



CSIR - National Institute of Oceanography



Geo-morphological studies for the sand mining clusters of Rivers in Goa

Zuari River

Submitted to

Goa State Biodiversity Board (GSBB)
C/o Department of Science, Technology and Environment,
Opp Saligao Seminary, Saligao, Bardez - Goa.
Tel: 0832-2407032 Fax: 0832-2407033



सीएसआईआर – राष्ट्रीयसमुद्रविज्ञानसंस्थान
CSIR-NATIONAL INSTITUTE OF OCEANOGRAPHY
(वैज्ञानिकतथाऔद्योगिकअनुसंधानपरिषद्)
(COUNCIL OF SCIENTIFIC & INDUSTRIAL RESEARCH)
दोना पावला, गोवा भारत / DONA PAULA, GOA - 403004 India



फ़ोन/Tel : 91(0)832-2450450
फैक्स /Fax: 91(0)832-2450602
इ-मेल/e-mail : ocean@nio.org
[http:// www.nio.org](http://www.nio.org)

Executive Summary

This report summarizes the details of field survey undertaken within ~ 53 km stretches of the Zuari River. It includes geological and geophysical data acquisition, analysis and important outcomes of the study. As per the project mandate Zuari River survey have been completed in two phases;

1. **Pre- Monsoon Survey** have been carried out during 7th to 13th January 2021. Geophysical data, including side scan sonar, single beam echo sounding, and high-resolution seismic, were acquired to study riverbed as well as subsurface characteristics of the Zuari river. Apart from this, grab sediment samples along 55 stations have also been acquired for Geochemical and grain size analysis.
2. **Post- Monsoon survey** have been carried out during 2nd to 4th January 2022. (53 Line Km side scan sonar, single beam echo sounding, and high-resolution seismic data were acquired to study the post-monsoon geomorphological changes along ~53 km of Zuari river course.

Key Observations

Sonography survey

- Spatial variations observed in the backscatter sonar intensity and ripple patterns.
- The Side Scan Sonar images of Zuari river shows varying smooth to rippled to heavily rugged riverbed morphology between off Chicalim to Sangameshwar.
- Point and mid-channel bars are more frequent in upstream region of the river.

Shallow Seismic 2D (H)R

- Sparker system achieved a subsurface penetration of ~3-25 m in the survey area.
- Due to the shallow depth of riverbed, multiples (up to second-order) are observed in the study area.
- Sand volume are estimated using side scan sonar image zonation of sand features, sediment thickness from seismic data.
- Based on EIA/EMP studies eight feasible sand mining regions are identified

Sediment Sampling

- Sediment samples were collected at different stations using small hand grab
- Sand dominates the sediments followed by silt.

Geo-Morphological studies for Zuari River - 2022

Contents

List of figures.....	iv
List of tables.....	vii
Chapter 1. Introduction.....	1
Background	1
Chapter 2. Data Acquisition.....	3
Geophysical data acquisition.....	3
General.....	3
Geodesy and controls.....	4
Survey Plan.....	4
Survey boats deployed for geophysical survey in Zuari river.....	5
Single Beam Echo sounder profiling	6
Data Acquisition Software.....	6
Navigation and Planning	6
Bathymetric Equipments and Softwares	6
Sparker data acquisition system.....	7
Side scan sonar	7
Sediment Sampling	8
Chapter 3. Data Processing.....	10
Geophysical data processing	10
High resolution Seismic data processing.....	10
Single beam bathymetry data processing	10
Side Scan Sonar Data Processing	10
Side Scan Sonar Data.....	11
Chapter 4. Interpretation	12
Major features identified from the side scan sonar (SSS) imaging	12
Color legends in Geophysical interpretation	15
Across Borim Bridge.....	16
Rachol-Shiroda ferry point	17

Geo-Morphological studies for Zuari River - 2022

Chandor-Ponchavadi	17
Ponchavadi-Xelvona	17
Ponchavadi-Curchorem	17
Chapter 5. Geological Observations	23
Material and Methods	23
Sediment Nomenclature	23
Sieve Size analysis	23
Results	24
Microscopic Analysis of geological samples of Zuari	26
Methodology	26
Salinity and pH	26
Results	27
Chapter 6. Post-Monsoon Geophysical Survey	41
Geophysical data acquisition:	41
Major features identified from the side scan sonar (SSS) imaging and high resolution seismic (HRS):	41
Side Scan Sonar Interpretation	41
Seismic Data Interpretation:	64
Chapter 7. Conclusions	70
Annexure 1	a

List of figures

Figure 1. Hydrographic Map of Goa. Insight zoom area of river Zuari.....	3
Figure 2. Google Map of the survey region (Zuari River).....	4
Figure 3. Boat deployed during the survey for side scan sonar (SSS) imaging, single beam echosounder profiling, high resolution seismic (HRS squid) survey and geological sampling across the Zuari river.5	
Figure 4.a) Hypack software used for recording Navigation and single beam echosounding data; b) Single beam echosounding system; c) Squid Sparkar System with 8 element streamer; d) Side Scan Sonar system (400kHz/900kHz).	8
Figure 5. sample (hand grab sampler) photographs	9
Figure 6. Flow diagram of side scan sonar data processing.....	10
Figure 7. Side Scan Sonar images. A) Riverbanks and small boulders, active mining, b) shadow zones of bridge pillars c) confluence of river channel d) active mining marks.....	11
Figure 8. Sonogram showing rock outcrop.....	12
Figure 9. Sonogram showing rock outcrop and debris near the riverbank.	13
Figure 10. Sonogram showing sand bar and ripple marks.....	14
Figure 11. Sonogram showing type-1 sand mining zone.....	15
Figure 12. Sonogram showing type-2 sand mining zone.....	15
Figure 13. Schematic representing the calculation of sediment resource along the river profile	16
Figure 14. Geophysical data across Borim bridge. (a) Side scan sonar (SSS) image (b) single beam echosounder bathymetry. (c) high resolution seismic data	18
Figure 15. Rachol-Shiroda ferry point geophysical data. (a) Side scan sonar (SSS) image (b) single beam echosounder bathymetry. (c) high resolution seismic data	19
Figure 16. Geophysical data across Chandor-Ponchavadi region. (a) Side scan sonar (SSS) image (b) single beam echosounder bathymetry. (c) high resolution seismic data	20
Figure 17. Geophysical data across Ponchavadi-Xelvona region, Navelim. (a) Side scan sonar (SSS) image (b) single beam echosounder bathymetry. (c) high-resolution seismic data	21
Figure 18. Geophysical data across the Ponchavadi-Curchorem region. (a) Side scan sonar (SSS) image (b) single beam echosounder bathymetry. (c) high-resolution seismic data	22
Figure 19. Geological Sample Locations.....	23

Geo-Morphological studies for Zuari River - 2022

- Figure 20. Side Scan Sonograms acquired near Taripanta playground and Mascarenhas organic farm during (A) pre-monsoon and (B) post-monsoon seasons. (A) highlights the presence of two sand bars and (B) shows the removal of sediment from the bars. 43
- Figure 21. Side Scan Sonograms acquired near Cotarli village (A) pre-monsoon and (B) post-monsoon seasons. (A) primarily highlights the presence of a sediment bar and (B) highlights thinning of the sediment bar to an extent that the underlying bedrock morphology 44
- Figure 22. Side Scan Sonogram acquired near Vakerwada-Vodlemol-Cacora region during (A) pre-monsoon and (B) post-monsoon seasons. (A) highlights the presence of a thin sediment bar along with rock outcrop and debris and (B) highlights the thickening of the sediment bar. 45
- Figure 23. Side Scan Sonogram acquired near Muguli-Vodlemol-Cacora region during (A) pre-monsoon and (B) post-monsoon seasons. (A) Shows the presence of sediment along with rock outcrop and debris. (B) highlights partial erosion of the sand bar..... 46
- Figure 24. Side Scan Sonogram acquired near Muguli-Solien math region during (A) pre-monsoon and (B) post-monsoon seasons. (A) Shows presence of thin mid-channel bars (B) highlights partial erosion of point bars and thinning of the mid-channel bar and the presence of type-2 sand mining signatures.... 47
- Figure 25. Side Scan Sonogram acquired near Comproi-Vodlemol-Cacora region during (A) pre-monsoon and (B) post-monsoon seasons. The sonograms highlight thinning of mid-channel bars and the appearance of bedrock after the monsoon..... 48
- Figure 26. Side Scan Sonogram acquired near Comproi region during (A) pre-monsoon and (B) post-monsoon seasons. (A) highlights riverbed morphology along with rock outcrops and debris at the bank. (B) highlights the presence of sand mining signature of type-2. 49
- Figure 27. Side Scan Sonogram acquired near Kamral-Comproi region during (A) pre-monsoon and (B) post-monsoon seasons. (A) highlights the presence of sand mining signatures and dumped residue sediment near the banks. (B) highlights obliteration of sand mining pits indicating sediment accumulation. 50
- Figure 28. Side Scan Sonogram acquired near Sanvordem-Kamral (upstream Sanvordem bridge) region during (A) pre-monsoon and (B) post-monsoon seasons. (A) Highlights relatively smooth riverbed morphology. (B) highlights the presence of exposed bedrock indication erosion in this region. 51
- Figure 29. Side Scan Sonogram acquired near Sanvordem-Baag Shirfod (downstream Sanvordem bridge) region during (A) pre-monsoon and (B) post-monsoon seasons. (A) shows drag marks on the riverbed. (B) highlights the obliteration of drag marks and the presence of a mid-channel bar in the region..... 53
- Figure 30. Side Scan Sonogram acquired near Ponchavadi-Bag-Xelvona region during (A) pre-monsoon and (B) post-monsoon seasons. (A) shows the presence of a sediment bar, type-2 sand mining signatures, and bedrocks. (B) shows an enlarged sediment bank bar at the same location and some fresh sand mining signatures along with the bedrock..... 54
- Figure 31. Side Scan Sonogram acquired near Ponchavadi-Xelvona region during (A) pre-monsoon and (B) post-monsoon seasons. (A) highlights the presence of a mid-channel bar with type-2 sand mining signature. (B) shows a thinned mid-channel bar and some remains of old mining signatures. 55

Geo-Morphological studies for Zuari River - 2022

- Figure 32. Side Scan Sonogram acquired near Ponchavadi-Chandor region during (A) pre-monsoon and (B) post-monsoon seasons. (A) highlights the presence of step-like features near the bank. (B) shows the washout of these features and a thin layer of sediment has covered the bank. 56
- Figure 33. Side Scan Sonogram acquired near Ponchavadi-Chandor region during (A) pre-monsoon and (B) post-monsoon seasons. (A) highlights the presence of mid-channel bars along with a few rock outcrops. (B) highlights thinning of one of the sand bars and signatures of sand mining. 57
- Figure 34. Side Scan Sonogram acquired near Mankem-Macasana region during (A) pre-monsoon and (B) post-monsoon seasons. (A) highlights a sediment ridge and the presence of past sand mining signatures. (B) shows the same ridge and mining signatures, which are still not completely washed out after the monsoon. Some new sand mining signatures are also observed in this region..... 58
- Figure 35. Side Scan Sonogram acquired near Soncrem (Shiroda)-Curtorim region during (A) pre-monsoon and (B) post-monsoon seasons. (A) highlights presence of type-2 sand mining signature. (B) highlights anomalous enhancement of the mining signature. 59
- Figure 36. Side Scan Sonogram acquired near Shiroda-Curtorim region during (A) pre-monsoon and (B) post-monsoon seasons. (A) highlights the presence of thinly covered bedrocks. (B) highlights the disappearance of the bedrock signature and some type-1 sand mining signatures. 60
- Figure 37. Side Scan Sonogram acquired near Borim-Loutolim region during (A) pre-monsoon and (B) post-monsoon seasons. (A) highlights the presence of medium-to-large ripple marks near Borim bank. (B) shows the post-monsoon sonogram of the same medium-to-large ripple marks. 61
- Figure 38. Side Scan Sonogram acquired near Durbhat-Verna region during (A) pre-monsoon and (B) post-monsoon seasons. These sonograms do not show any significant change in the riverbed morphology after monsoon..... 62
- Figure 39. Side Scan Sonogram acquired near Madkai-Verna region during (A) pre-monsoon and (B) post-monsoon seasons. These sonograms do not show any significant change after the monsoon..... 63
- Figure 40. High-resolution seismic data: a) pre-monsoon seismic data, b) post-monsoon seismic data, and c) sediment thickness from the reference layer between the survey period near Cortalim Zuari bridge.66
- Figure 41. High-resolution seismic data: a) pre-monsoon seismic data, b) post-monsoon seismic data, and c) sediment thickness variation from reference layer between the survey period near Borim bridge. .67
- Figure 42. High-resolution seismic data: a) pre-monsoon seismic data, b) post-monsoon seismic data, and c) sediment thickness variation between the survey period near the Ponchavadi-Chandor region..... 68
- Figure 43. High-resolution seismic data: a) pre-monsoon seismic data, b) post-monsoon seismic data, c) sediment thickness variation between the survey period near the Sanvordem - Baag Shirfod region.. 69
- Figure 44. Sand sediment grain size distribution from upstream to river mouth..... 70
- Figure 45. Possible Sand mining regions after considering EIA/EMP studies 71

List of tables

Table 1. Geodetic survey parameters..... 4

Table 2. Nomenclature of Zuari River (Pre-monsoon) sand samples were done by following standard Rock-Color Chart prepared by the Rock-Color Chart Committee (representing the U.S. Geological Survey, GSA, the American Association of Petroleum Geologists, the Society of Economic Geologists, and the Association of American State Geologists 24

Table 3. Cumulative percentage of passing of Zuari River sediment samples as per IS 650 requirements 24

Table 4. Weight percentage of sand, silt, and clay fractions in Zuari River sediments 25

Table 5. The pH and salinity variation of the sand samples for 3stage fresh water washing 27

Table 6. Grain size variation from microscopic analysis of dry sediment samples data 29

Table 7. Photomicrographic images of dry sediments 31

Table 8. Total Volume (Cubic m) and Weight (Ton) in selected regions and volume (cubic m) and weight (ton) within 3meter mining depth 72

Chapter 1. Introduction

Background

Undoubtedly sand is an essential part of a river ecosystem. Like flow and fish, it helps rivers stay healthy, sand is critical for groundwater recharge, replenishing the nutrients in moving water, and providing habitat to numerous forms of aquatic and riparian fauna. Sand has become an essential component of most modern infrastructure. From roads to buildings and other structures, the usage of sand is ubiquitous all over the planet. Sand mining is the extraction of sand from beaches, seabeds, and riverbeds. The dredging and mining often cause several alterations to the physical characteristics of both rivers and riverbeds. The erosion caused by mining the sea or a river floor can also adversely affect the region's biodiversity (river and riparian habitats). Although, several policy measures have been undertaken, the sheer demand for sand worldwide has given rise to an extensive network of sand mining operators, including in Goa, India.

To address the impact of sand mining on the health of the riverine systems of Goa, four major rivers have been identified: *Terekhol, Chapora, Mandovi, and Zuari* rivers. In each of these rivers, a total of twenty-four active sand mining clusters have been identified (Annexure-I). Other than the above four, Goa harbors a few more rivers. This project also includes carrying out studies in nine other rivers (*Sal, Talpona, Galjibag, Cumbarjua, Valvanti, Mapusa, Sinquerim, Khandepar, Kushavati*) and sand mining areas in second phase of this project. Presently there is no data available for the rivers with respect to sand, its availability, areas, and its extraction etc. Goa State Biodiversity Board (GSBB), an autonomous body of the Government of Goa under Department of Science, Technology and Environment, would like to carry out a study to understand the geo-morphology, bathymetry, sand budgetary and flow dynamics of these clusters and the impact of sand mining on the biodiversity of these identified river clusters in Goa. GSBB has approached CSIR- National Institute of Oceanography (CSIR-NIO), since the CSIR-NIO has scientific expertise, infrastructural and logistic facilities, and capability for carrying out such studies.

"In the present report the study is focused on the river Zuari for Geomorphological studies for the sand mining clusters (Fig.1)."

Chapter 2. Data Acquisition: provides the detailed information about the geophysical survey and various equipments deployed during the survey. Side scan sonar (SSS) for imaging the geomorphology of the riverbed, single beam echo sounding for imaging the riverbed

Geo-Morphological studies for Zuari River - 2022

depth, high resolution seismic (HRS, squid) system for imaging the subsurface below the riverbed.

Chapter 3. Data Processing: provides the detailed information about the geophysical data processing and various parameters for processing the side scan sonar (SSS), single beam echo-sounding, high resolution seismic (HRS). Geological sampling locations are given and sampling protocol followed.

Chapter 4. Interpretation: provides the detailed interpretation and cross correlation between different geophysical data sets across the Zuari river. Various geomorphological features associated with the sand distribution (sand ripple marks, sand bars), riverbank, active mining, exposed bed rock and riverbank erosion is identified from side scan sonar data, corresponding bathymetry using single beam echo-sounding data and subsurface sediment thickness (probably sand) using high-resolution seismic data.

Chapter 5. Geological observations: provides the detailed analysis and observations from the geological samples collected across the river Zuari.

Chapter 6. Post-monsoon geophysical survey: provides the major features identified from the side scan sonar (SSS) images and high resolution seismic (HRS) data. Comparison of pre- and post-monsoon SSS images have been done to study changes in important riverbed morphological features. Seismic data has also been interpreted to include a pre- and post-monsoon comparison of the riverbed aggradation or erosion.

Chapter 7. Conclusion: provides key points from geophysical data interpretation, including high resolution shallow seismic data, side scan sonar data and single beam bathymetry data. Also includes a gist of important geological observations made from grab samples.

Chapter 2. Data Acquisition

Geophysical data acquisition

With a ~145 km long stretch, Zuari River is the longest river of Goa. Zuari River basin constitute the second largest basin of Goa after Mandovi River. With about 975 km² area between Netravali and Mormugao bay, it constitutes about 27% of the total area of Goa. It originates in the Sahyadri Hills as Uguem and Sanguem rivers and after flowing on zigzag stretch till Sanguem Taluka, it conjoins. The river after the confluence of Sanguem and Uguem is referred as Zuari River. Thereafter, Zuari flows in the north-western direction through the talukas of Sanguem, Quepem, Ponda, Tiswadi, Mormugao, and Salcete. It covers approximately 55 km, from Sanguem confluence point, before finally debouching in the Arabian Sea at Mormugao Bay. For present study, the geophysical survey has been conducted from the river Mouth in the downstream to Sangmeshwar temple (Sanguem) in the upstream.

General

Geophysical survey is a systematic collection of multi-platform geophysical data for spatial studies. Such surveys have many applications in geology, archaeology, mineral and energy exploration, oceanography, and engineering. These surveys are used in industry as well as, for academic research. Such surveys are classified as seismic and non-seismic and provide various levels of detail. But all generate useful data based on the purposes for which the surveys are conducted. In the present study, the geophysical surveys carried out include seismic, sonography survey along with the single beam survey for the Zuari river (Fig.1).

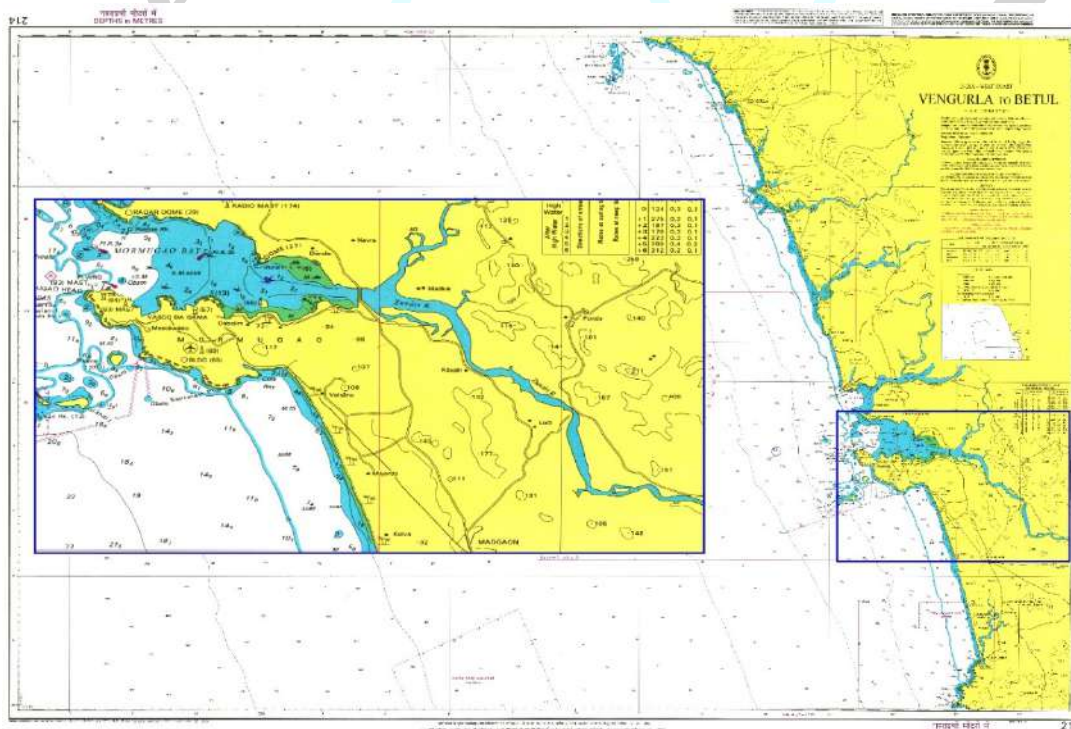


Figure 1. Hydrographic Map of Goa. Insight zoom area of river Zuari.

Geo-Morphological studies for Zuari River - 2022

Geodesy and controls

The survey was conducted in WGS 84 datum i.e., World Geodetic System version 84 spheroid, which is invariably used by the various constellation of the Global Navigation Satellite System (GNSS).

GEODETTIC PARAMETERS	
Satellite Datum	
Spheroid	WGS-84
Datum	WGS 84
Semi-Major Axis	6378137.000 m
Semi Minor Axis	6356752.314 m
Inverse Flattening	298.2572
Projection Parameters	
Grid Projection	Universal Transverse Mercator
Latitude of Origin of Projection	0° (Equator)
Longitude of Origin of Projection	75° E, Zone 43
Hemisphere	North
False Easting (meters)	500000
False Northing (meters)	0
Scale Factor on CM	0.9996
Units	Meters

Table 1. Geodetic survey parameters

Survey Plan

The entire geophysical survey was planned in two phases. Phase-I consists of a side scan sonar survey (SSS), single beam echosounder profiling, and seismic sparker survey, along the navigating channel in the Zuari river. Phase-II consists of sediment samples collection by using hand-grab sampling equipment. (Google map; Fig.2).



Figure 2. Google Map of the survey region (Zuari River)

Survey boats deployed for geophysical survey in Zuari river

Two different boats are deployed for various geophysical survey in Zuari river for side scan sonar (SSS), single beam echosounder profiling, and high resolution seismic (HRS) (Fig.3).



Figure 3. Boat deployed during the survey for side scan sonar (SSS) imaging, single beam echosounder profiling, high resolution seismic (HRS squid) survey and geological sampling across the Zuari river.

Single Beam Echo sounder profiling

Data Acquisition Software

The acquisition software used is HYPACK[®] Max (Fig.4a), a marine surveying, positioning, and navigation software package. The software provides interface between various sensors such as motion sensor, heave sensor, global positioning system, echosounder, seismic data acquisition and side-scan sonar. The acquisition hardware is composed of three separate units: a GPS system on the survey vessel (rover), a motion sensor (vessel heave, pitch, and roll), and a Single beam echosounder. All the above hardware units were interfaced with acquisition system (HYPACK[®] Max). The acquisition software combines the data streams from the various components into a single raw data file, with each device string referenced by a device identification code and timestamped to the nearest millisecond.

The raw data, thus, gets recorded on hard disk of the computer, which was then copied to the portable hard disc. The time stamping to navigation and other geophysical data was accomplished in Greenwich Mean Time (GMT) provided by the Global Positioning System (GPS) receiver clock throughout the survey.

Navigation and Planning

The survey track lines were planned, oriented, in the navigation channel with the help of local navigator as no depth values are readily available in such a way that the underway survey would fulfil the objectives of the project indicated in the WORK. The survey vessel is navigated and maneuvered along navigation track lines by the master of the survey boat. In order to assist the master in track navigation, a helmsman monitor was placed in the wheel house of the vessel. This was interfaced to the data acquisition PC, running one of the most widely used software package called HYPACK[®] Max. It is basically a Windows PC based integrated software package for automated hydrographic data acquisition and processing routines, developed by Xylem Inc., USA.

The data from the GPS receiver, motion sensor, and echosounder are streamed in real time to a computer running the Windows operating system. Along with this, it also provides tools to i) Design preplanned survey track lines ii) Navigate along the planned track lines iii) Provide position data to other geophysical systems (echo sounder and high-resolution sub-bottom profiler) iv) Log raw position and depth data and v) Realize the quality control in real time navigation.

Bathymetric Equipments and Softwares

The single beam bathymetric survey equipment used for the survey consists of boat-based hull mounted Bathy-500HD echosounder. The Bathy-500HD is a high-resolution, precision echo sounder. It is basically a triple frequency echosounder having 33kHz, 50kHz and 210kHz frequency acoustic bursts (Fig.4a, 4b). It is designed exclusively for hydrographic marine surveys up to 100 meters of water depth. It meets or exceeds all current IHO hydrographic requirements for single beam echo sounders.

The Bathy-500HD system is configured as a flexible acoustic measurement sensor device capable of providing an excellent solution for shallow water hydrographic applications. Both applications make use of the appropriate signal processing features to perform accurate and reliable bottom digitizing. The Bathy-500HD makes use of

sophisticated algorithms for first/peak bottom echo detection, automatic mode controls for: receiver gain, bottom tracking, pulse length and power level controls greatly reduce the probability of inaccurate bottom detection/tracking.

Bathymetric surveys allow us to measure the depth of a riverbed as well as, to map the underwater features on the riverbed. Bathymetric charts are typically produced to support safety of surface navigation, and usually show river-floor relief or terrain as contour lines and selected depths soundings.

Sparker data acquisition system

High-resolution shallow seismic system (make: Applied Acoustics Squid 500) was deployed to acquire the sub-bottom information of the region. The system includes Power Supply, Trigger capacitor bank, (Fig. 4c), hydrophone streamer array and an acquisition unit (model Mini-Trace II). In this technique, a source of seismic energy (squid system) is towed behind the survey vessel just below the water surface. The transmitted pulse travels through the water column and sub-surface and are reflected when changes in acoustic impedance are encountered. Acoustic impedance changes commonly occur at the boundaries, i.e., interfaces between water and sediments, inter-sediments, and sediments and basement.

The reflected pulses travel back towards the sea surface, and the reflections are detected by an 8-element hydrophone. These reflections are converted to an electrical signal, which is amplified and converted to digital samples and stored in the hard disk of the data acquisition system (Mini Trace II) in native GeoTrace format. This data is then processed, filtered and displayed in graphic form as a function of travel time. The raw data is copied in SEG Y format and later processed at CSIR-NIO using seismic data processing software Pro-MAX.

Side scan sonar

EdgeTech 4125 digital side scan sonar digital geophysical data acquisition system was used for SSS data on board (Fig.4d)

Rub Test: The side-scan sonar system was set up on the deck of the respective survey vessels and a 'rub test' was carried out on both port and starboard transducers of the tow fish.

Wet Test: The tow fish was, thereafter, lowered into the water and a 'wet test' was performed to check that echo from targets were returning to both the channels. The gain and grey-scale settings were adjusted to balance the port and starboard channels of the side-scan sonar system.

Side-scan sonar data was acquired using EdgeTech discover 4125 digital data acquisition system.

The raw data was recorded in *.jsf, and *.xtf format and the xtf format is used for processing the data. The EdgeTech acquisition software displayed the real time acoustic data on the computer screen for online quality control (QC). Output was controlled by specifying or editing various parameters, e.g., filter settings, automatic bottom tracking settings for known fish height at any time, time variable gain settings, output file format (XTF) settings. SonarWiz data processing software package was finally used to process the acquired side scan sonar data.

Geo-Morphological studies for Zuari River - 2022

Dual-channel dual frequency EdgeTech 4125 side-scan sonar performed well during the survey. The tow system was operated using recommended manufacturers procedures. The tow fish was towed astern of the survey vessel over an arm.

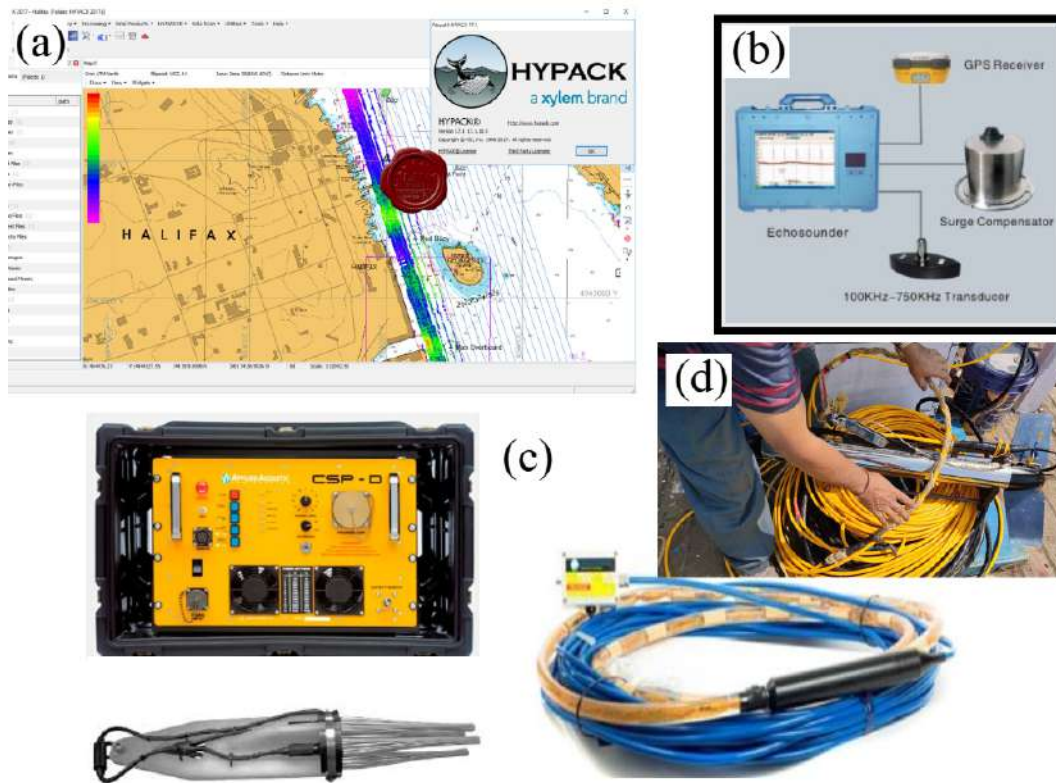


Figure 4. a) Hypack software used for recording Navigation and single beam echosounding data; b) Single beam echosounding system; c) Squid Sparkar System with 8 element streamer; d) Side Scan Sonar system (400kHz/900kHz).

Sediment Sampling

In Phase-II we have carried out sediment sampling at selected locations based on the side scan sonar images across the Zuari River region (Fig. 5). The sediment samples are collected for geological analysis and cross correlated with the geological features interpreted from side scan sonar (SSS) to understand riverbed morphology.



Figure 5. sample (hand grab sampler) photographs

Chapter 3. Data Processing

Geophysical data processing

High resolution Seismic data processing

The raw seismic data collected across the Zuari river for subsurface imaging is processed for increasing the signal to noise ratio for better subsurface imaging. Raw data was loaded with Seismic Unix processing software and applied bandpass filtering 400-450-1900-2000. We have seen 1st order to 3rd order riverbed multiples

Single beam bathymetry data processing

Raw single beam echosounder bathymetry data collected along the navigation track line is processed for the tide correction based on the tide gauge.

Side Scan Sonar Data Processing

Raw data processing and analysis is carried out through "SonarWiz5" software following processing steps listed in Fig. 6. Common processing steps include bottom tracking, signal processing (automatic gain control, beam angle correction, time varying gain), and offset & layback correction for determining towed sensor positions. The resultant side scan sonar image is created by mosaicking which is a process of assembling geo-referenced sonar images from adjacent track lines to create a comprehensive image of the riverbed that represents the acoustic character of the riverbed of the survey area. Finally, processed data and images are exported into formats compatible with Geographical Information Systems/other spatial image analysis software.

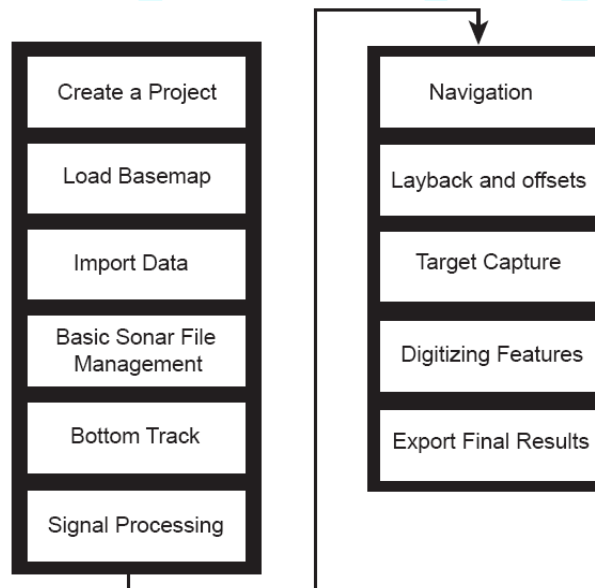
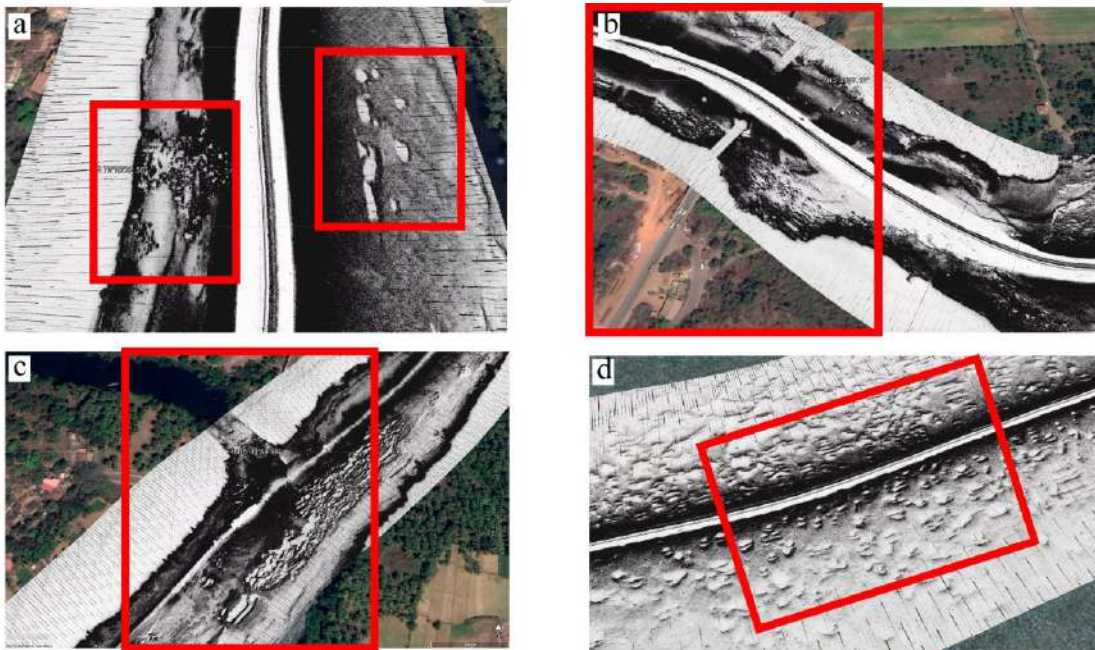


Figure 6. Flow diagram of side scan sonar data processing

Side Scan Sonar Data

The side scan sonar (SSS) is deployed from the starboard side ~ 0.5 m below water column and towed. The survey is navigated along the channel at ~3.5 knots speed, and the continuous data is collected from mouth of the Zuari River (Off Chicalim) to Sangameshwar (Fig. 2). The side scan sonar data have been recorded with a 100 m swath range in both (i.e., star and port) side of the boat, which provided total coverage of 200 m. The side scan sonar image is the intensity image of the backscatter from the riverbed and riverbanks.

Fig. 7 shows side scan sonar images of various salient features from different locations within the river basin. Fig.7a shows riverbanks, rock debris at the riverbank, and a few sand extraction marks on the riverbed. Fig.7b shows side scan sonar image on google map overlay, highlights roads at the river-banks, rock outcrops, and rock debris along with bridge pillar base and its shadow. Fig.7c highlights a tributary's confluence points that join the main-



stream and sand mining marks. Fig.7d shows sand extraction marks.

Figure 7. Side Scan Sonar images. A) Riverbanks and small boulders, active mining, b) shadow zones of bridge pillars c) confluence of river channel d) active mining marks.

Chapter 4. Interpretation

Major features identified from the side scan sonar (SSS) imaging

Riverbed morphology through the side scan sonar images have been carefully analyzed to infer the sand distribution, and to mark active sand mining zones in the study area. The processed images are presented along with a key map in figures 14 to 18. The analysis of the side scan sonar images reveals that the riverbed is carpeted by sediments in the entire surveyed area except at few locations. Apart from this, riverbank rock outcrops and rock debris are also identified. These rock debris and riverbank rock outcrops are predominant upstream Sanvordem. Some representative side scan sonar images outlining rock outcrops, rock debris, sand bar and sand mining signatures are shown in figures 8-12.

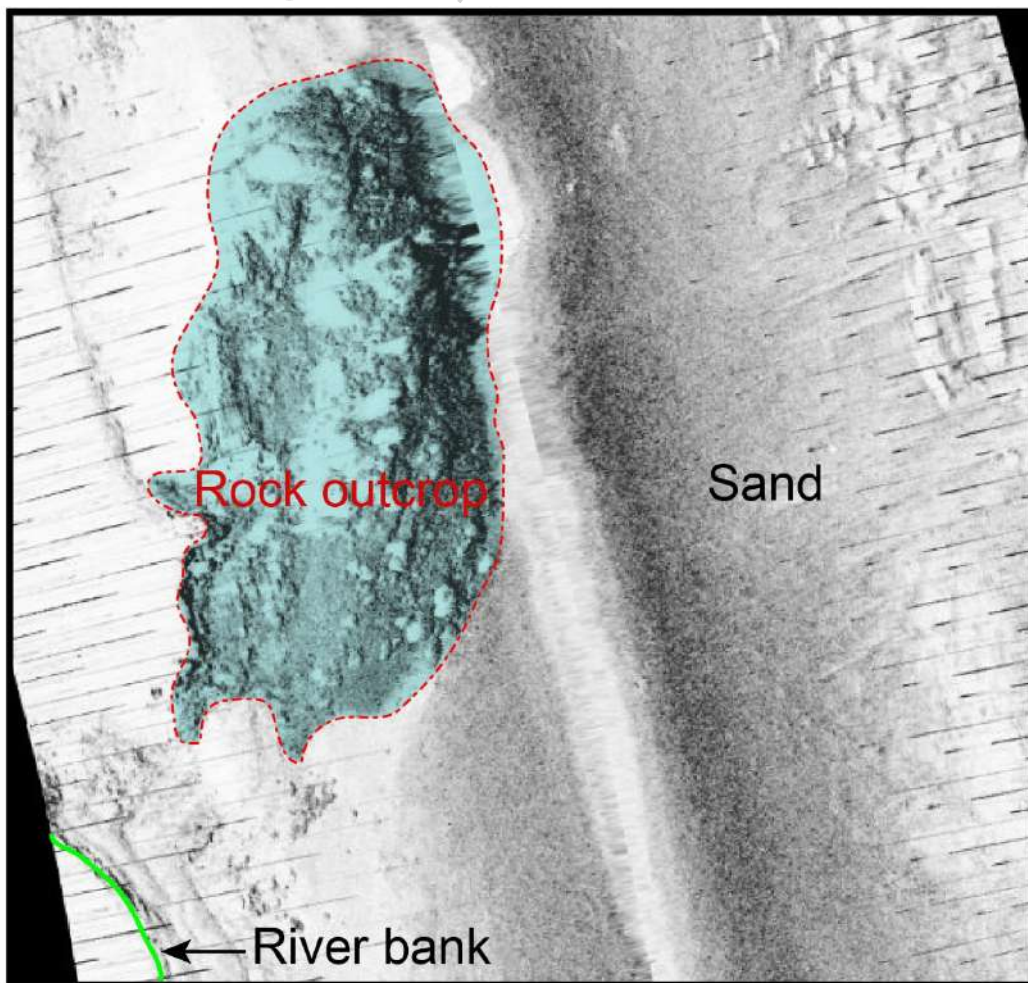


Figure 8. Sonogram showing rock outcrop.

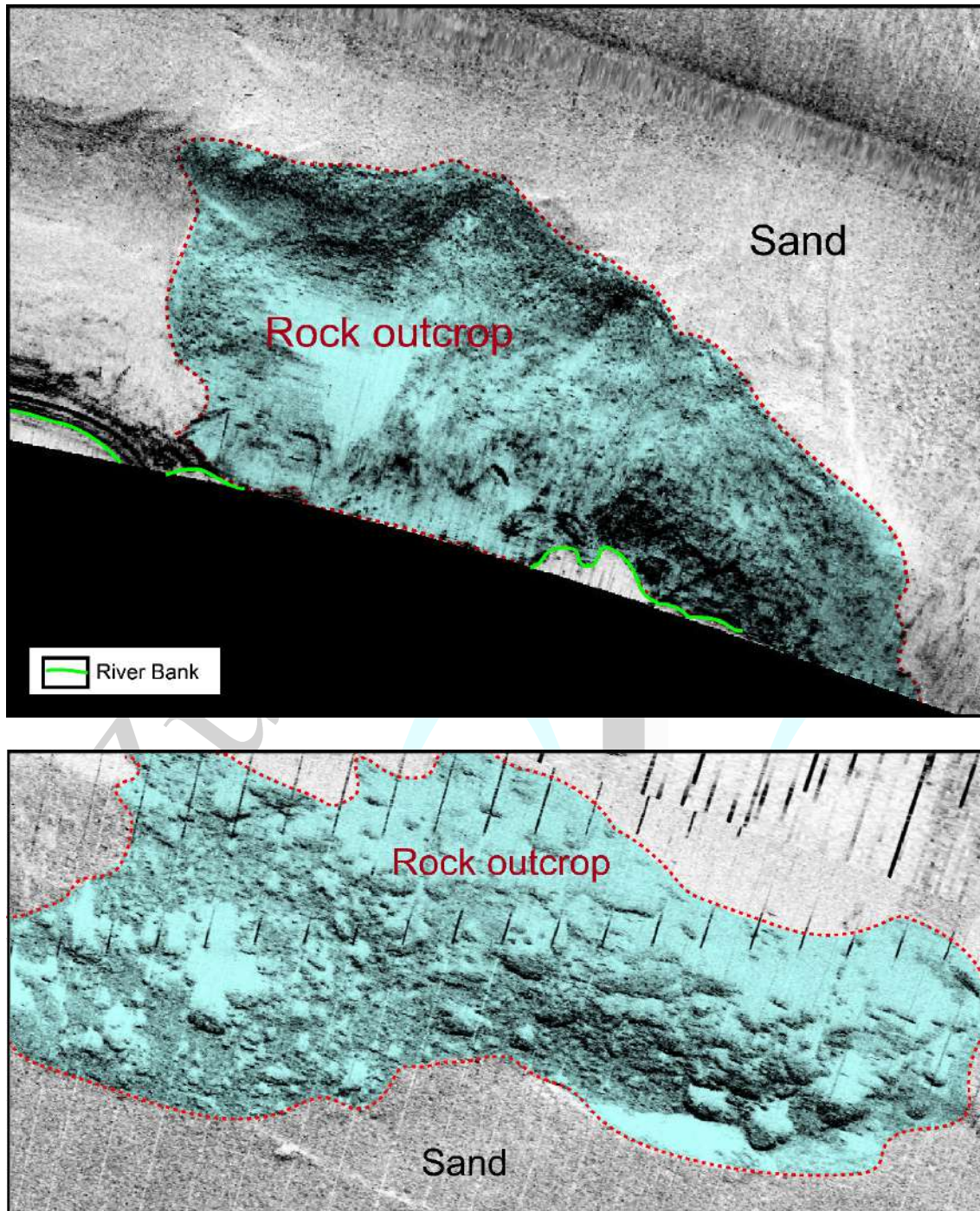


Figure 9. Sonogram showing rock outcrop and debris near the riverbank.

Based on the presence of morphological features such as ripple marks and sand bar, along with tonal and textural variation in the backscatter, sand deposits on the riverbed are identified as shown in Fig.10. The riverbed, in the entire surveyed area, is predominantly comprised sand. Sand boundaries in each sonogram have been delineated and presented for select locations in figures.14-18.

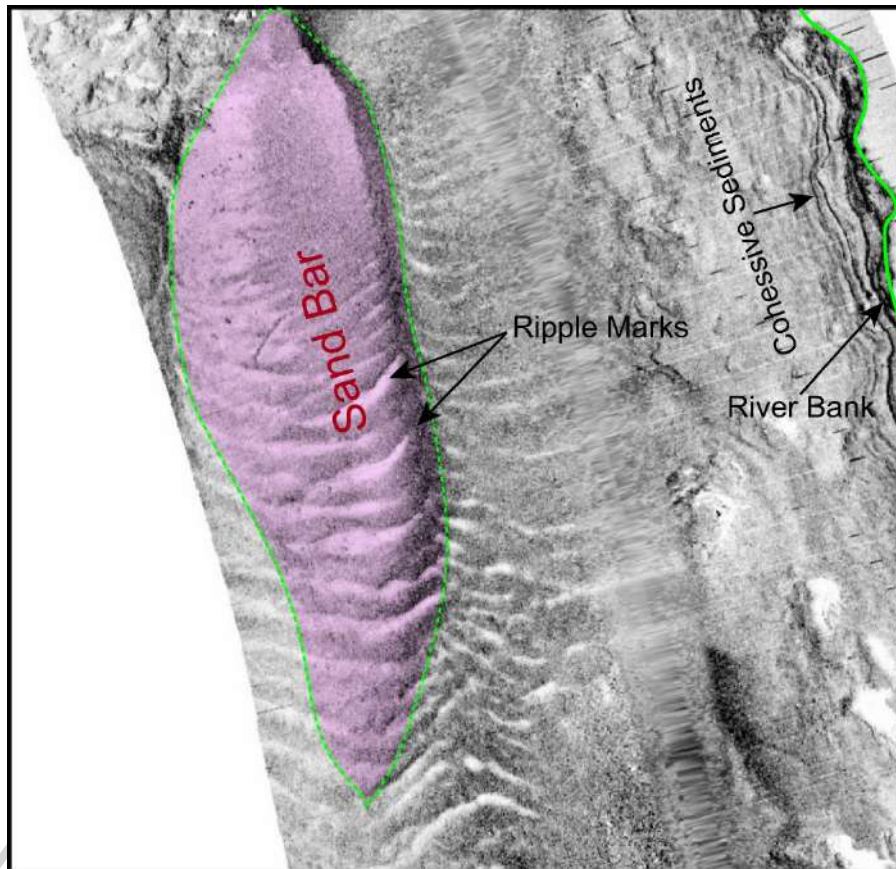


Figure 10. Sonogram showing sand bar and ripple marks.

At certain locations, side scan sonar images show zones with signatures of sediment excavation. These zones are interpreted as active sand mining zones. Based on the appearances of excavation marks, these active sand mining zones are categorized in two types. In type-1 mining zone, excavation marks are generally elongated. One excavation mark ~22 m long and ~4 m wide is shown in Fig.11.

In type-2 mining zone, the excavation marks are more rounded. A representative excavation mark of ~20-25 m diameter is shown in Fig. 12. Two different types of excavation marks signify variation in sand mining practice.

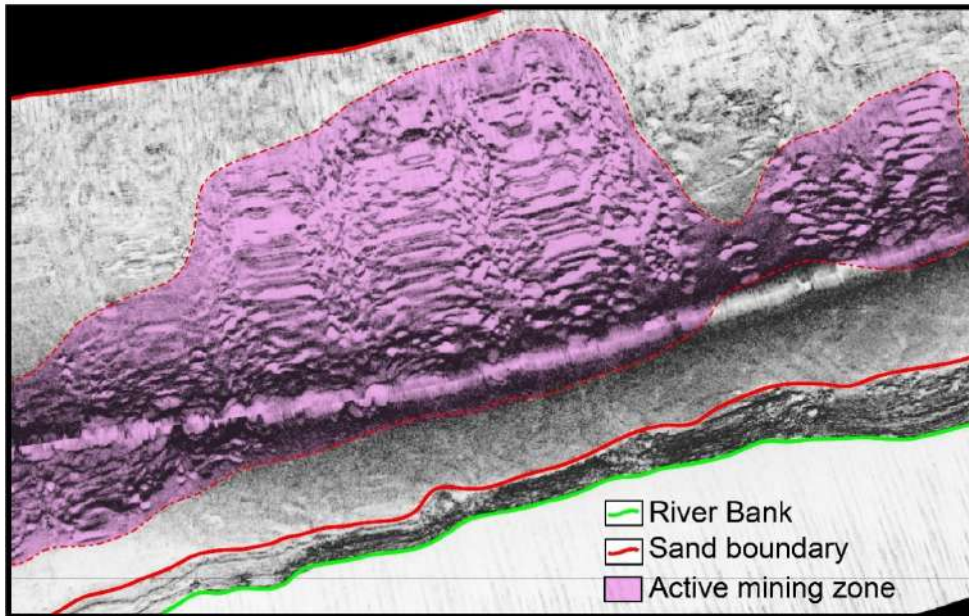


Figure 11. Sonogram showing type-1 sand mining zone

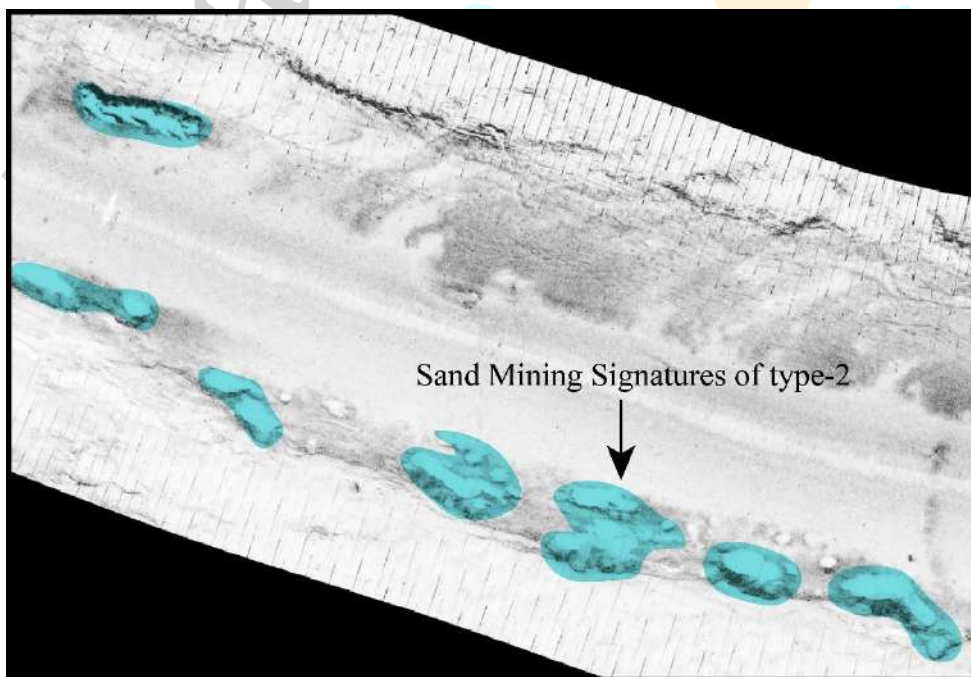


Figure 12. Sonogram showing type-2 sand mining zone.

Color legends in Geophysical interpretation

Integrated geophysical plot highlighting the geomorphology based on side scan sonar (SSS) imaging, riverbed bathymetry using single beam echo sounding and sediment thickness derived from high-resolution sparker seismic (HRS) is shown from Figures 14 to 18. The side scan sonar (SSS) image is referenced with WGS84 Universal Transverse Mercator (UTM) coordinate system and relative distance mode. In the side scan sonar images, the top X-axis is

UTM-X, right Y-axis is UTM-Y. The bottom and left axis show relative distance in m. The side scan sonar profile in Figures 14a-18a is interpreted with confirmed sand boundaries (red solid line), unconfirmed sand boundary (dotted red), outcrop (cyan), riverbank (green), active mining region (pink solid), geological sample locations (green dot) and the HRS seismic track is highlighted in solid blue line with the trace no. The bridges across the river are shown with Yellow and interpreted sand bars as solid black lines. Figures 14b-18b represent single beam echo sounder data (solid blue) providing the riverbed depth profile along survey line. Figures 14c-18c show interpreted riverbed (green) and bedrock (red) which are used for the calculation of sediment thickness.

The seismic data is acquired in time domain and is converted to depth by using a constant velocity of 1500 m/s and is also corrected for tides. The sediment volumes are calculated as follows.

The difference between the bedrock and riverbed provides the sediment thickness along the seismic track. We assume the sediment thickness to be zero at the boundary of the sand zone. Assuming a linear sediment thickness between the seismic track line and boundary of sand zone, the cross section is calculated from the area of triangle as shown in Figure 13. The volume is calculated by multiplying the cross-section area with the incremental distance along the survey line.

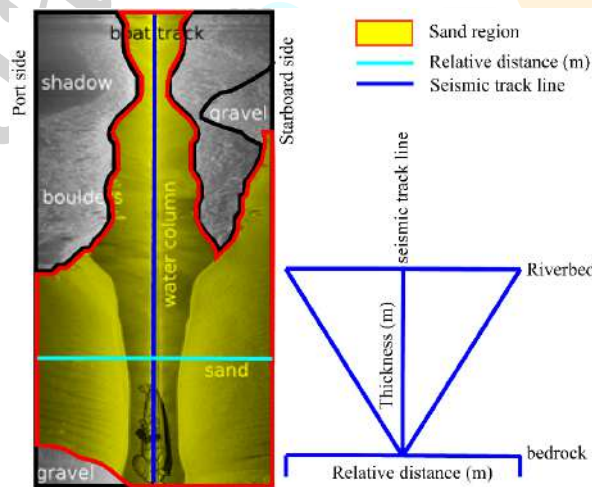


Figure 13. Schematic representing the calculation of sediment resource along the river profile

The total weight of the sediment (sand) in tonnage is calculated by multiplying the volume with the bulk density of sediment of 1.6 g/cm^3 (equivalent to 1.6 Tonnes/m^3).

Across Borim Bridge

The SSS image across Borim Bridge covers an area of $(200 \times 2200) \text{ m}^2$ from the center of the navigation (blue track line). It shows the sand boundary (red), Borim bridge pillar (yellow) rock outcrop (cyan) and riverbank (green) (Fig.14a). Single beam bathymetry data shows the riverbed depth varying between ~ 5.0 - 13.5 m . One depression is identified from the single beam bathymetry (Fig.14b) and seismic data (Fig.14c) where the depth of riverbed increases from 6.0 m to 13.5 m . One geological sample location (**station 16**) is within the span of side scan sonar image (Fig.14a). The details of sediment sample analysis are provided in Table 3.

The seismic data, interpreted in both time and depth domain, shows the riverbed depth varies between ~5.2-13.6 m (green) and bedrock (red) between ~18.5-26.4 m (Fig. 14c). A total minable volume of ~**411681 cubic m**, and ~**658690 Tons** (weight) of sand is available.

Rachol-Shiroda ferry point

The SSS images across **Rachol-Shiroda ferry point** covers an area of (200x2100) m² from the center of the navigation (blue track line). It shows the sand boundary (red), and riverbank (green) (Fig.15a). Single beam bathymetry data (Fig.15b) shows the riverbed depth varying between ~4.3-14.2 m. One geological sample location (**stations 20**) is within the span of side scan sonar image (Fig.15a). The details of sediment sample analysis are provided in Table 3. The seismic data, interpreted in both time and depth domain, shows the riverbed depth varies between ~4.2-14.3m (green) and bedrock (red) between ~11.5-20.5m (Fig. 15c). A total minable volume of ~**432219 cubic m**, and ~**691550 Tons** (weight) of sand is available.

Chandor-Ponchavadi

The SSS image across **Chandor-Ponchvadi region** covers an area of (200x2000) m² from the center of the navigation (blue track line). It shows the sand boundary (red), active mining zone (magenta), and riverbank (green) (Fig.16a). Single beam bathymetry data shows the riverbed depth varying between ~3.5-9.6 m (Fig.16b). One geological sample location (**stations 26**) is within the span of side scan sonar image (Fig.16a). The details of sediment sample analysis are provided in Table 3. The seismic data, interpreted in both time and depth domain, shows the riverbed depth varies between ~3.7-9.5 m (green) and bedrock (red) between ~7.4-20.2 m (Fig.16c). A total minable volume of ~**549391 cubic m**, and ~**879026 Tons** (weight) of sand is available.

Ponchavadi-Xelvona

The SSS image across **Ponchavadi-Xelvona** region covers an area of (200x2200) m² from the center of the navigation (blue track line). It shows the sand boundary (red), mining locations (magenta), rock outcrops (cyan), and riverbank (green) (Fig.17a). Single beam bathymetry data shows the riverbed depth varying between ~3.4-9.6 m (Fig.17b). One geological sample location (**station 28**) is within the span of side scan sonar image (Fig.17 a). The details of sediment sample analysis are provided in Table 3. The seismic data, interpreted in both time and depth domain, shows the riverbed depth varies between ~3.6-9.5 m (green) and bedrock (red) between ~13.8-18.6 m (Fig.17c). A total minable volume of ~**287541 cubic m**, and ~**460066 Tons** (weight) of sand is available.

Ponchavadi-Curchorem

The SSS image across **Ponchavadi-Curchorem** region covers an area of (200x2000) m² area from the center of the navigation (blue track line). It shows the sand boundary (red), mining locations (magenta), rock outcrops (cyan), and riverbank (green) (Fig.18a). Single beam bathymetry data shows the riverbed depth varying between ~6.2-9.6 m (Fig.18b). The seismic data, interpreted in both time and depth domain, shows the riverbed depth varies between ~6.1-9.5 m (green) and bedrock (red) between ~8.3-16.8 m (Fig.18c). A total minable volume of ~**244861 cubic m**, and ~**391777 Tons** (weight) of sand is available.

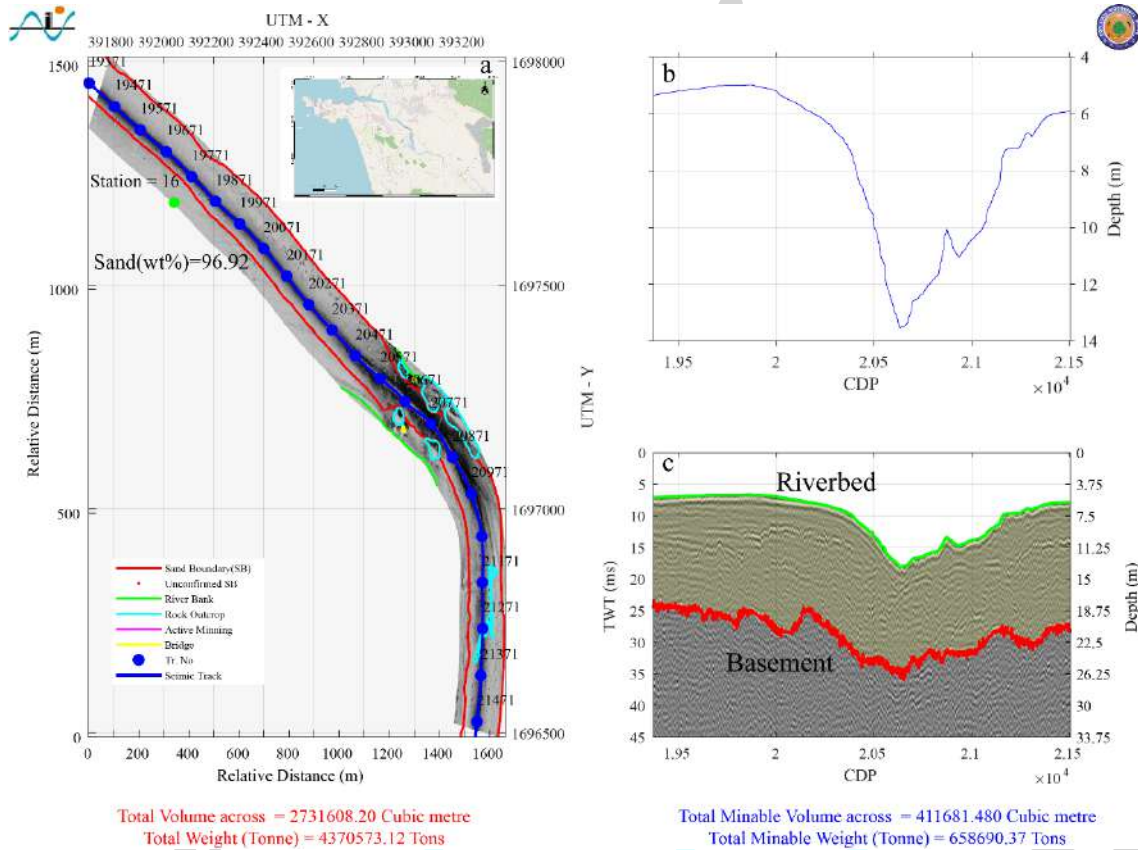


Figure 14. Geophysical data across Borim bridge. (a) Side scan sonar (SSS) image (b) single beam echosounder bathymetry. (c) high resolution seismic data

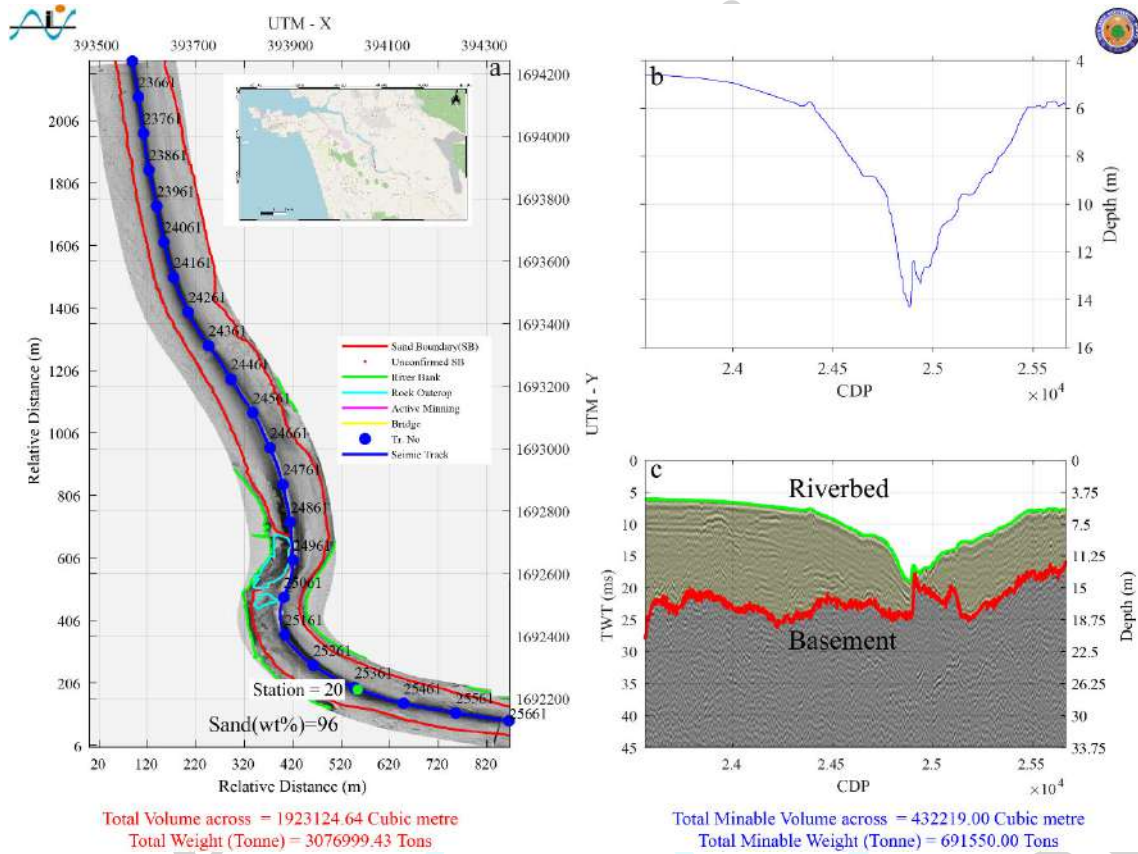


Figure 15. Rachol-Shiroda ferry point geophysical data. (a) Side scan sonar (SSS) image (b) single beam echosounder bathymetry. (c) high resolution seismic data

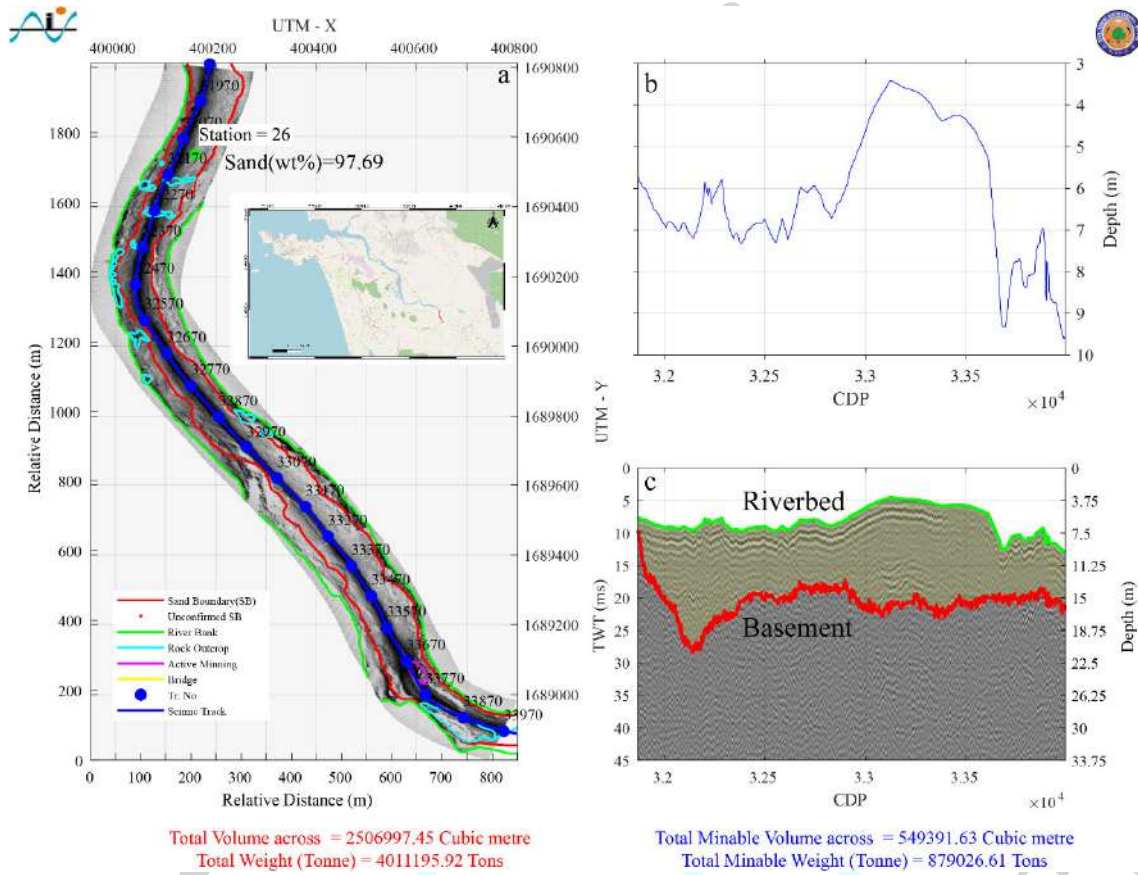


Figure 16. Geophysical data across Chandor-Ponchavadi region. (a) Side scan sonar (SSS) image (b) single beam echosounder bathymetry. (c) high resolution seismic data

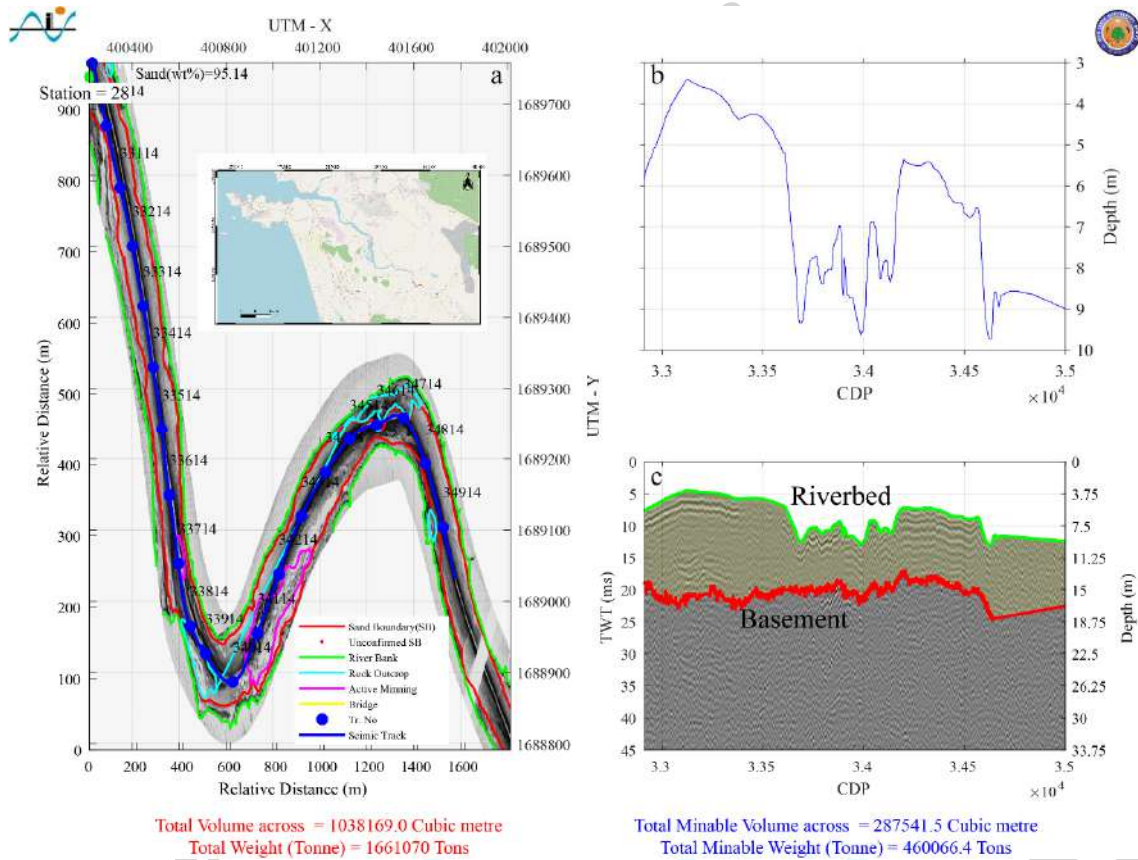


Figure 17. Geophysical data across Ponchavadi-Xelvona region, Navelim. (a) Side scan sonar (SSS) image (b) single beam echosounder bathymetry. (c) high-resolution seismic data

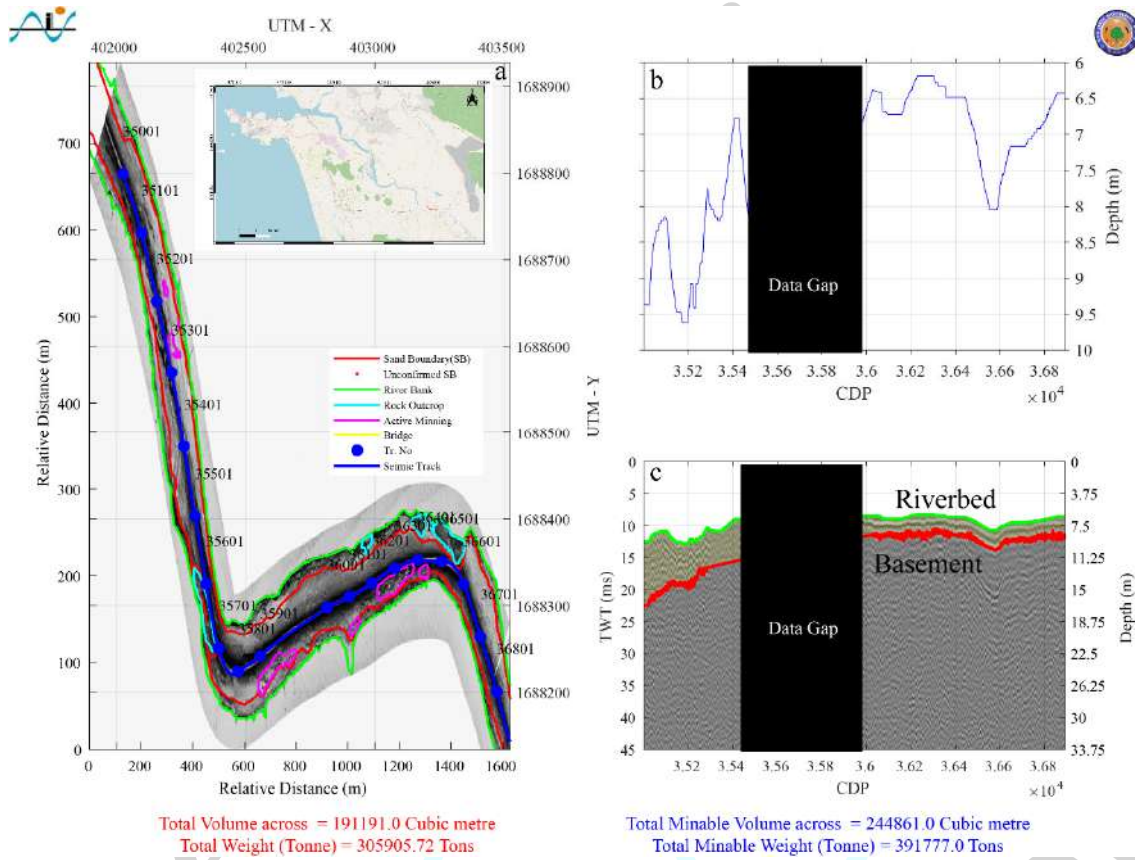


Figure 18. Geophysical data across the Ponchavadi-Curchorem region. (a) Side scan sonar (SSS) image (b) single beam echosounder bathymetry. (c) high-resolution seismic data

Chapter 5. Geological Observations

Material and Methods

A total of fifty-five (55) surface sediment samples (uppermost 5 cm) covering several parts of Zuari River were collected using a Van Veen grab sampler (Fig.21). Samples were packed in containers and stored at CSIR-NIO's sample storage repository. The samples are used for Salinity (PPT), pH, Chloride (PPM), sediment nomenclature (grain size through sieving analysis), and microscopic observations for grain sorting, mineral composition, and grain angularity.

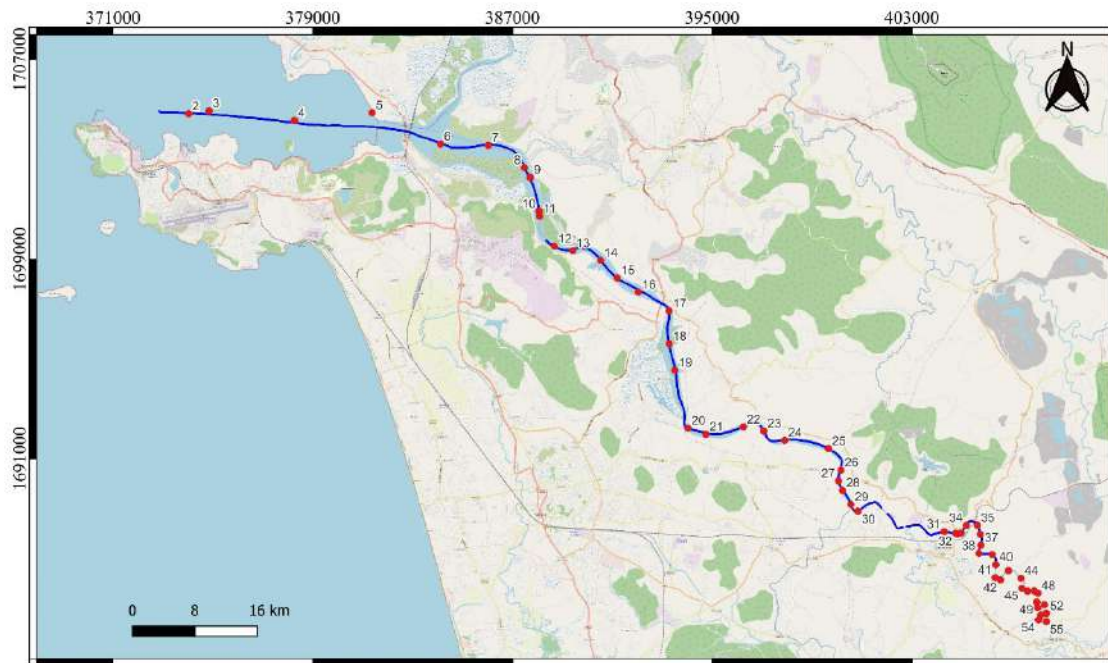


Figure 19. Geological Sample Locations

Sediment Nomenclature

Nomenclature of Zuari River sediment samples were done following standard Rock-Color Chart prepared by the Rock-Color Chart Committee (*representing the U.S. Geological Survey, GSA, the American Association of Petroleum Geologists, the Society of Economic Geologists, and the Association of American State Geologists*). The rock color chart for selected stations is provided in Table 2.

Sieve Size analysis

As per IS 650 requirement, bulk sediment samples of about 50 g were dried, weighed, and wet-sieved for 20 mins with an automated sieve shaker (Fritsch Analysette) creating following sieved fractions $> 2000 \mu\text{m}$, $1600 - 2000 \mu\text{m}$, $1000 \mu\text{m} - 1600 \mu\text{m}$, $850 \mu\text{m} - 1000 \mu\text{m}$, $500 \mu\text{m} - 850 \mu\text{m}$, $200 \mu\text{m} - 500 \mu\text{m}$, and $90 \mu\text{m} - 200 \mu\text{m}$. Cumulative percentage passing (%) for four stations were calculated following ASTM standards (Table 3). Weight percentage of sand ($> 63 \mu\text{m}$), silt ($4 \mu\text{m} - 63 \mu\text{m}$) and clay ($< 4 \mu\text{m}$) in Zuari river sediments are presented in Table 4.

Geo-Morphological studies for Zuari River - 2022

Results

Moderately-well sorted, fine-medium-coarse grained sand is found in majority of the sediment samples from Zuari River. The bulk sediment grain size in most of the samples is dominated by sand fraction. In general, sand content in Zuari River sediments ranges between 57.15 - 99.22 (wt %), silt content ranges between 0.0 – 40.0 (wt %), and clay content ranges between 0.0 - 15.87 (wt %) (Table 4).

Sampling Station No	Colour	Rock Colour Chart	Sorting
1	Moderate yellowish brown	10YR 5/4	Moderately sorted
16	Moderate brown	5YR 4/4	Moderately sorted
36	Moderate yellowish brown	10YR 5/4	Poorly sorted to moderately sorted
55	Moderate brown	5YR 4/4	Moderately sorted

Table 2. Nomenclature of Zuari River (Pre-monsoon) sand samples were done by following standard Rock-Color Chart prepared by the Rock-Color Chart Committee (representing the U.S. Geological Survey, GSA, the American Association of Petroleum Geologists, the Society of Economic Geologists, and the Association of American State Geologists)

Table 3. Cumulative percentage of passing of Zuari River sediment samples as per IS 650 requirements

Stn. No	Latitude	Longitude	Sieve Size (mm)	Sieve Size (µm)	Cumulative percentage passing (%)
1	15°25'13.17" N	73°48'44.42" E	2	2000	100
			1.6	1600	100
			1	1000	99.92
			0.85	850	99.92
			0.5	500	99.22
			0.2	200	96.5
			0.09	90	76.68
16	15°21'12.89" N	73°59'39.08" E	2	2000	100
			1.6	1600	100
			1	1000	99.92
			0.85	850	99.92
			0.5	500	80.66
			0.2	200	53.84
			0.09	90	44.2
35	15°16'10.63" N	74° 07'15.66 " E	2	2000	100
			1.6	1600	100
			1	1000	99.4

Geo-Morphological studies for Zuari River - 2022

			0.85	850	99.4
			0.5	500	98.84
			0.2	200	97.84
			0.09	90	94.3
55	15°14'05.52" N	74°08'48.97" E	2	2000	42.18
			1.6	1600	41.78
			1	1000	24.82
			0.85	850	24.38
			0.5	500	9.7
			0.2	200	5.86
			0.09	90	5.04

Table 4. Weight percentage of sand, silt, and clay fractions in Zuari River sediments

STATION NO.	LATITUDE	LONGITUDE	Sand (Wt.%)	Silt (Wt.%)	Clay (Wt.%)
1	15.419966 N	73.820136 E	96.91	2.25	0.00
2	15.417321 N	73.826015 E	77.02	15.48	5.49
3	15.418388 N	73.833639 E	94.41	4.80	0.00
4	15.415066 N	73.865525 E	76.23	13.09	7.84
5	15.41804 N	73.894483 E	82.21	16.08	0.00
6	15.406829 N	73.920026 E	78.00	15.99	2.45
7	15.406429 N	73.937903 E	94.37	2.53	0.00
8	15.398417 N	73.951419 E	89.20	9.97	0.00
9	15.394908 N	73.953598 E	71.33	26.70	0.00
10	15.382602 N	73.956994 E	80.42	15.90	0.00
11	15.380866 N	73.957203 E	82.36	15.75	0.00
12	15.369993 N	73.962750 E	97.69	0.80	0.00
13	15.368445 N	73.969667 E	97.40	0.72	0.00
14	15.364991 N	73.980007 E	98.65	0.95	0.00
15	15.358658 N	73.986383 E	96.91	1.40	0.00
16	15.353576 N	73.994187 E	96.92	3.02	0.00
17	15.346771 N	74.005727 E	96.12	2.80	0.00
18	15.334901 N	74.005815 E	97.89	0.05	0.00
19	15.325346 N	74.007927 E	92.56	5.37	0.00
20	15.304355 N	74.012943 E	NO SAMPLE		
21	15.302155 N	74.019595 E	93.65	5.62	0.00
22	15.304885 N	74.033559 E	97.92	0.02	0.00
23	15.303400 N	74.041240 E	90.74	8.12	0.00
24	15.300097 N	74.049030 E	96.89	2.55	0.00
25	15.297163 N	74.065381 E	95.84	2.60	0.00
26	15.289411 N	74.070089 E	97.69	2.20	0.00
27	15.285503 N	74.069239 E	99.15	0.05	0.00
28	15.282075 N	74.070664 E	95.14	4.05	0.00

Geo-Morphological studies for Zuari River - 2022

29	15.276971 N	74.073880 E	98.59	0.85	0.00
30	15.274536 N	74.076459 E	93.92	5.07	0.00
31	15.267268 N	74.108706 E	97.02	2.95	0.00
32	15.266687 N	74.113011 E	97.29	2.37	0.00
33	15.266787 N	74.115052 E	94.34	4.84	0.00
34	15.269594 N	74.116977 E	57.15	24.61	15.87
35	15.269631 N	74.121018 E	87.36	12.48	0.00
36	15.26635 N	74.122170 E	83.46	15.90	0.00
37	15.262439 N	74.122392 E	94.72	4.82	0.00
38	15.259475 N	74.121714 E	97.39	1.55	0.00
39	15.259076 N	74.126658 E	97.89	2.10	0.00
40	15.255422 N	74.127988 E	94.87	3.47	0.00
41	15.250715 N	74.127788 E	97.62	2.00	0.00
42	15.249918 N	74.129793 E	58.67	40.00	0.00
43	15.253267 N	74.132721 E	91.01	7.99	0.00
44	15.250521 N	74.137417 E	99.22	0.00	0.00
45	15.246962 N	74.137703 E	93.61	4.80	0.00
46	15.245856 N	74.139838 E	95.16	4.07	0.00
47	15.245986 N	74.142300 E	98.83	1.10	0.00
48	15.245132 N	74.143749 E	95.13	3.30	0.00
49	15.241944 N	74.143347 E	97.24	2.55	0.00
50	15.239885 N	74.143679 E	99.19	0.00	0.00
51	15.240966 N	74.146140 E	87.13	12.20	0.00
52	15.237808 N	74.146905 E	96.62	0.85	0.00
53	15.237224 N	74.144904 E	99.02	0.00	0.00
54	15.23548 N	74.144026 E	93.69	3.30	0.00
55	15.234868 N	74.146935 E	94.38	4.07	0.00

Microscopic Analysis of geological samples of Zuari

Methodology

Sand samples collected along the river course were air-dried and subsequently treated with 20 ml oxalic acid (0.055M; pH = 0.34) overnight to remove Fe-oxide coatings from the mineral grains. Then the oxalic acid was decanted, and the residual solid was repeatedly washed properly with Mili-Q water and dried for microscopic observation. A Leica M205 C microscope was used for the observation. The photomicrographs are attached (Station 1 to 55).

Salinity and pH

Salinity and pH of the sand samples were measured by using a refractometer (Cole Parmer) and pH meter (Eutech, pH Testr 20), respectively. 5g of air-dried sediment samples were washed three times with 25 ml Mili-q water. Salinity and pH were measured for each wash. Refractometer is calibrated by using Milli-Q and pH meter calibrated by using buffer solution of pH values 4, 7, and 10.

Results

1. The pH value of most of the samples are above 7 and observed variation in pH after washing maybe because of the leaching out of carbonates and bicarbonate. In station 30, pH value less than 4 after first wash and after second wash it showed ~ 6 which may indicate the carbonate and bicarbonate abundance (*Table 5*).
2. River mouth locations (Station 1 -10) contain very fine sand ($\sim 0.05 \text{ mm}$) and shell fragments, grain size increases gradually going to the river head locations (Station 20-30) $\sim 2 \text{ cm}$.
3. Most of the stations contain quartz, iron oxides and weathered rock fragments rich in iron (*Table 6*).
4. The pH of most of the samples is less than seven after the first wash, which indicates the acidic nature of the samples. Second and third washing makes the leaching out of carbonate and bicarbonate.
5. Micro-photographic images show that all grains are very large and rich in iron, particularly in station six samples.
6. Most of the stations quartz and iron oxides are more and large.

Table 5. The pH and salinity variation of the sand samples for 3stage fresh water washing

Stations	First wash		Second Wash		Third Wash	
	pH	Salinity	pH	Salinity	pH	Salinity
1	7.84	0	8.1	0	8.32	0
2	8.23	0	8.38	0	9.08	0
3	8.7	0	8.81	0	9.52	0
4	8.81	0	9.06	0	9.12	0
5	9.38	0	9.3	0	9.33	0
6	8.52	1	8.7	0	8.96	0
7	8.34	0	8.64	0	8.42	0
8	7.63	0	8.26	0	8.32	0
9	6.46	0	7.18	0	7.42	0
10	6.79	0	6.86	0	7.34	0
11	6.83	0	7.13	0	7.1	0
12	7.74	0	8.24	0	8.8	0
13	7.47	0	7.82	0	7.89	0
14	7.33	0	7.92	0	7.88	0
15	7.7	0	7.94	0	8.52	0
16	7.68	0	8.09	0	8.79	0
17	7.23	0	7.32	0	7.8	0
18	7.44	0	7.74	0	7.86	0
19	7.38	0	7.14	0	7.72	0
20	7.5	0	7.34	0	7.44	0
21	7.63	0	7.92	0	7.53	0
22	7.11	0	7.16	0	7.55	0
23	7.05	0	7.27	0	7.42	0
24	7.61	0	7.65	0	7.8	0
25	7.26	0	6.96	0	7.12	0

Geo-Morphological studies for Zuari River - 2022

26	7.53	0	7.46	0	8.18	0
27	7.47	0	7.99	0	7.82	0
28	7.3	0	7.42	0	7.35	0
29	6.89	0	7.29	0	7.24	0
30	3.6	0	6.06	0	7.08	0
31	7.62	0	7.32	0	7.4	0
32	6.95	0	7.18	0	7.50	0
33	7.01	0	6.72	0	6.74	0
34	6.53	0	6.23	0	6.45	0
35	6.6	0	6.72	0	7.42	0
36	6.96	0	7.05	0	6.96	0
37	5.81	0	6.08	0	6.16	0
38	6.76	0	7.31	0	7.38	0
39	6.3	0	6.55	0	6.63	0
40	7.14	0	7.28	0	7.36	0
41	7.04	0	7.41	0	7.44	0
42	7.12	0	7.04	0	7.26	0
43	7.1	0	7.2	0	7.33	0
44	6.94	0	7.12	0	7.24	0
45	6.7	0	7.01	0	7.18	0
46	5.25	0	5.67	0	5.95	0
47	6.09	0	6.48	0	6.63	0
48	6.66	0	5.97	0	6.18	0
49	6.74	0	7.34	0	7.62	0
50	6.88	0	7.05	0	7.13	0
51	6.96	0	7.16	0	7.29	0
52	7.1	0	6.85	0	7.08	0
53	7.33	0	7.52	0	7.63	0
54	6.41	0	6.13	0	7.04	0
55	6.07	0	7.08	0	7.24	0

Geo-Morphological studies for Zuari River - 2022

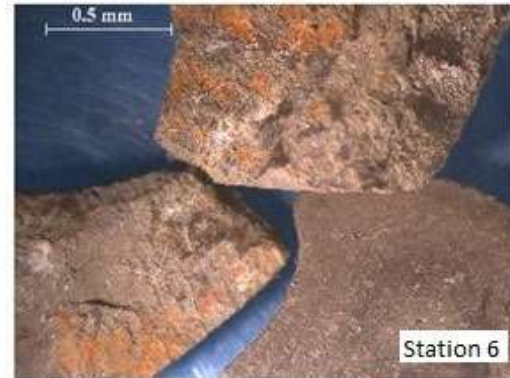
Table 6. Grain size variation from microscopic analysis of dry sediment samples data

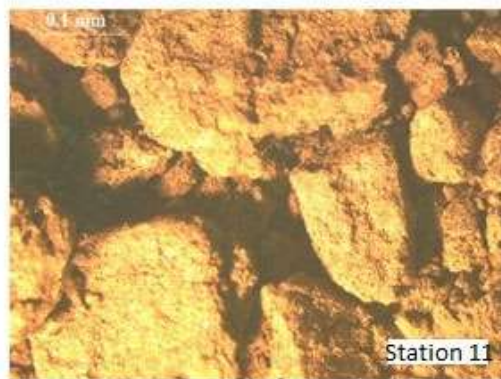
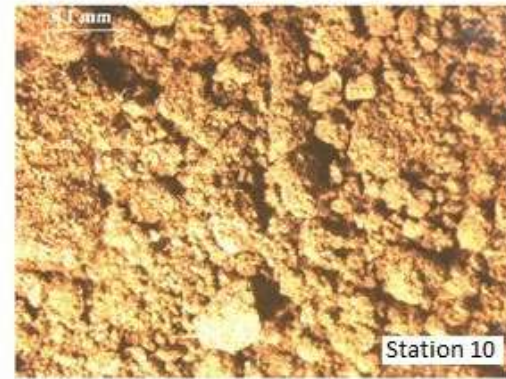
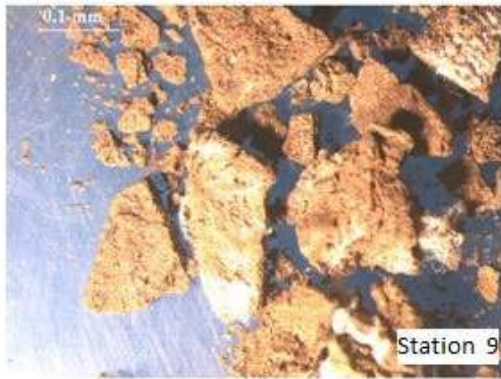
Zuari River	Large grain size (mm)	Small grain size (mm)	Remarks
Station 1	-	-	Quartz rich very fine sand
Station 2	-	-	Quartz rich very fine sand
Station 3	0.06	0.01	Iron oxides, quartz and phyllite
Station 4	0.03	0.01	Iron oxides, quartz, wood fragments, and phyllite
Station 5	0.03	0.01	Iron oxides, quartz, shell fragments and phyllite
Station 6	-	-	Iron rich very fine sand
Station 7	0.12	0.02	Iron oxides and quartz
Station 8	0.12	0.01	Iron oxides, quartz, and rock fragments
Station 9	-	-	Very fine sand with iron oxides
Station 10	-	-	Very fine sand
Station 11	-	-	Very fine sand
Station 12	0.14	0.015	Quartz, rock fragments and lot of iron oxides
Station 13	0.012	0.005	Iron oxides, quartz, phyllite, wood fragments & well sorted grains
Station 14	0.122	0.01	Iron oxides, quartz, wood fragments & well sorted grains
Station 15	0.04	0.01	Iron oxides, quartz, shell fragments
Station 16	0.05	0.012	Well sorted iron oxides, quartz, rock & wood fragments
Station 17	0.012	0.005	Iron oxides, quartz, phyllite, wood fragments & well sorted grains
Station 18	0.07	0.007	Quartz, rounded to semi rounded iron oxides and phyllite
Station 19	0.012	0.005	Iron oxides, quartz, phyllite, wood fragments & well sorted grains
Station 20	13	0.02	Iron oxides, quartz, rock fragments and poor sorting
Station 21	0.07	0.02	Iron oxides, quartz, shell fragments and well sorted
Station 22	0.04	0.012	Well sorted iron oxides, quartz, and phyllite
Station 23	0.03	0.02	Iron oxides, quartz, and rock fragments
Station 24	0.07	0.02	Iron oxides, quartz, phyllite, wood, shell, and rock fragments
Station 25	23	0.08	Iron oxides, quartz and rock fragments, very poor sorting
Station 26	17	0.02	Iron oxides, quartz and rock fragments, very poor sorting
Station 27	25	0.02	Iron oxides, quartz, rock and shell fragments, very poor sorting
Station 28	30	0.02	Iron oxides, quartz, phyllite, and rock fragments, very poor sorting
Station 29	20	0.03	Iron oxides, quartz, phyllite, and rock frag-

Geo-Morphological studies for Zuari River - 2022

			ments, very poor sorting
Station 30	10	0.015	Iron oxides, quartz, phyllite and rock, shell and wood fragments, poor sorting
Station 31	23	0.035	Quartz, iron oxides, phyllite, and rock fragments
Station 32	30	7	Iron oxides and quartz
Station 33	20	0.03	Iron oxides, quartz, and rock fragments
Station 34			Very fine sand rich in iron
Station 35	20	9	Iron oxides, quartz, and wood fragments
Station 36			Phyllite rich in iron
Station 37	30	0.04	Iron oxides and quartz
Station 38	20	0.14	Iron oxides, quartz, and rock fragments
Station 39	53	23	Quartz
Station 40	30	3	Weathered grains of quartz, iron oxides and rock fragments
Station 41	20	0.05	Weathered grains of quartz, iron oxides
Station 42	32	32	Quartz
Station 43	25	6	Iron oxides and quartz
Station 44	55	2	Iron oxides, quartz, and rock fragments
Station 45	35	0.1	Weathered grains of quartz, iron oxides and wood fragments
Station 46	45	0.1	Including very fine sand grains and large grains of quartz and iron oxides
Station 47	23	2	Iron oxides, quartz, and rock fragments
Station 48	42	2	Iron oxides, quartz, and rock fragments
Station 49	35	20	Iron oxides, quartz
Station 50	20	4	Iron oxides, quartz, and rock fragments
Station 51	55	40	Iron oxides, quartz
Station 52	29	0.125	Quartz, iron oxides and weathered rocks
Station 53	40	15	Quartz, iron oxides and weathered rocks
Station 54	21	0.12	Quartz, iron oxides and weathered rocks
Station 55	25	0.12	Quartz, iron oxides and weathered rocks

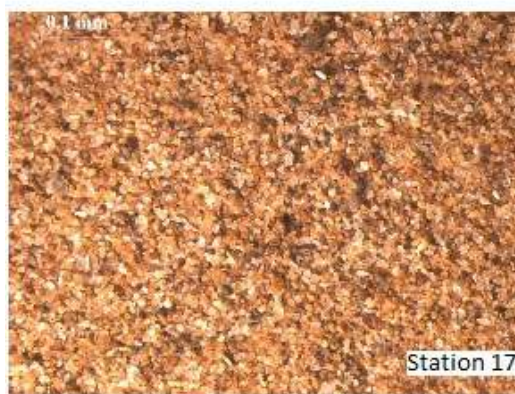
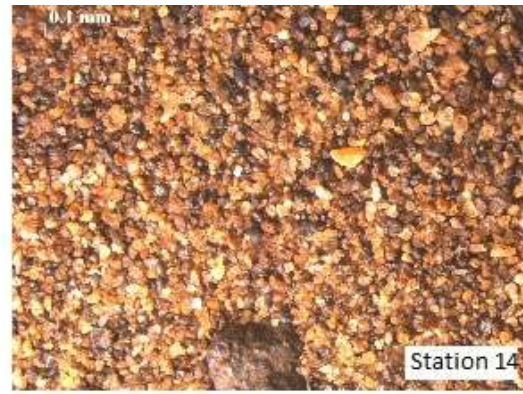
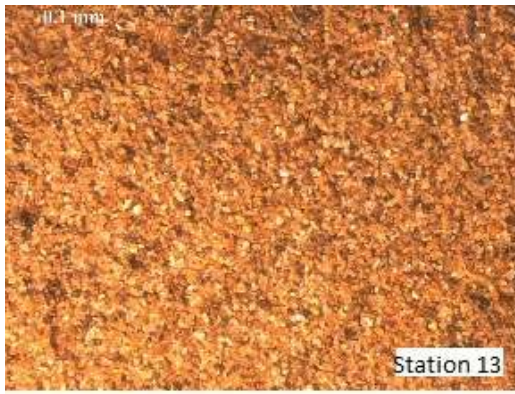
Table 7. Photomicrographic images of dry sediments





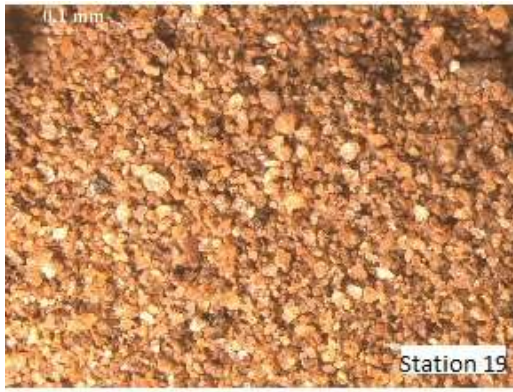
Survey Report

Geo-Morphological studies for Zuari River - 2022



Survey Report

Geo-Morphological studies for Zuari River - 2022



Survey Report

Geo-Morphological studies for Zuari River - 2022



Survey Report

Geo-Morphological studies for Zuari River - 2022



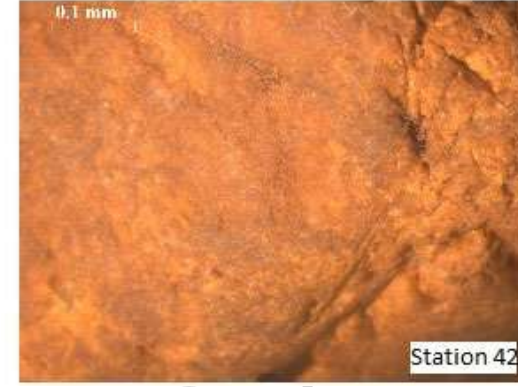
Survey Report

Geo-Morphological studies for Zuari River - 2022



Survey Report

Geo-Morphological studies for Zuari River - 2022



Survey Report

Geo-Morphological studies for Zuari River - 2022



Survey Report

Geo-Morphological studies for Zuari River - 2022



Chapter 6. Post-Monsoon Geophysical Survey

Geophysical data acquisition:

The post-monsoon geophysical data comprising side scan sonar (SSS), high resolution seismic (HRS), and single beam echo-sounding data was acquired in the Zuari river, to understand the post-monsoon geomorphological and subsurface variations. The analysis of these changes provides information about new deposition or erosion of riverbed as well as replenishment of mining zones.

Major features identified from the side scan sonar (SSS) imaging and high resolution seismic (HRS):

Riverbed morphology through the side scan sonar images is analyzed to infer the post-monsoon changes in riverbed geomorphology. Similarly, high-resolution seismic data are interpreted to infer post-monsoon variation in sediment thickness. The time-lapse study of SSS and HRS data acquired during the post-monsoon season (January 2022) and pre-monsoon season (January 2021) helps in demarcating regions of aggradation or erosion of the riverbed and replenishment of mining pits due to monsoonal activity.

Side Scan Sonar Interpretation

Side scan sonar data provide regional riverbed morphology, and a comparison of side scan sonograms between pre- and post-monsoon seasons may reveal information about the changes in riverbed morphology. Detailed analysis of SSS data acquired during pre- and post-monsoon seasons have been carried out to identify the variation in Zuari riverbed geomorphology due to monsoonal activity. Several geomorphological changes such as erosion and deposition of mid-channel/point bars, the disappearance of sandbar ripple marks and deposition of non-cohesive sediments, partial to complete washout of old mining pits, and signature of fresh mining pits at some locations are observed. Pre- and post-monsoon comparisons of geomorphological features in representative areas are presented in this report. Figures 20 to 28 highlight major geomorphological changes observed between Sanguem and Sanvordem. Figure 20 highlights the pre- and post-monsoon side scan sonograms across Sanguem Taluk near Taripanta playground: (A) shows sediment bars/lags deposits with ripple marks during the pre-monsoon period and (B) shows the same deposits after the monsoon. The absence of ripple marks and appearance of bedrock features indicates predominantly erosion of sediments in this region. Similarly, Figure 21A highlights a sediment bar along with rock outcrops/debris observed near Cotarli village in Sanguem Taluk (downstream Dando) and Figure 21B shows the same deposit after the monsoon. Again, a reduction in the sediment thickness and appearance of bedrock morphology are observed. The appearance of bedrock morphology shows substantial erosion of the sediments.

Figure 22 shows SSS images near to Vakerwada village of Sanguem Taluka: (A) depicts the presence of a thin sediment bar alongside rock outcrops during the pre-monsoon season and (B) depicts the same sediment bar after the monsoon. Some prominent ripple marks are observed which indicate an increase in the thickness of the sediment bar.

Geo-Morphological studies for Zuari River - 2022

Therefore, the region shows an aggradation of sediments. Figure 23 highlights SSS images near Muguli village of Sanguem Taluka: (A) depict the presence of a bank bar alongside rock outcrops and (B) shows a partially eroded sand bar after the monsoon indicating sediment erosion in the region. Figure 24 highlights pre- and post-monsoon SSS images acquired near Soliem Math of the Vodlemol-Cacora region: (A) depicts rock outcrops along the riverbanks and some point bars and (B) depicts eroded sediment bar towards Soliem Math and type-2 mining signature towards Muguli village. The thinning of the point and mid-channel bars indicates predominant erosion of sediments in this region. Figure 25 shows SSS images acquired near the Vodlemol-Cacora-Comproi region: (A) highlights sediment lag deposits during the pre-monsoon period and (B) shows the same deposits after the monsoon. The sediments are eroded, and bedrock is exposed in this region. Figure 26 highlights pre- and post-monsoon SSS images acquired near the Comproi village region: (A) shows some rocky outcrops at the riverbanks and (B) highlights some post-monsoon mining signature (type-2) near the riverbank. Figure 27 depicts pre- and post-monsoon side scan sonogram near Kamral-Comproi village region: (A) highlights sand mining signature of type-2 and some dumped sediment near the riverbanks and (B) shows complete obliteration of mining signature with some remains of dumped sediments near the banks. The obliteration of mining pits suggests sediment accumulation during the monsoon season. Figure 28 shows SSS images near the Kmaral-Sanvordem region: (A) highlights smooth riverbed and (B) shows the presence of rock outcrops after the monsoon season. The appearance of rocks indicates predominant erosion in this region.

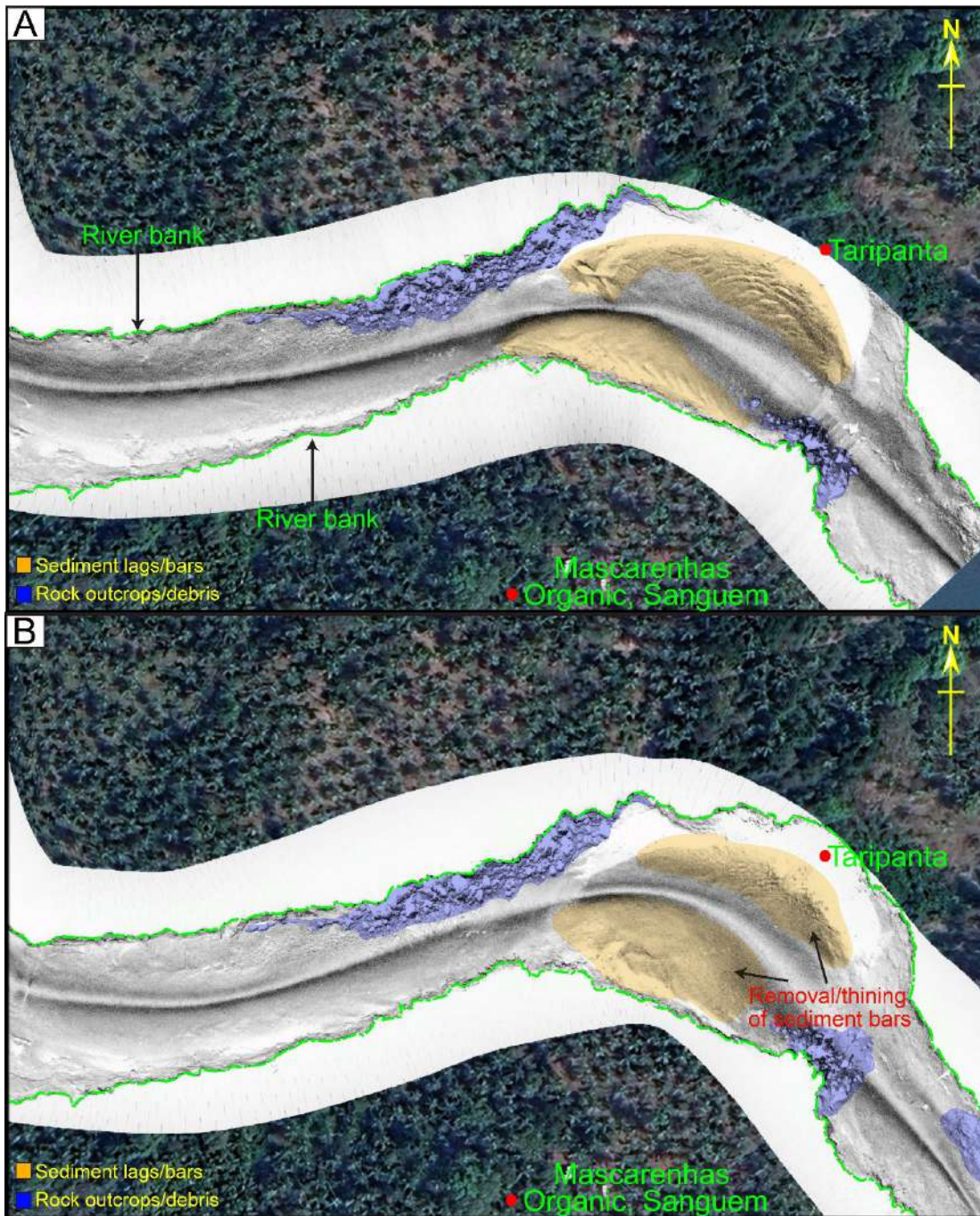


Figure 20. Side Scan Sonograms acquired near Taripanta playground and Mascarenhas organic farm during (A) pre-monsoon and (B) post-monsoon seasons. (A) highlights the presence of two sand bars and (B) shows the removal of sediment from the bars.

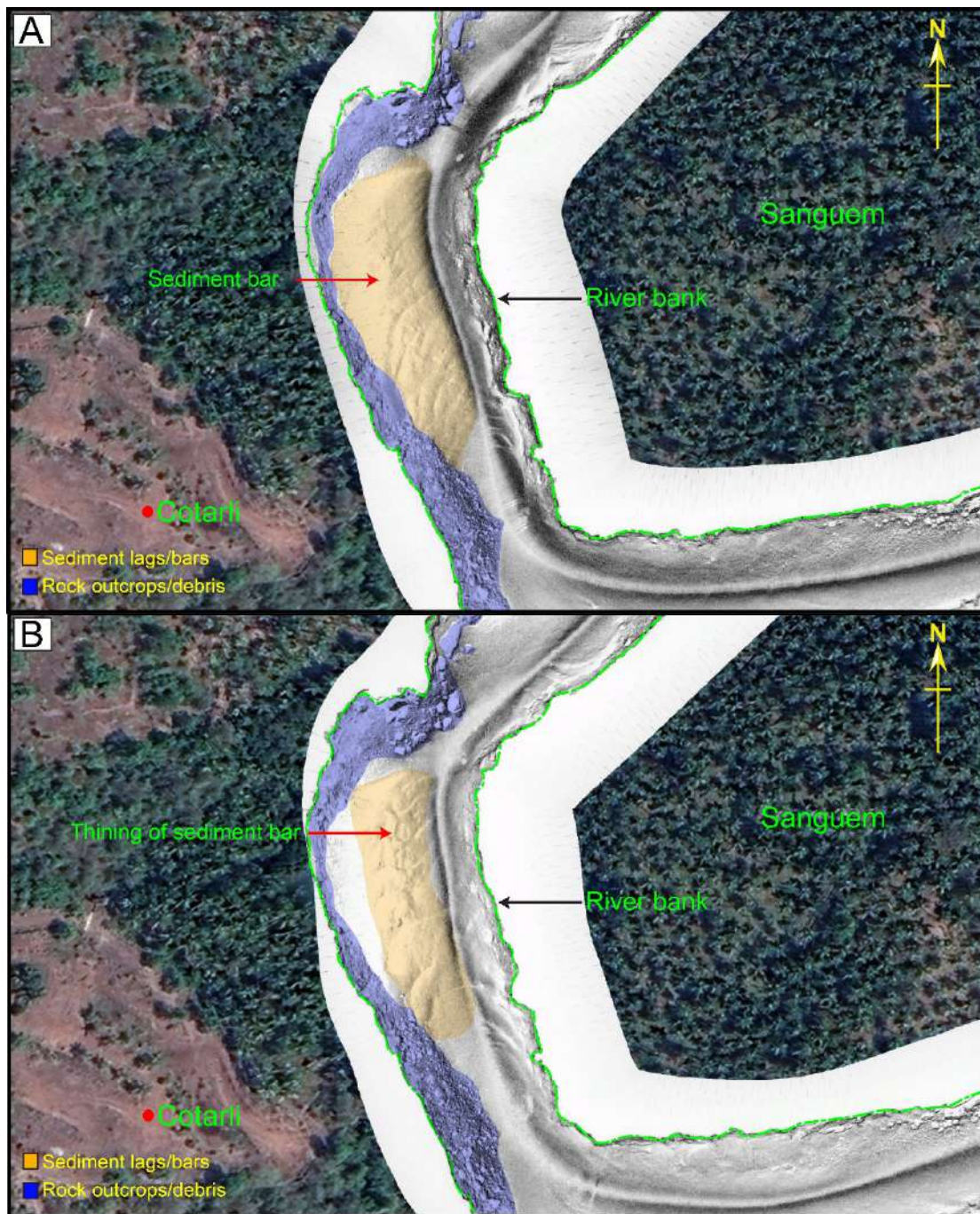


Figure 21. Side Scan Sonograms acquired near Cotarli village (A) pre-monsoon and (B) post-monsoon seasons. (A) primarily highlights the presence of a sediment bar and (B) highlights thinning of the sediment bar to an extent that the underlying bedrock morphology

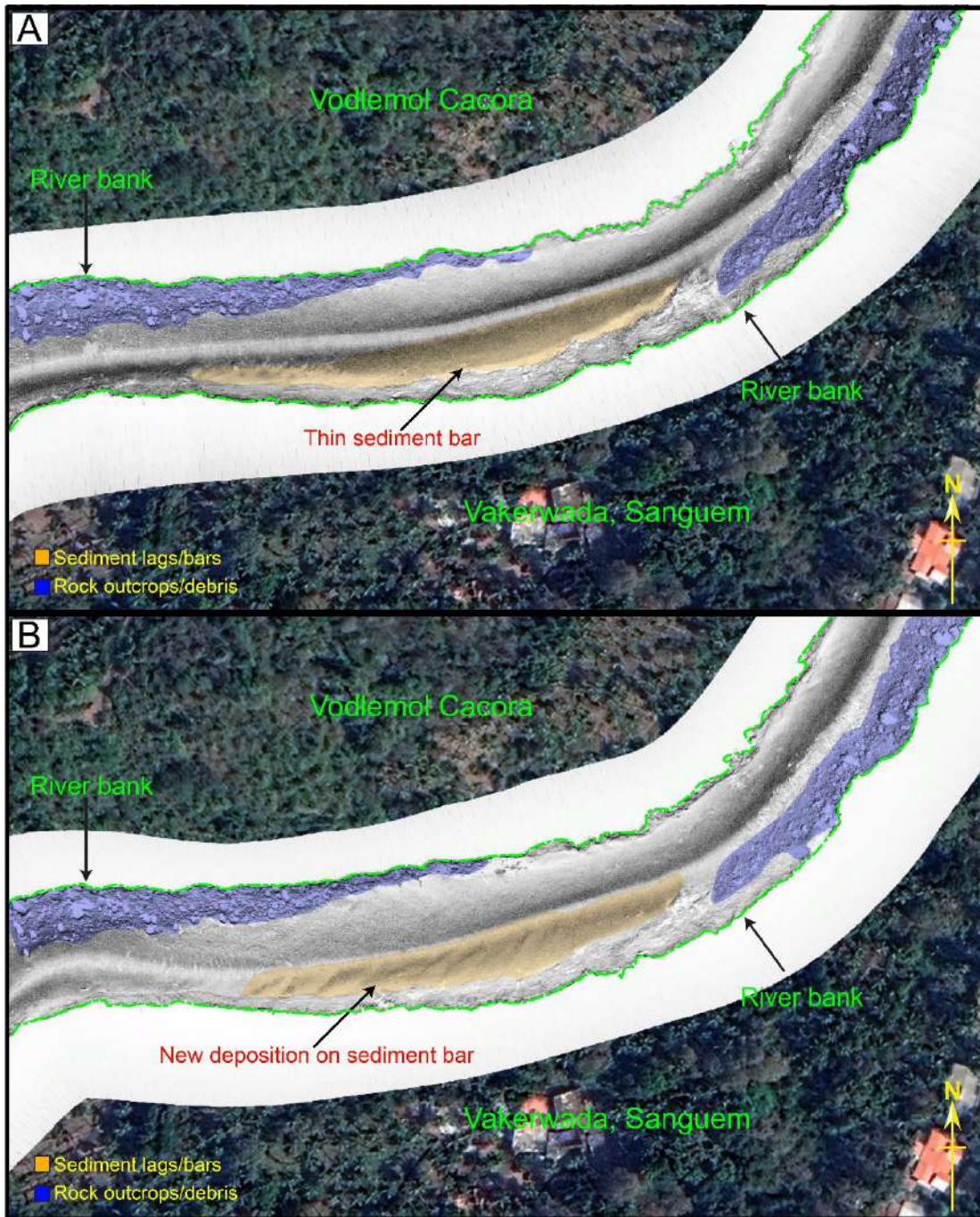


Figure 22. Side Scan Sonogram acquired near Vakerwada-Vodlemol-Cacora region during (A) pre-monsoon and (B) post-monsoon seasons. (A) highlights the presence of a thin sediment bar along with rock outcrop and debris and (B) highlights the thickening of the sediment bar.

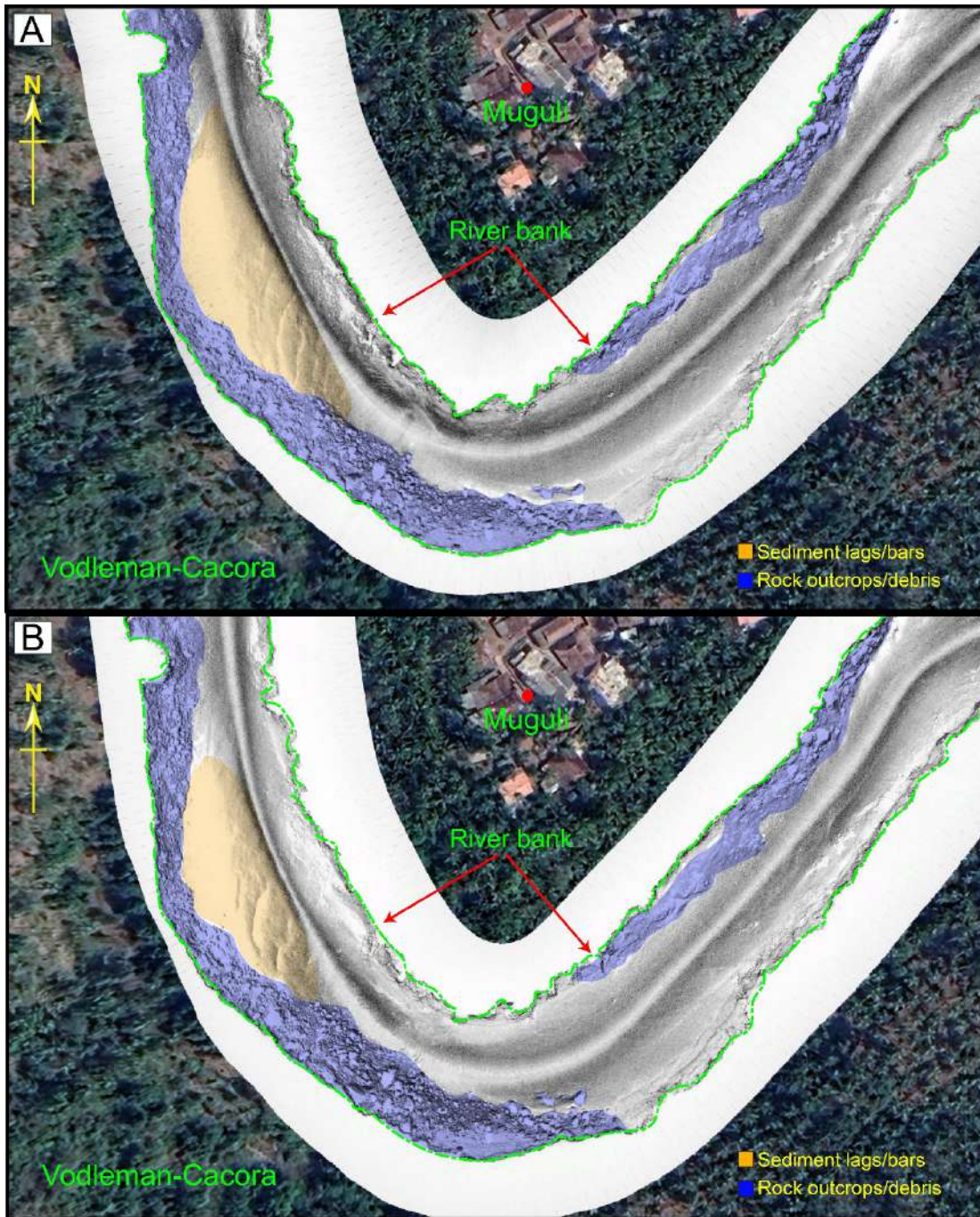


Figure 23. Side Scan Sonogram acquired near Muguli-Vodlemol-Cacora region during (A) pre-monsoon and (B) post-monsoon seasons. (A) Shows the presence of sediment along with rock outcrop and debris. (B) highlights partial erosion of the sand bar.

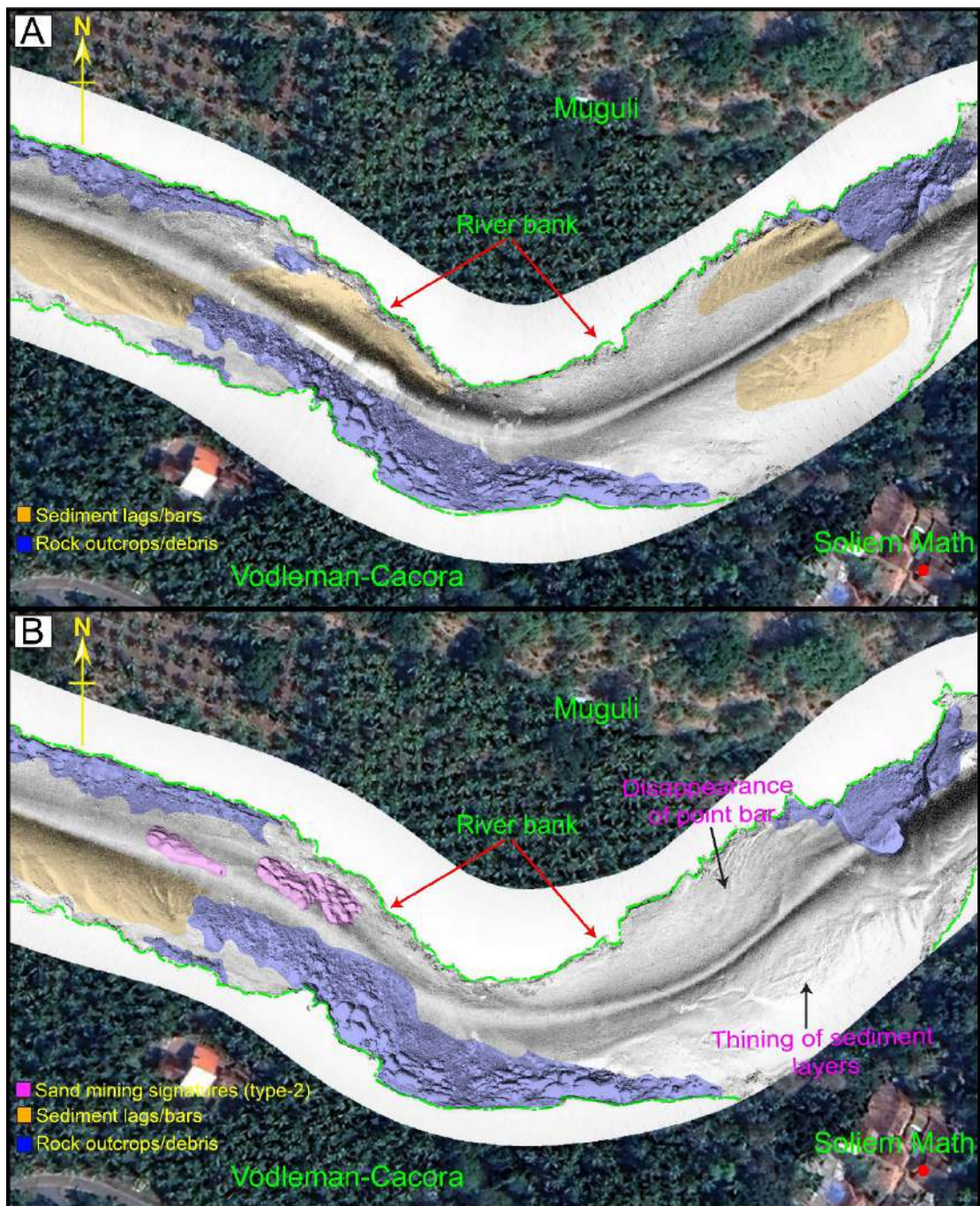


Figure 24. Side Scan Sonogram acquired near Muguli-Sollem math region during (A) pre-monsoon and (B) post-monsoon seasons. (A) Shows presence of thin mid-channel bars (B) highlights partial erosion of point bars and thinning of the mid-channel bar and the presence of type-2 sand mining signatures.

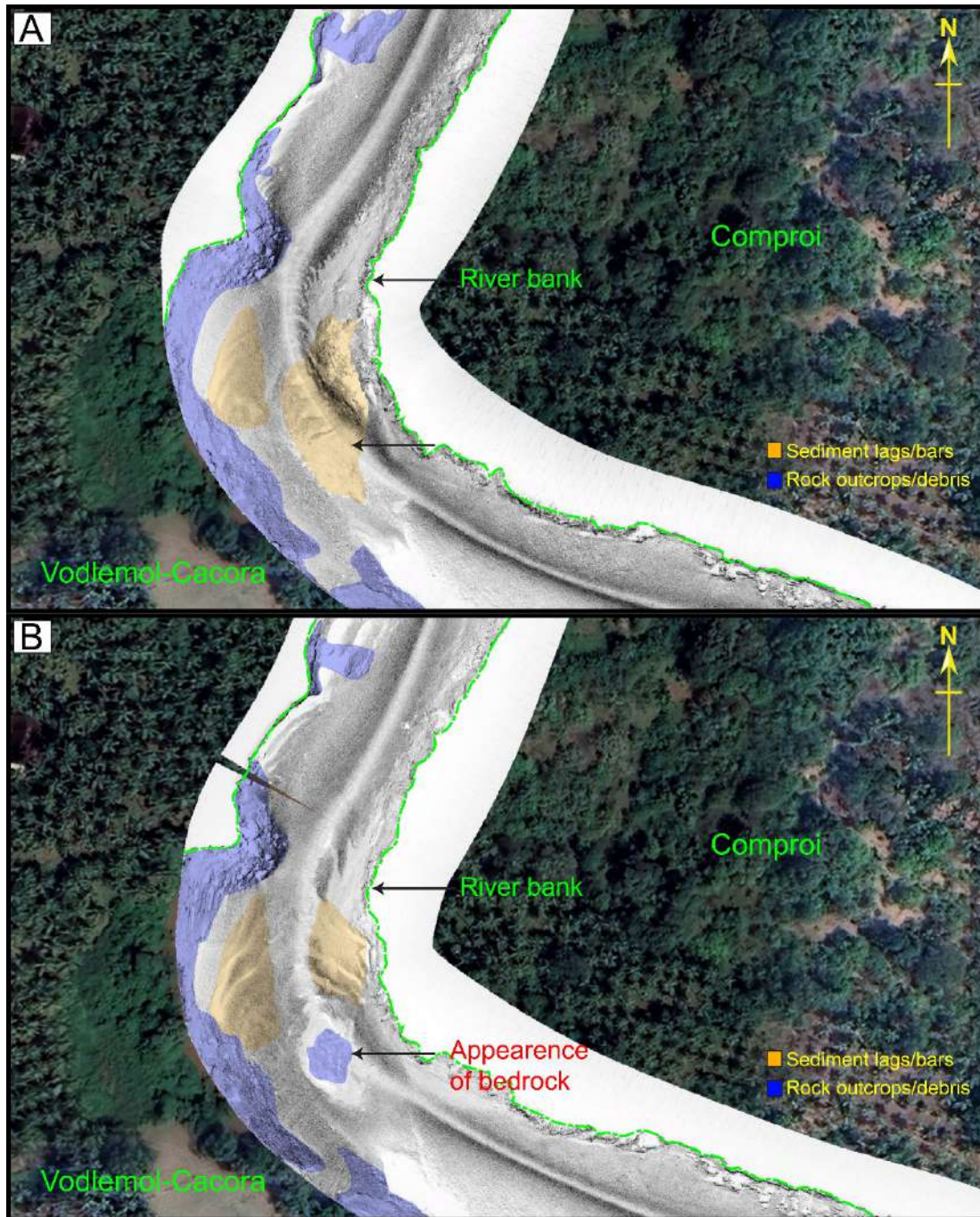


Figure 25. Side Scan Sonogram acquired near Comproi-Vodlemol-Cacora region during (A) pre-monsoon and (B) post-monsoon seasons. The sonograms highlight thinning of mid-channel bars and the appearance of bedrock after the monsoon.

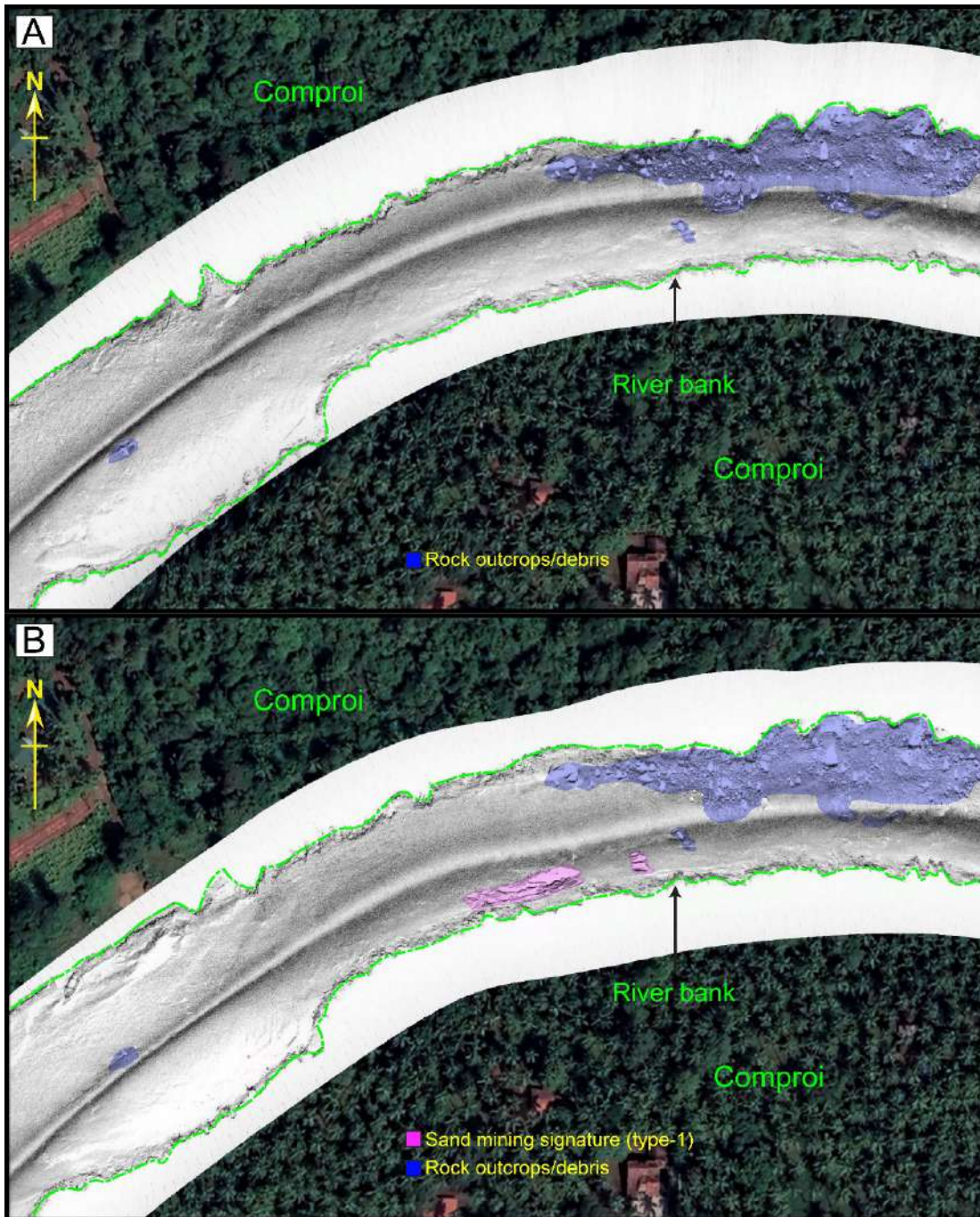


Figure 26. Side Scan Sonogram acquired near Comproi region during (A) pre-monsoon and (B) post-monsoon seasons. (A) highlights riverbed morphology along with rock outcrops and debris at the bank. (B) highlights the presence of sand mining signature of type-2.

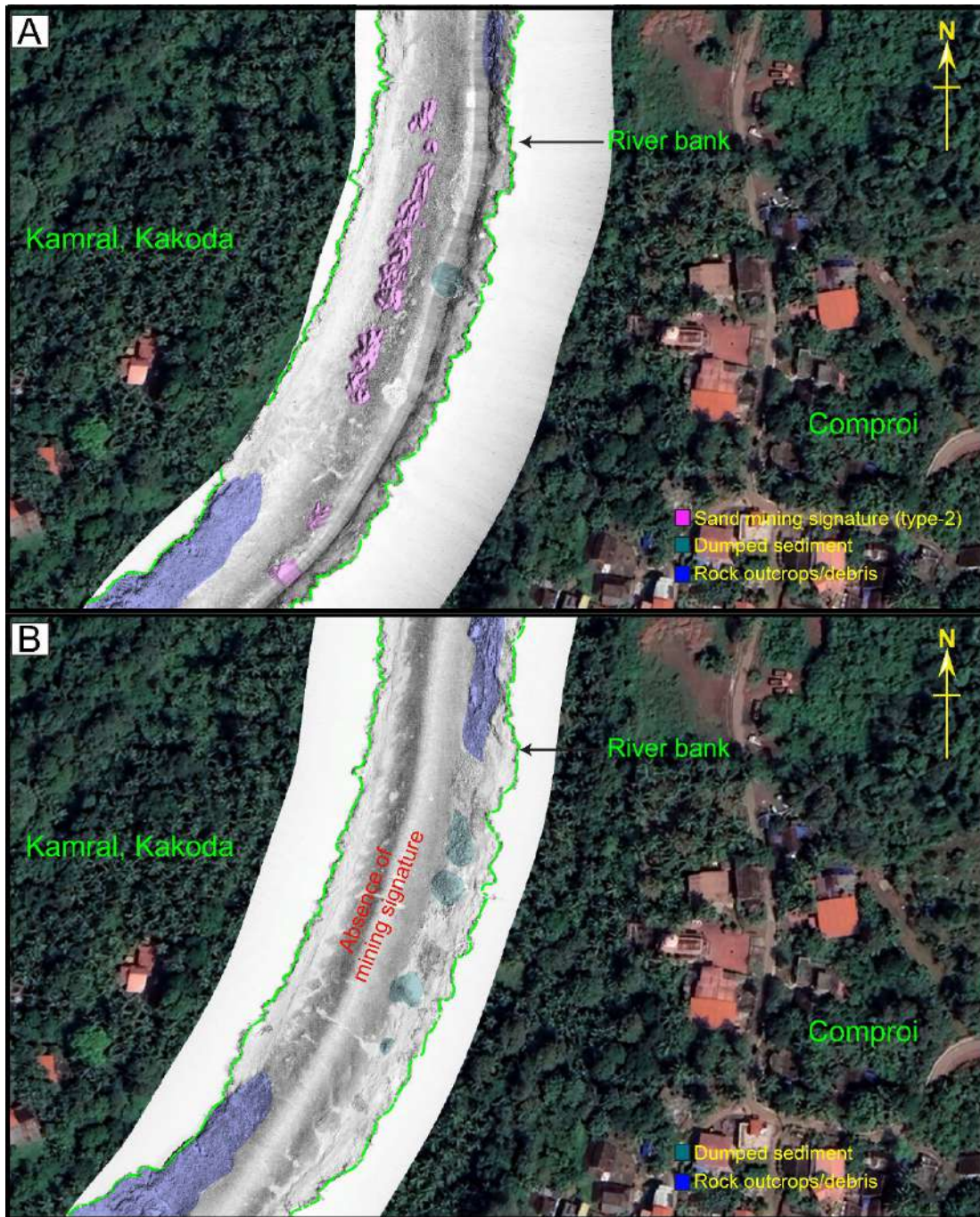


Figure 27. Side Scan Sonogram acquired near Kamral-Comproi region during (A) pre-monsoon and (B) post-monsoon seasons. (A) highlights the presence of sand mining signatures and dumped residue sediment near the banks. (B) highlights obliteration of sand mining pits indicating sediment accumulation.



Figure 28. Side Scan Sonogram acquired near Sanvordem-Kamral (upstream Sanvordem bridge) region during (A) pre-monsoon and (B) post-monsoon seasons. (A) Highlights relatively smooth riverbed morphology. (B) highlights the presence of exposed bedrock indication erosion in this region.

Figures 29 to 39 highlight major morphological changes observed in side-scan sonograms between Sanvordem and Madkai-Verna region during pre- and post-monsoon seasons. Figure 29 shows the pre- and post-monsoon SSS images near the Sanvordem-Baag-Shirford region: (A) shows some drag marks of the pre-monsoon period and (B) highlights the obliteration of the drag marks and the presence of a new mid-channel bar/lag after the monsoon.

The disappearance of drag marks and the presence of a mid-channel bar suggest sediment accumulation and local redistribution of sediment in this region. Figure 30 highlights the pre- and post-monsoon SSS images near the Ponchavadi-Bag-Xelvona region: (A) shows the presence of a sand bar and thinly covered bedrock outcrop during the pre-monsoon period. It also shows the presence of type-2 sand mining signatures. Prominent drag marks are also observed near the sand bar. (B) shows the presence of the same bar and thinly covered rock outcrop along with fresh mining pits after the monsoon. The signature of drag marks is partially washed out and pre-monsoon mining pits are completely filled indicating sediment accumulation along with local redistribution. Figure 31 shows SSS images acquired near the Ponchavadi-Xelvona region: (A) highlights a mid-channel bar and some type-2 sand mining signatures of the pre-monsoon period. The sand mining starts from the downstream part of the mid-channel bar and extends further downstream towards the Kushawati confluence point. (B) shows the same bar after the monsoon. Partial filling of mining pits and thinning of mid-channel bar indicates predominantly local redistribution of the sediment in this region. Figure 32 highlights pre- and post-monsoon sonograms near the Ponchavadi-Chandor region between the Kushawati river and Guirdolim rivulet: (A) shows the presence of step-like features along the riverbank during the pre-monsoon period and (B) shows the same area after the monsoon. The region is devoid of any such features rather a thin layer of non-cohesive sediment is observed indicating sediment accumulation. Figure 33 depicts sonograms near the Ponchavadi-Chandor region (downstream Guirdolim rivulet confluence point): (A) shows pre-monsoon riverbed morphology highlighting sand bars at both the bank along with a few rock outcrops and (B) depicts the morphology of the same location after the monsoon. It shows the presence of sand mining signature at downstream Guirdolim's mouth and some sand bars. The bar towards the Guirdolim side has been thinned indicating a local redistribution of sediments. Figure 34 shows sonograms acquired near Mankem (Shiroda)-Macasana (Curtorim) region during (A) pre-monsoon and (B) post-monsoon seasons. (A) highlights the presence of a sediment ridge along with rough riverbed morphology caused by mining in the past. (B) highlights the same sediment ridge and some fresh mining signature after the monsoon. The old sand mining signatures are partially washed out and some fresh mining signatures of type-2 are observed indicating restricted local sediment redistribution and insufficient sediment supply. Also, the sediment ridge is observed at the same location during both seasons and may indicate the boundary between non-cohesive and cohesive sediments. Figure 35 shows the SSS images acquired near Soncrem (Shiroda) and Curtorim region: (A) highlights the presence of sand mining signature in the pre-monsoon period and (B) shows an anomalous enlargement of the same mining signature to ~35 m wide and ~84 m long pit. It also shows the presence of a mid-channel bar near this pit indicating a significant perturbation of the flow pattern at this location.

Figure 36 depicts the side scan sonar sonogram acquired near Socrem (Shiroda)-Ungirim (Curtorim) region during the (A) pre-monsoon and (B) post-monsoon seasons. (A) highlights the presence of thinly sedimented bedrock in this region and (B) shows type-1 sand mining signatures. The bedrock is not observed after the monsoon indicating sediment accumulation or local redistribution of sediments in this region. Figure 37 shows the SSS images acquired near Borim-Loutolim region during (A) pre-monsoon and (B) post-monsoon seasons. The sonograms show medium-to-large-sized ripple marks which do not change after the monsoon. The similarity of images indicates an absence of any major depositional or erosion or local sediment redistribution event in this region. Figures 38 and 39 show pre- and post-

monsoon sonograms near Durbhat-Verna and Madkai-Verna regions, respectively. Similar to the Borim-Loutolim region, no significant geomorphological changes are observed which indicates minimal deposition/erosion or sediment redistribution process in this region.

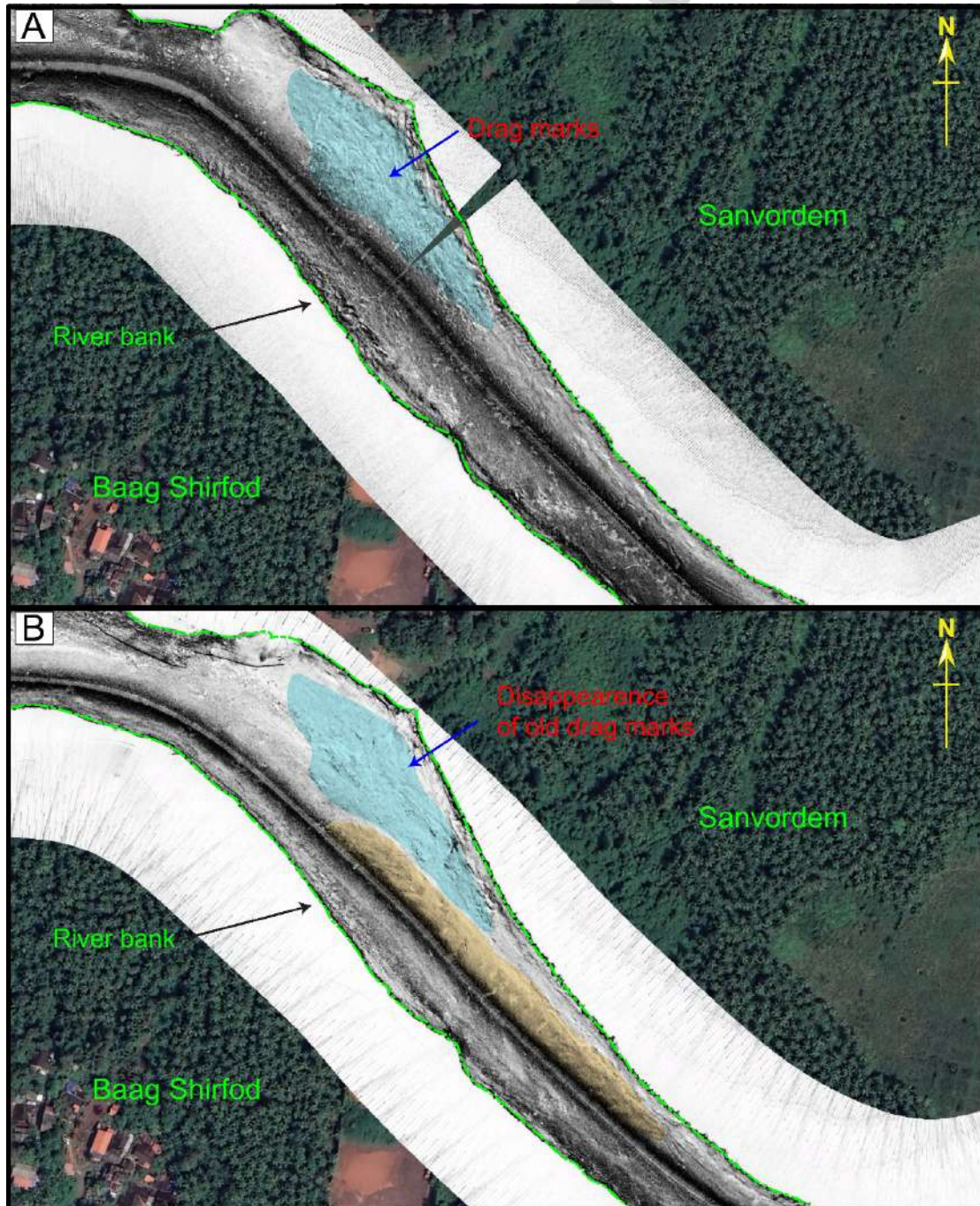


Figure 29. Side Scan Sonogram acquired near Sanvordem-Baag Shirfod (downstream Sanvordem bridge) region during (A) pre-monsoon and (B) post-monsoon seasons. (A) shows drag marks on the riverbed. (B) highlights the obliteration of drag marks and the presence of a mid-channel bar in the region.

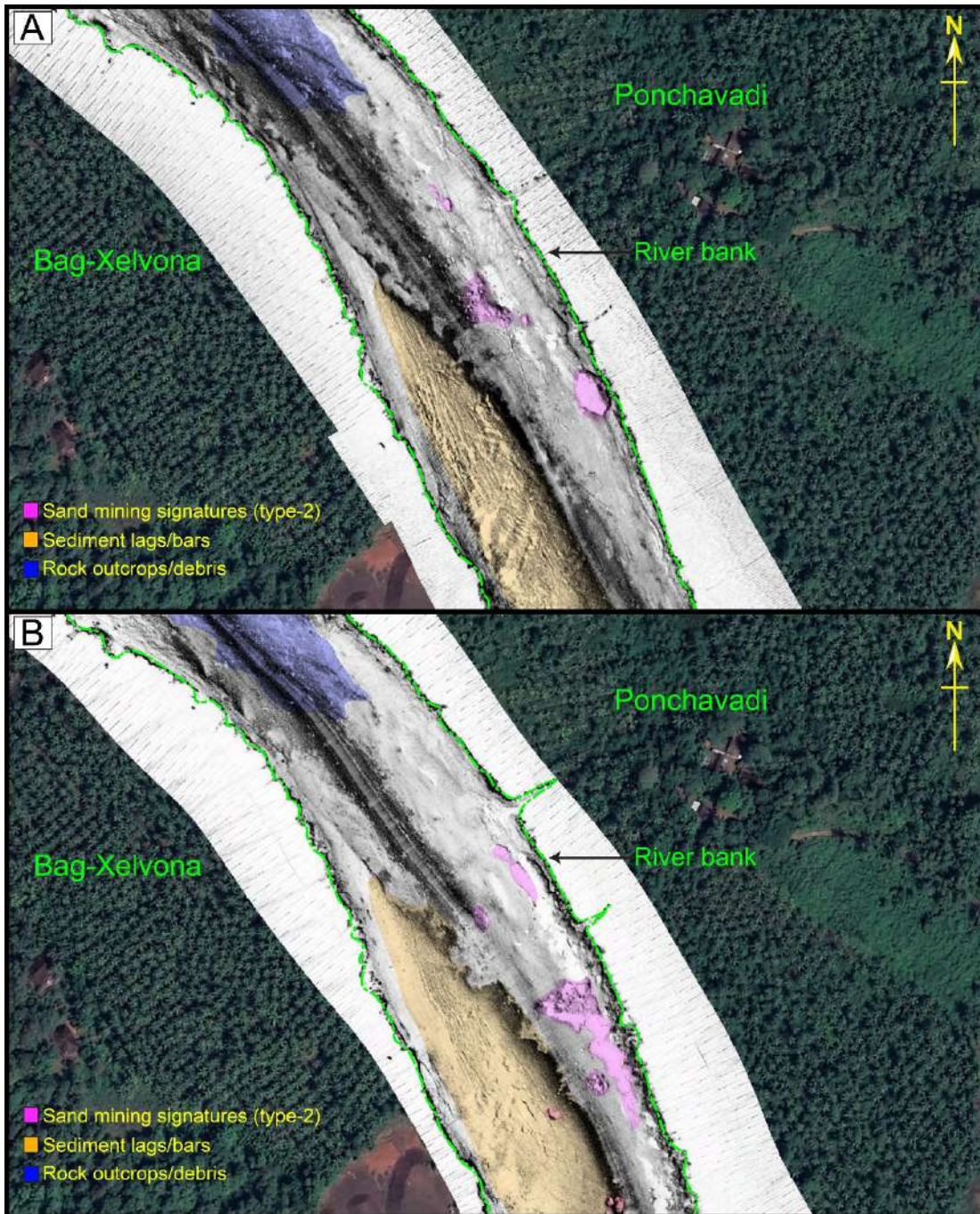


Figure 30. Side Scan Sonogram acquired near Ponchavadi-Bag-Xelvona region during (A) pre-monsoon and (B) post-monsoon seasons. (A) shows the presence of a sediment bar, type-2 sand mining signatures, and bedrocks. (B) shows an enlarged sediment bank bar at the same location and some fresh sand mining signatures along with the bedrock.

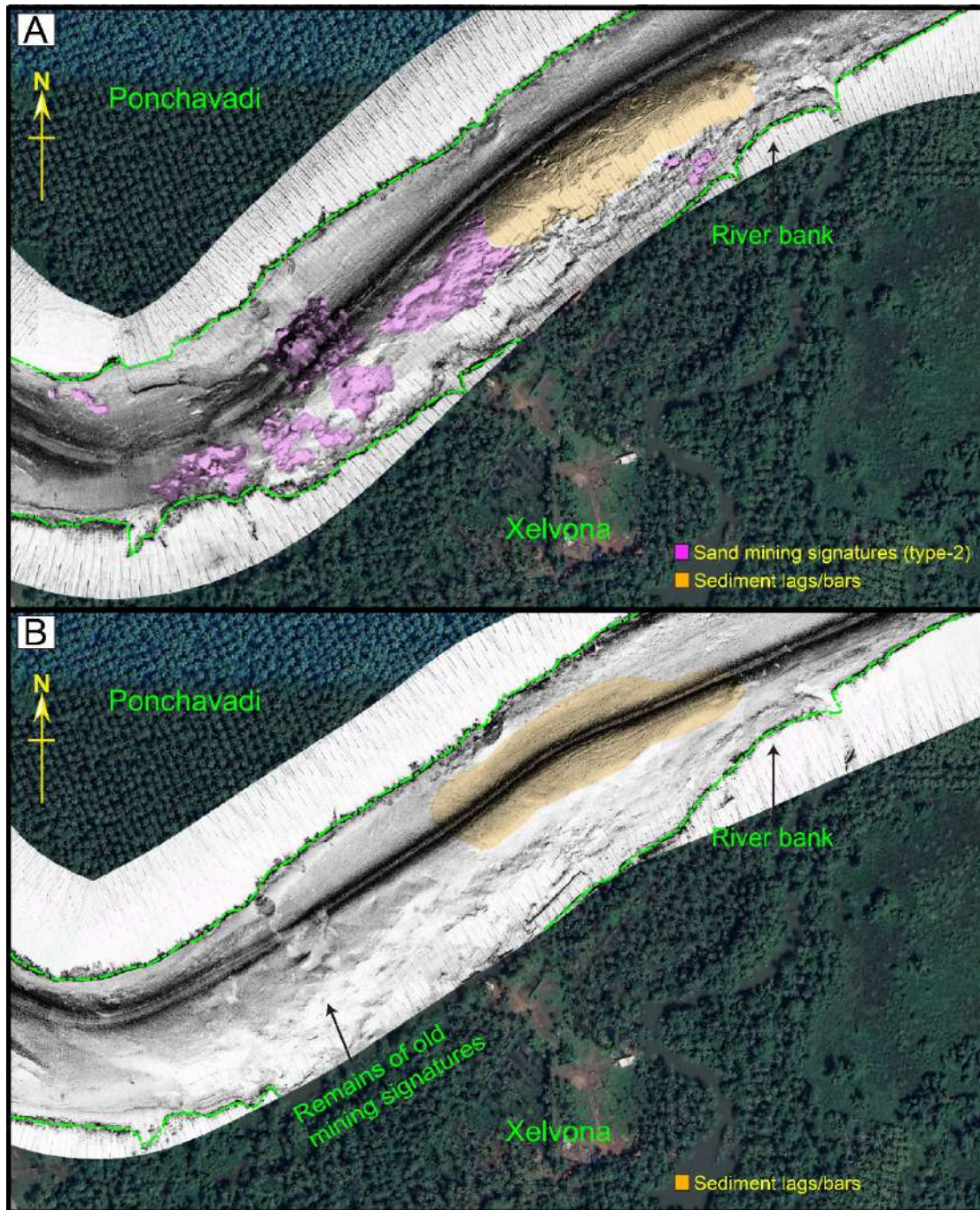


Figure 31. Side Scan Sonogram acquired near Ponchavadi-Xelvona region during (A) pre-monsoon and (B) post-monsoon seasons. (A) highlights the presence of a mid-channel bar with type-2 sand mining signature. (B) shows a thinned mid-channel bar and some remains of old mining signatures.

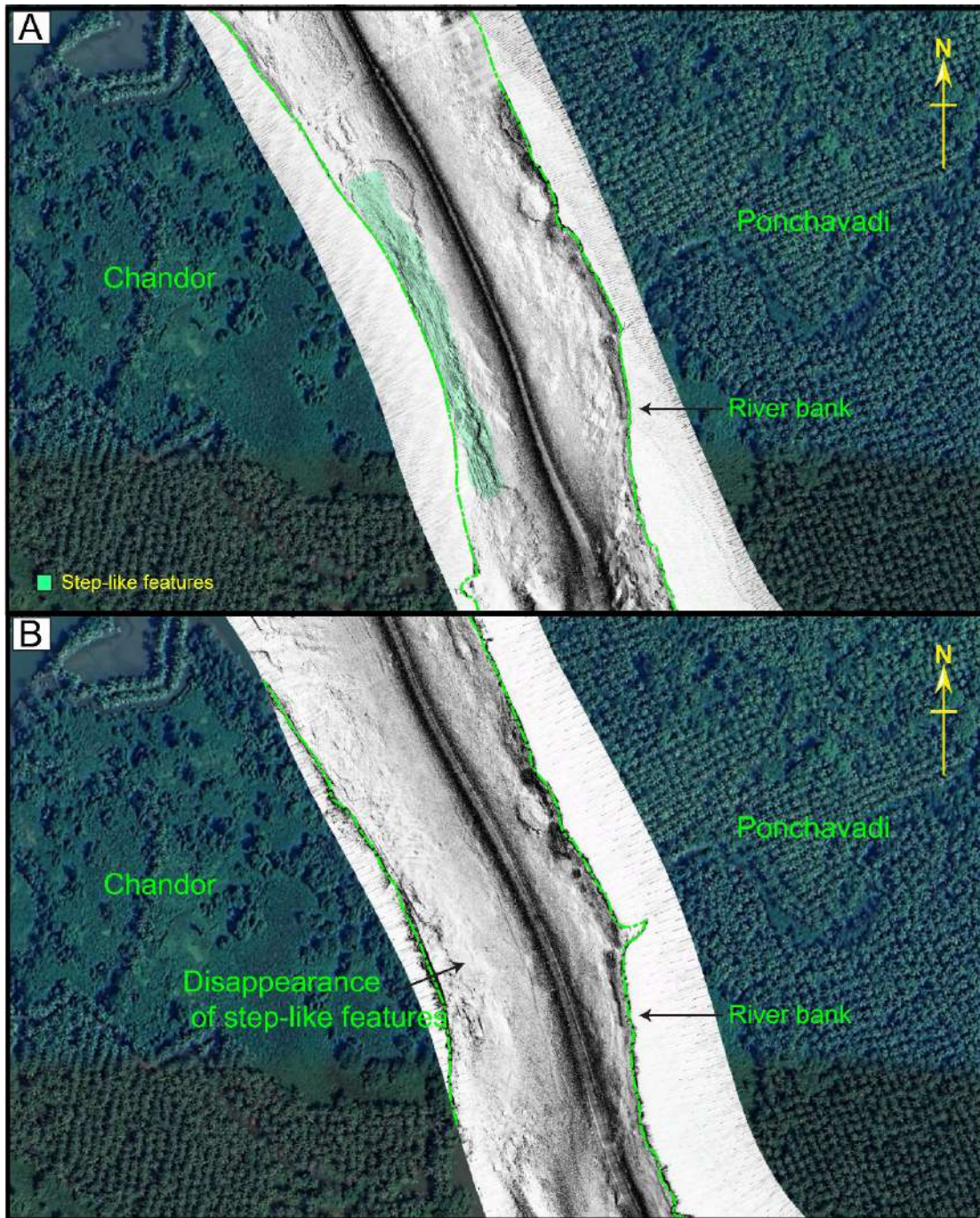


Figure 32. Side Scan Sonogram acquired near Ponchavadi-Chandor region during (A) pre-monsoon and (B) post-monsoon seasons. (A) highlights the presence of step-like features near the bank. (B) shows the washout of these features and a thin layer of sediment has covered the bank.

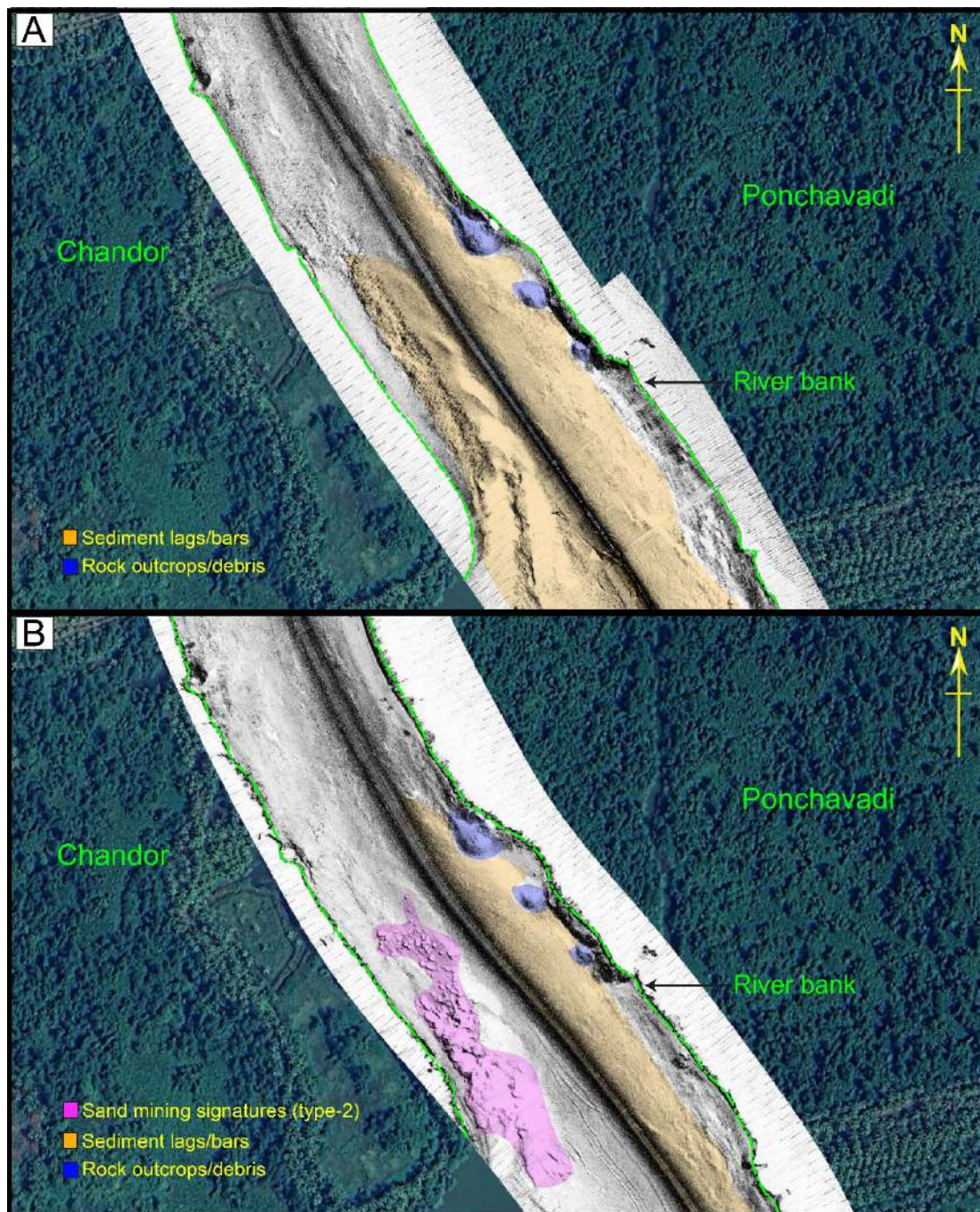


Figure 33. Side Scan Sonogram acquired near Ponchavadi-Chandor region during (A) pre-monsoon and (B) post-monsoon seasons. (A) highlights the presence of mid-channel bars along with a few rock outcrops. (B) highlights thinning of one of the sand bars and signatures of sand mining.

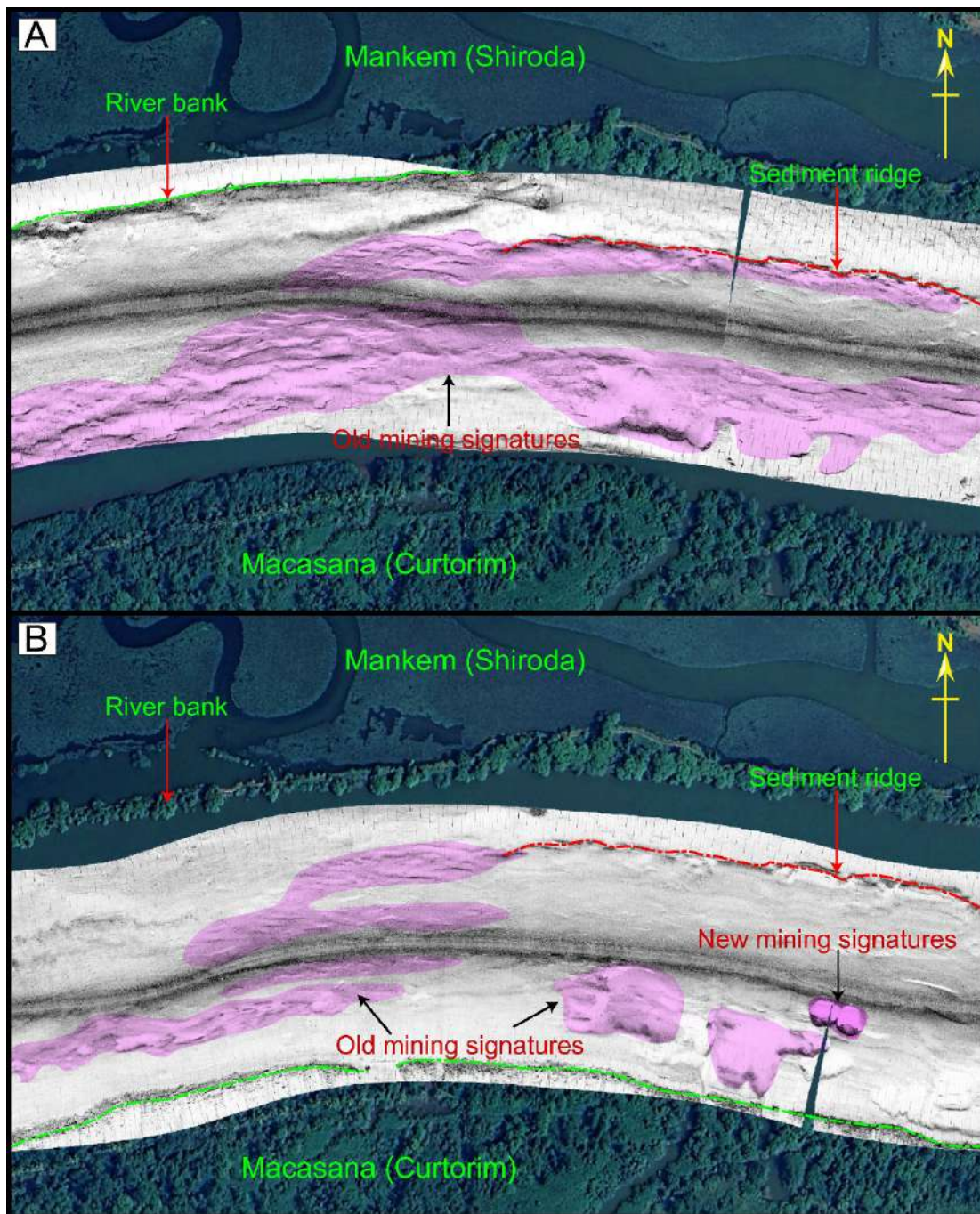


Figure 34. Side Scan Sonogram acquired near Mankem-Macasana region during (A) pre-monsoon and (B) post-monsoon seasons. (A) highlights a sediment ridge and the presence of past sand mining signatures. (B) shows the same ridge and mining signatures, which are still not completely washed out after the monsoon. Some new sand mining signatures are also observed in this region.

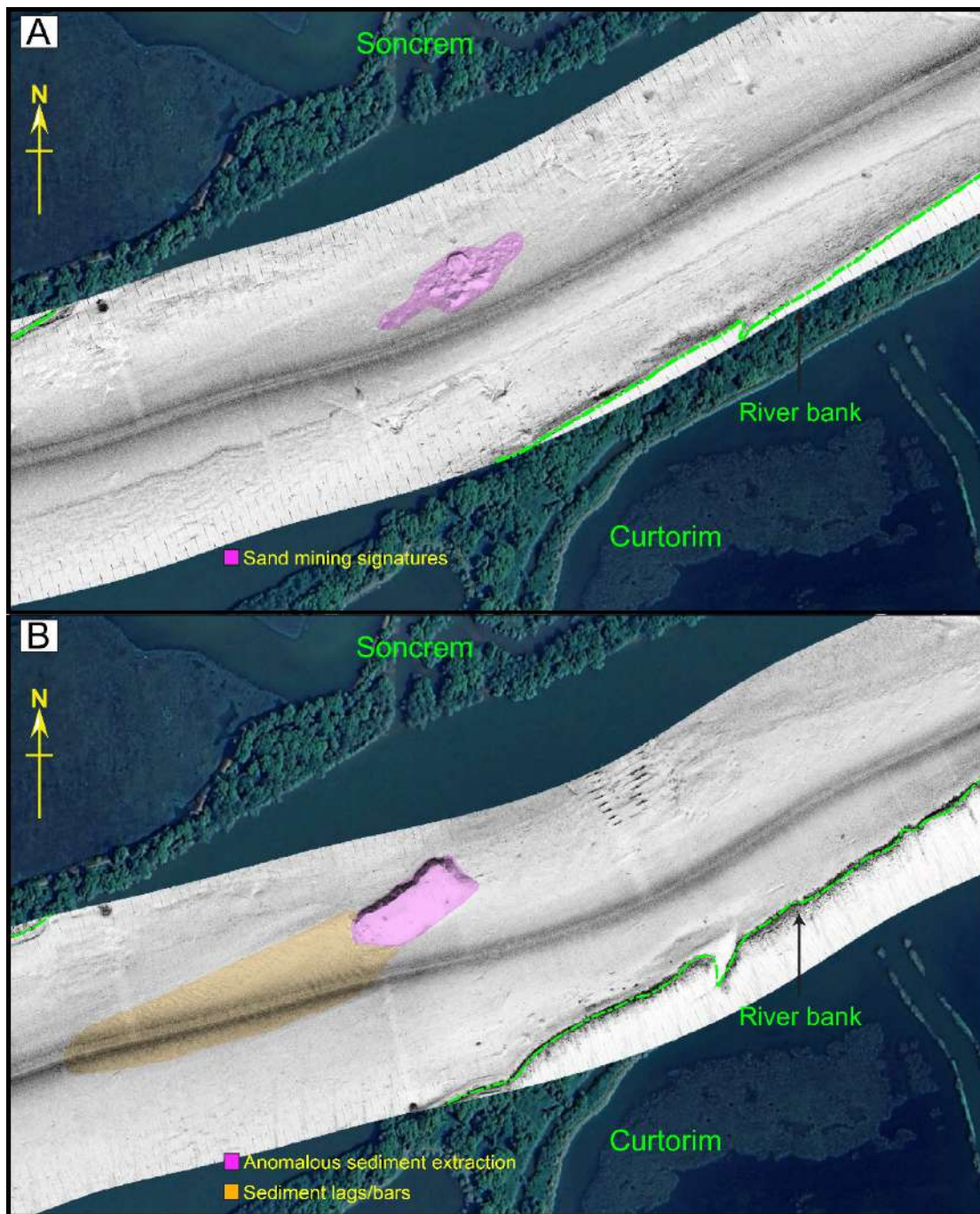


Figure 35. Side Scan Sonogram acquired near Soncrem (Shiroda)-Curtorim region during (A) pre-monsoon and (B) post-monsoon seasons. (A) highlights presence of type-2 sand mining signature. (B) highlights anomalous enhancement of the mining signature.

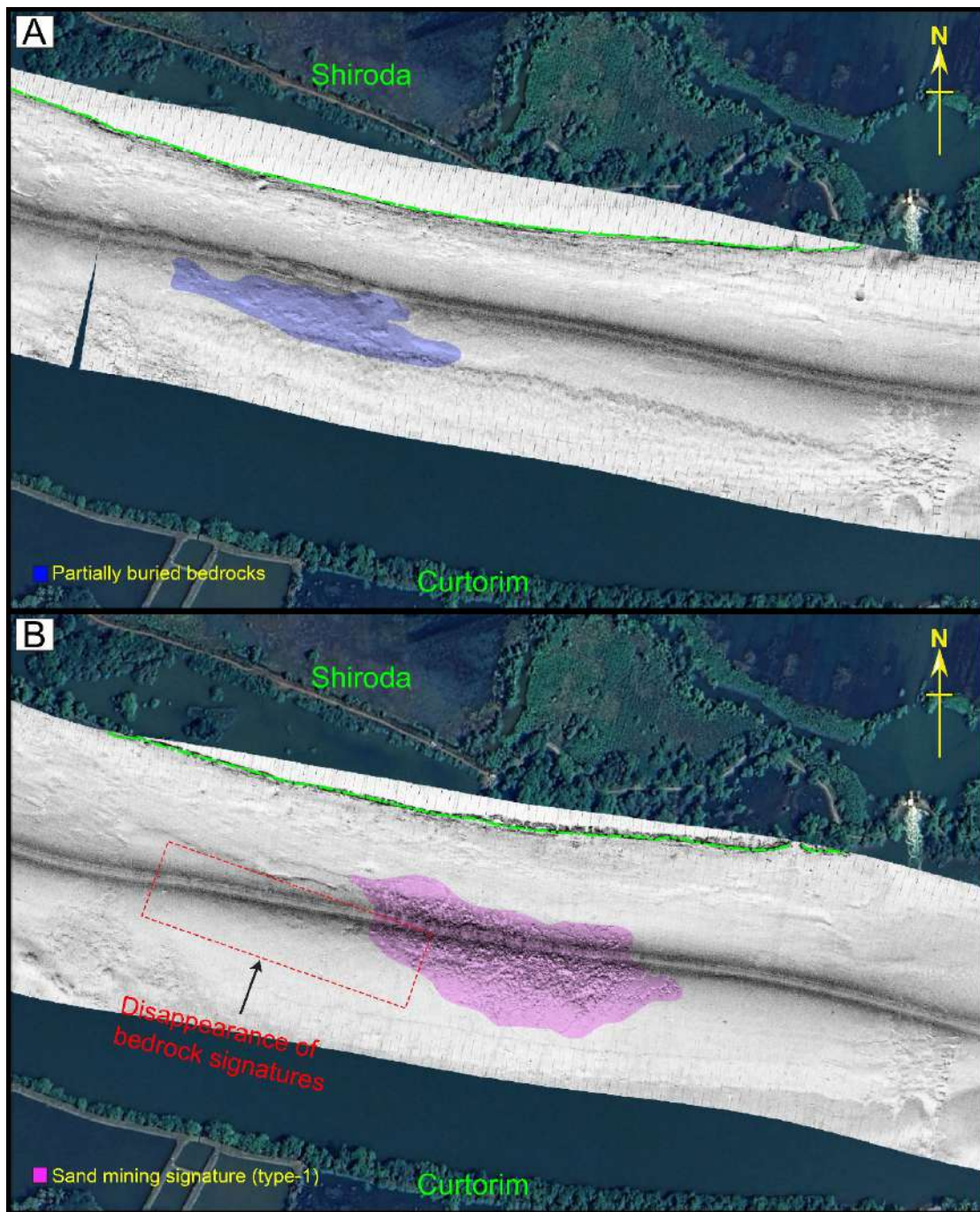


Figure 36. Side Scan Sonogram acquired near Shiroda-Curtorim region during (A) pre-monsoon and (B) post-monsoon seasons. (A) highlights the presence of thinly covered bedrocks. (B) highlights the disappearance of the bedrock signature and some type-1 sand mining signatures.

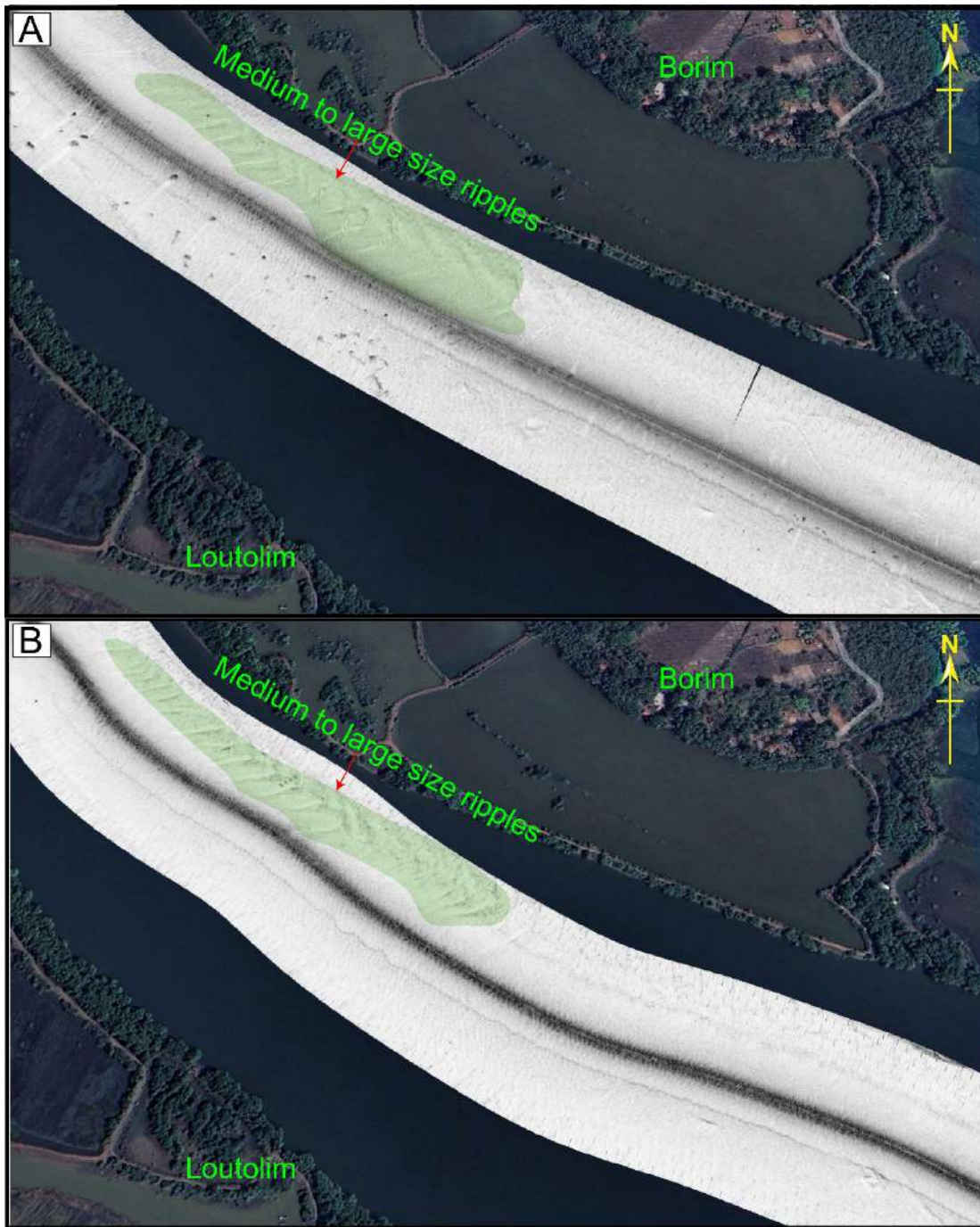


Figure 37. Side Scan Sonogram acquired near Borim-Loutolim region during (A) pre-monsoon and (B) post-monsoon seasons. (A) highlights the presence of medium-to-large ripple marks near Borim bank. (B) shows the post-monsoon sonogram of the same medium-to-large ripple marks.

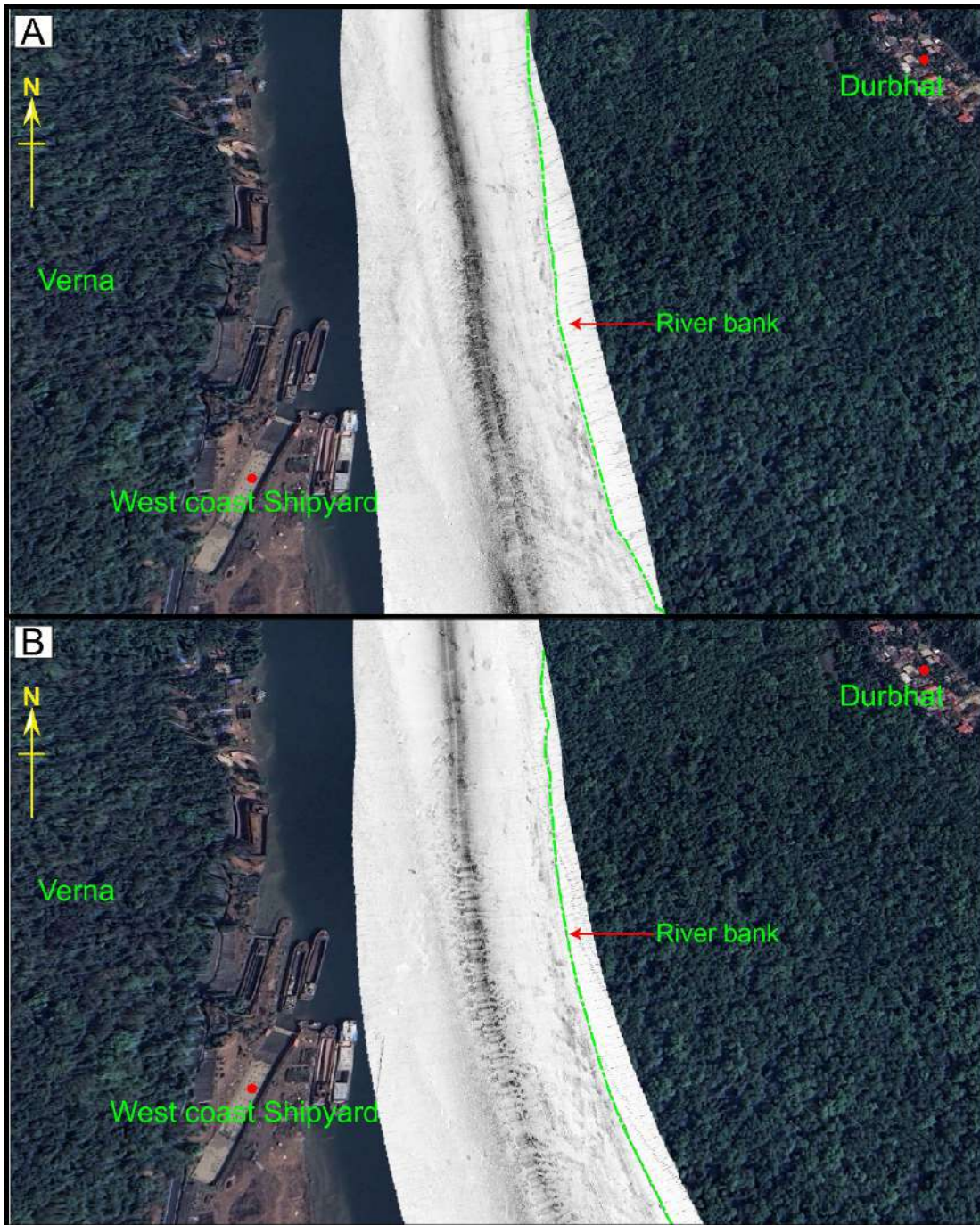


Figure 38. Side Scan Sonogram acquired near Durbhat-Verna region during (A) pre-monsoon and (B) post-monsoon seasons. These sonograms do not show any significant change in the riverbed morphology after monsoon.

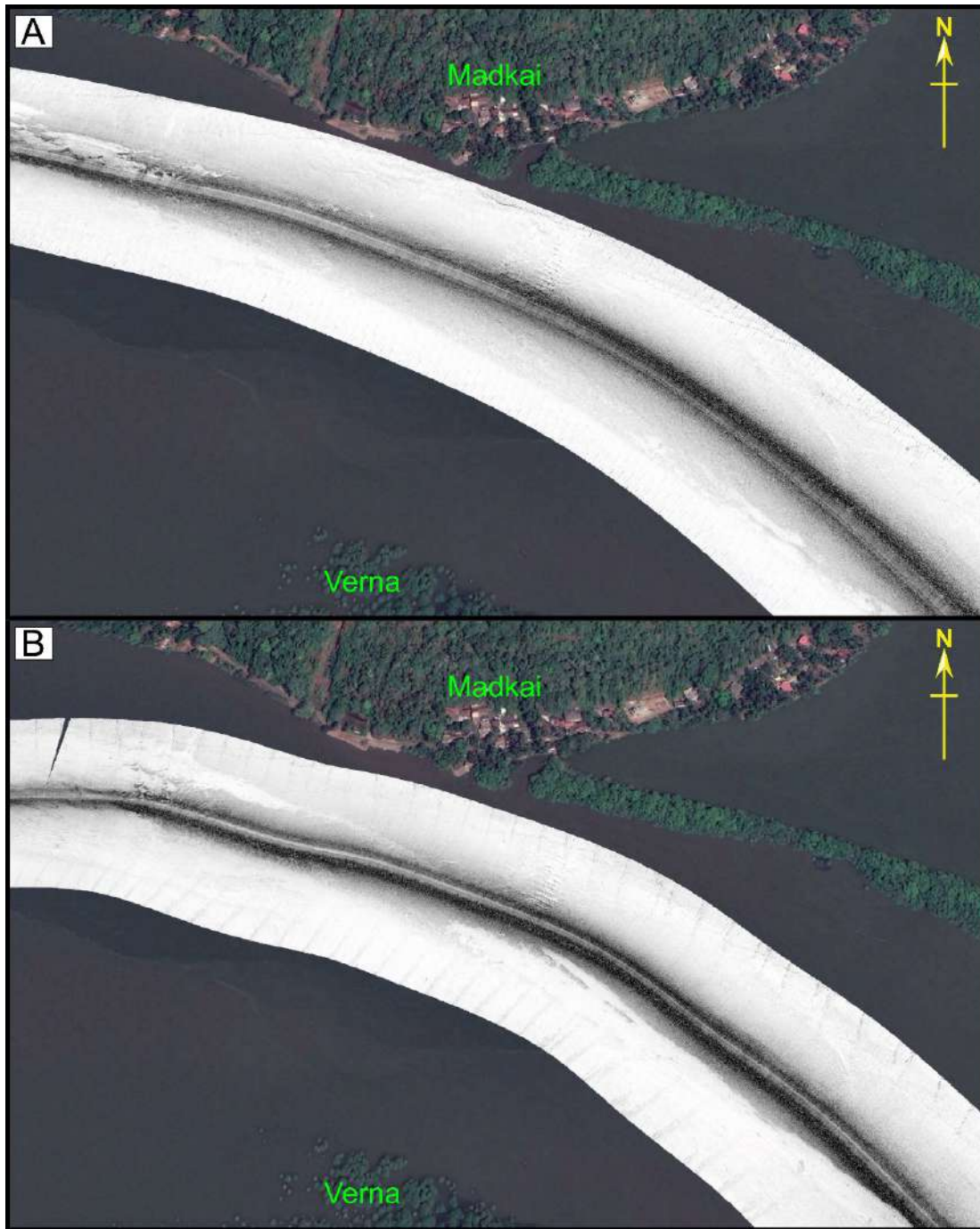


Figure 39. Side Scan Sonogram acquired near Madkai-Verna region during (A) pre-monsoon and (B) post-monsoon seasons. These sonograms do not show any significant change after the monsoon.

The following geomorphological changes like bar thinning, lag removal, sediment accumulation, complete or partial washout of sand mining signatures or drag marks, and exposure or burial of bedrocks are studied in the Zuari river. Based on the observed geomorphological changes, the Zuari River can be classified into three different regions:

1. Sangmeshwar temple to Sanvordem bridge,
2. Downstream Sanvordem to Borim bridge, and
3. Downstream Borim bridge.

The region between Sangmeshwar temple to Sanvordem bridge show thinning of sediment bar/lag, bedrock exposure, deposition of new sediment bar/lag at some locations, fresh signatures of sand mining, and signatures related to sediment dumps. Thinning of sediment bar/lag and bedrock exposure are prevalent in this region indicating predominant erosion. Although, some locations show sediment deposition as well as local sediment redistribution.

The region downstream of Sanvordem bridge to Borim bridge shows deposition of new sediment bar/lag, the disappearance of bedrock exposure, complete obliteration of sand mining signatures and drag marks, and disappearance of step-like features along riverbanks. These changes indicate that the sediment eroded from the upstream Sanvordem bridge is deposited in this region. The change in geomorphological features suggest significant sediment accumulation near the Sanvordem-Baag Xelvona region. The sediments transported from the Kushawati river and Guirdolim rivulet might have contributed to the sediment supply in this region.

The region downstream of the Borim bridge shows minor changes in the riverbed morphology. A negligible amount of sediments reaches upto this extent of the river.

Seismic Data Interpretation:

The riverbed and basement/reference reflector are interpreted from the pre-monsoon and post-monsoon high-resolution seismic data. These are compared to identify locations of aggradation/degradation of the riverbed in the Zuari river. However, following the same track-line in pre- and post-monsoon seasons is difficult due to the navigational constraints and boat/barge traffic on the river. Therefore, an integrated data analysis approach is followed to reach the final conclusions. The analysis of pre-and post-monsoon seismic data revealed significant to insignificant aggradation/degradation of the riverbed through the Zuari river. At a few locations in the upstream region, aggradation/degradation of the riverbed are significant, whereas it is largely insignificant in the downstream region. Irrespective of their magnitude, these variations can only be categorized as local in nature. These variations reflect the local adjustment of the river during the monsoon season. In the present report, a few representative regions in the upstream and downstream regions of the Zuari river have been highlighted.

Figures 40 a, b shows the pre-and post-monsoon seismic data acquired in the Zuari river near Cortalim. A common reference layer has been identified. No significant change in the depth of reference subsurface layers is observed after the monsoon indicating a similar tidal level during the surveys. Therefore, we compared variation in the pre-and post-monsoon sediment thickness with respect to the reference layer as shown in Figure 40c. Observed sediment thickness variation between pre- post-monsoon surveys is insignificant and does not

Geo-Morphological studies for Zuari River - 2022

show any clear aggradation/degradation trend in this region except a local redistribution at a few locations where it varies within the ~ 0.5 m range.

Figure 41 a, b highlights the pre-and post-monsoon seismic data near the Borim bridge. Again, A common reference layer has been identified. The depth of the reference layer and the structures of subsurface layers appear to be similar between pre-and post-monsoon surveys indicating similar tidal levels. Therefore, the variation in the pre-and post-monsoon sediment thickness with respect to the reference layer is compared. A significant amount of riverbed aggradation of ~ 1 m is observed the far upstream of the Borim bridge. The magnitude of aggradation decreases towards the bridge and close to the bridge a sediment degradation of $\sim 0.5-0.7$ m is observed. Again, in downstream of the bridge, aggradation of the riverbed is observed which becomes insignificant further downstream (Fig. 41c). These observations indicate a local redistribution of the sediment where deposition processes are leading.

Figures 42 a, and b shows the pre-and post-monsoon seismic data near the Ponchavadi-Chandor region. The basement reflector's depth, though the basement reflector doesn't show considerable change, the riverbed and embedded reflectors show some discernible changes in the region as shown in Figure 42 a & b. A comparison of sediment thickness variation shows aggradation of the riverbed in the upstream region and a large degradation of the riverbed in the downstream region. The aggradation varies between 0.2 m to 1.5 m whereas the degradation is prominent in the downstream. The pre-and post-monsoon comparison of side scan sonar data from the same region also show significant geomorphological changes like the formation of a sand bar, local redistribution of sediments as well as sand mining signatures.

Figures 43a, b highlights the pre- and post-monsoon seismic data near the Sanvordem-Baag-shirfod region. Some new sets of reflectors are observed after the monsoon, which may correspond to the newly deposited sedimentary layer with variable thickness. The basement depths are almost similar, indicating similar tidal level during the survey. the variation of sediment thickness for the pre- and post-monsoon surveys are compared (Fig. 43c). The sediment thickness of the area has increased after the monsoon season (Fig. 43c). The SSS data also shows geomorphological changes related to the aggradation of sediments and the offset between the survey track-lines are small. Overall, the region shows aggradation of the riverbed of the order of ~ 0.5 to 3.0 m.

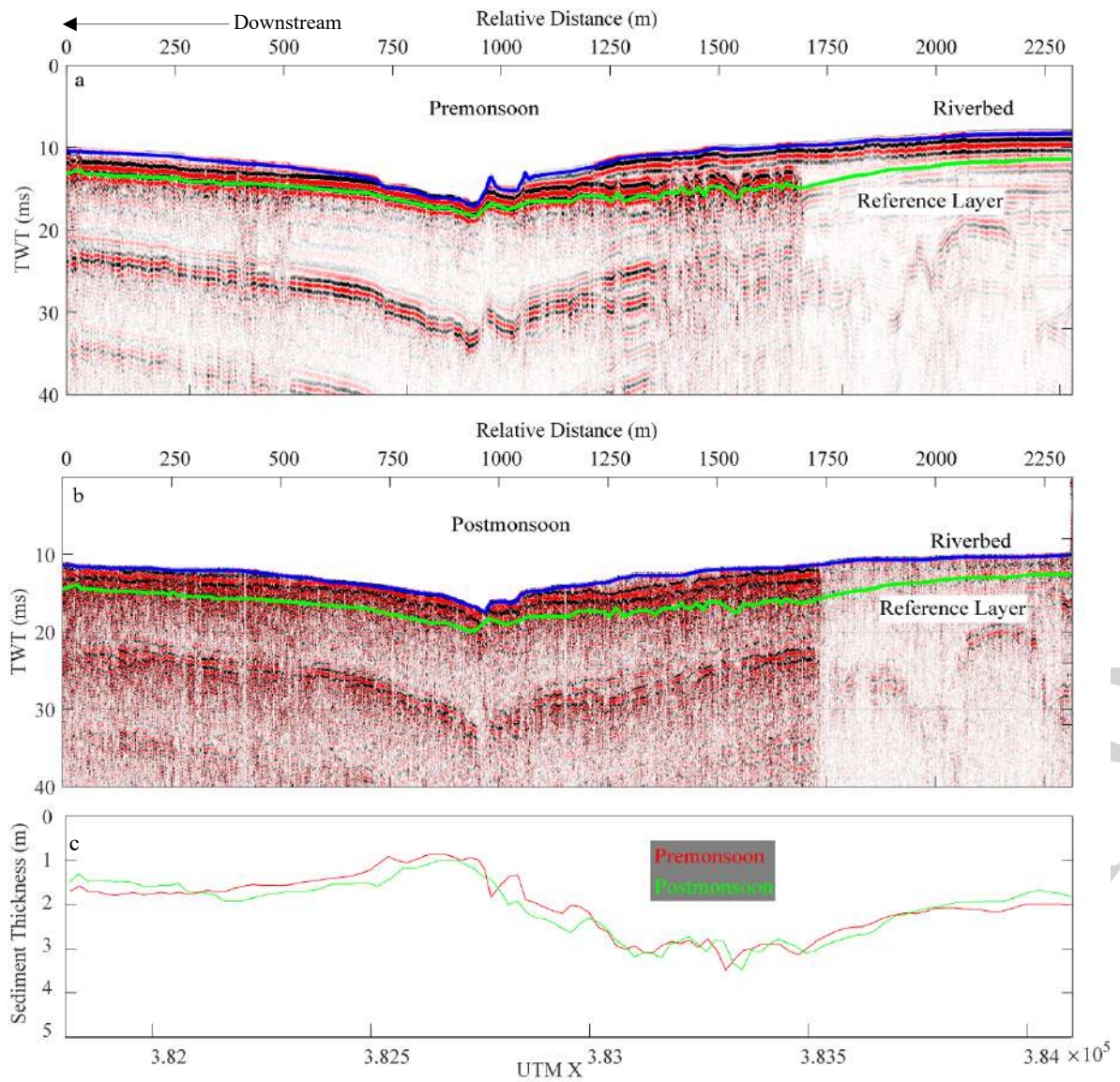


Figure 40. High-resolution seismic data: a) pre-monsoon seismic data, b) post-monsoon seismic data, and c) sediment thickness from the reference layer between the survey period near Cortalim Zuari bridge.

Geo-Morphological studies for Zuari River - 2022

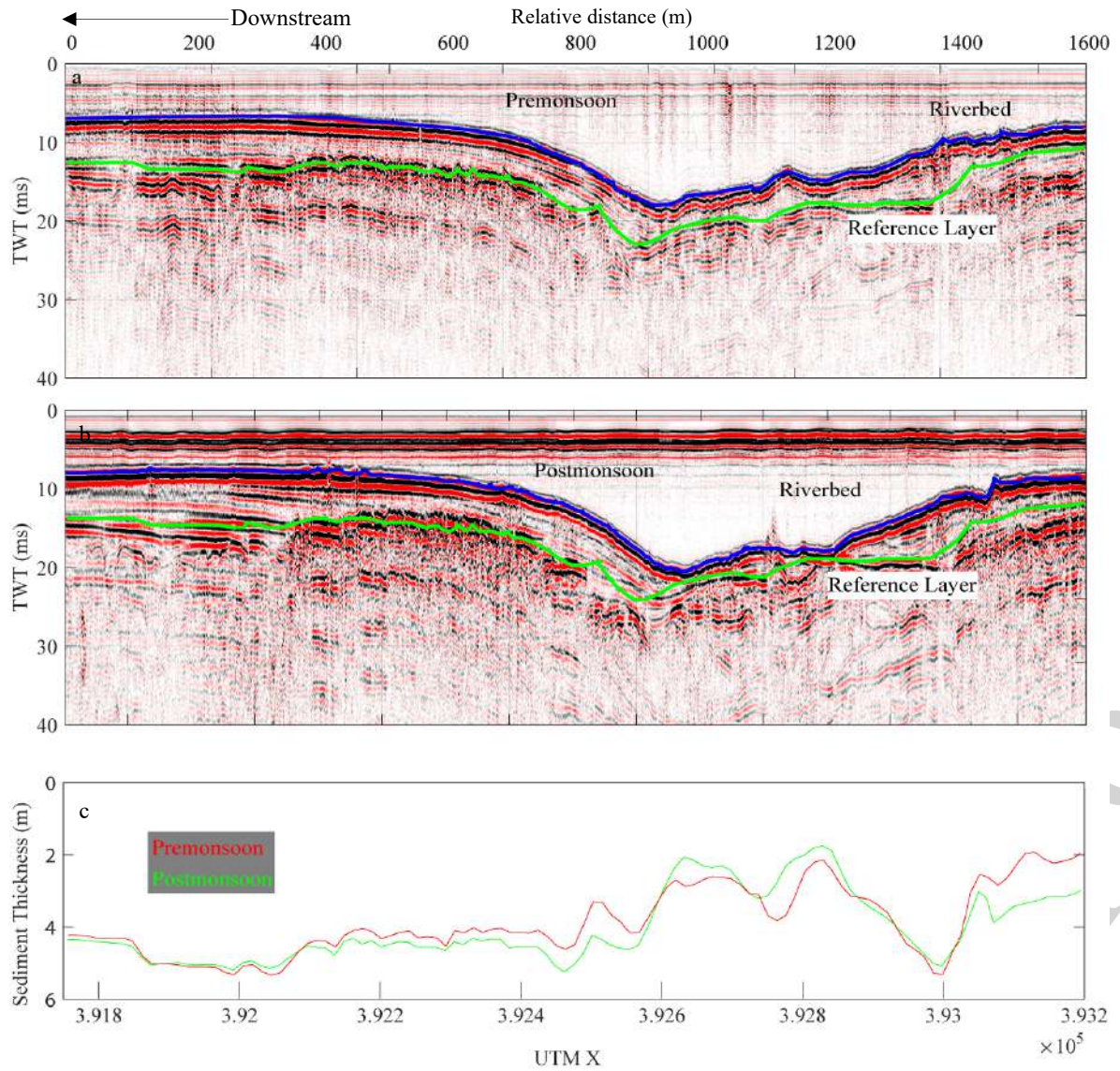


Figure 41. High-resolution seismic data: a) pre-monsoon seismic data, b) post-monsoon seismic data, and c) sediment thickness variation from reference layer between the survey period near Borim bridge.

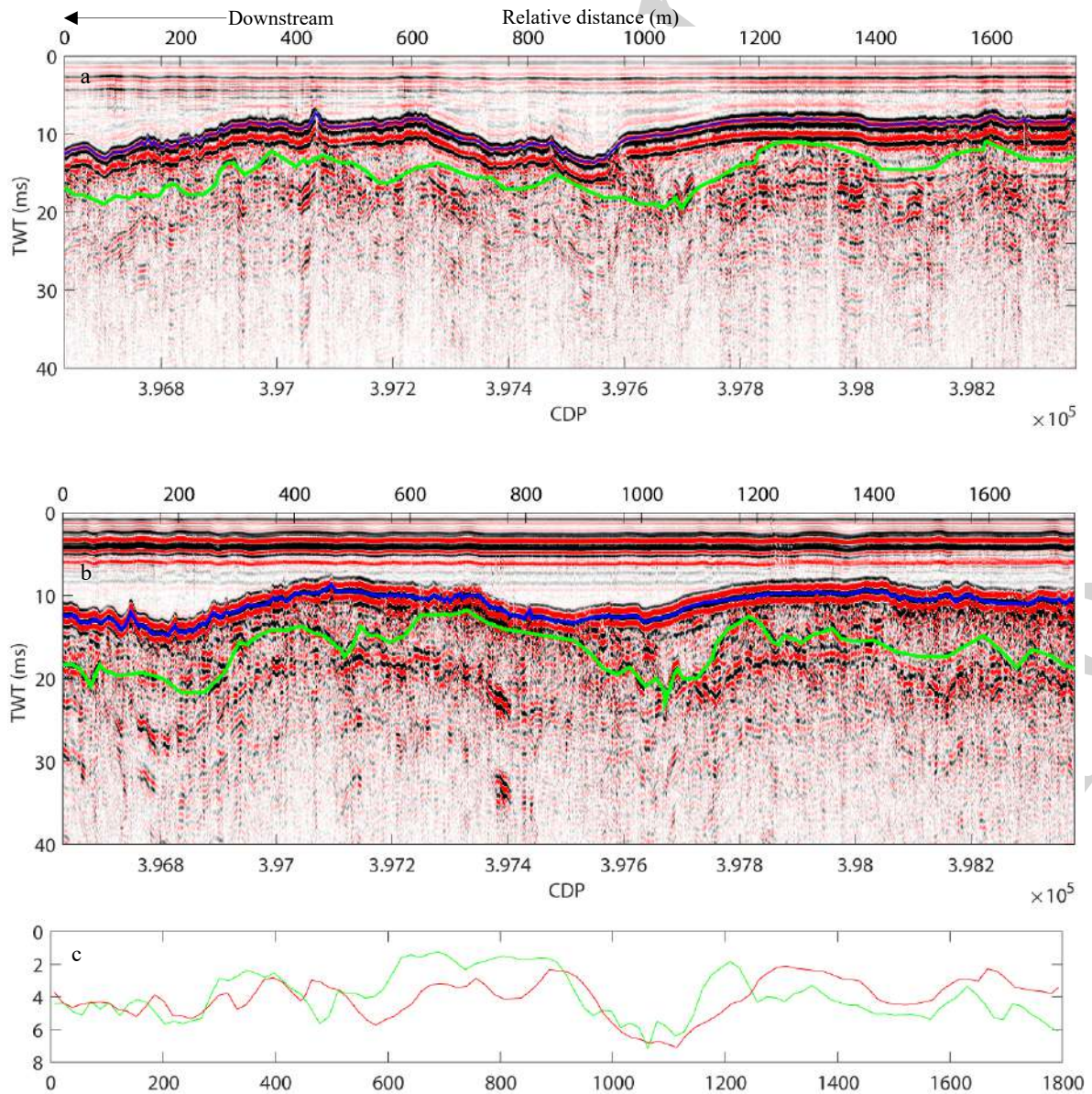


Figure 42. High-resolution seismic data: a) pre-monsoon seismic data, b) post-monsoon seismic data, and c) sediment thickness variation between the survey period near the Ponchavadi-Chandor region.

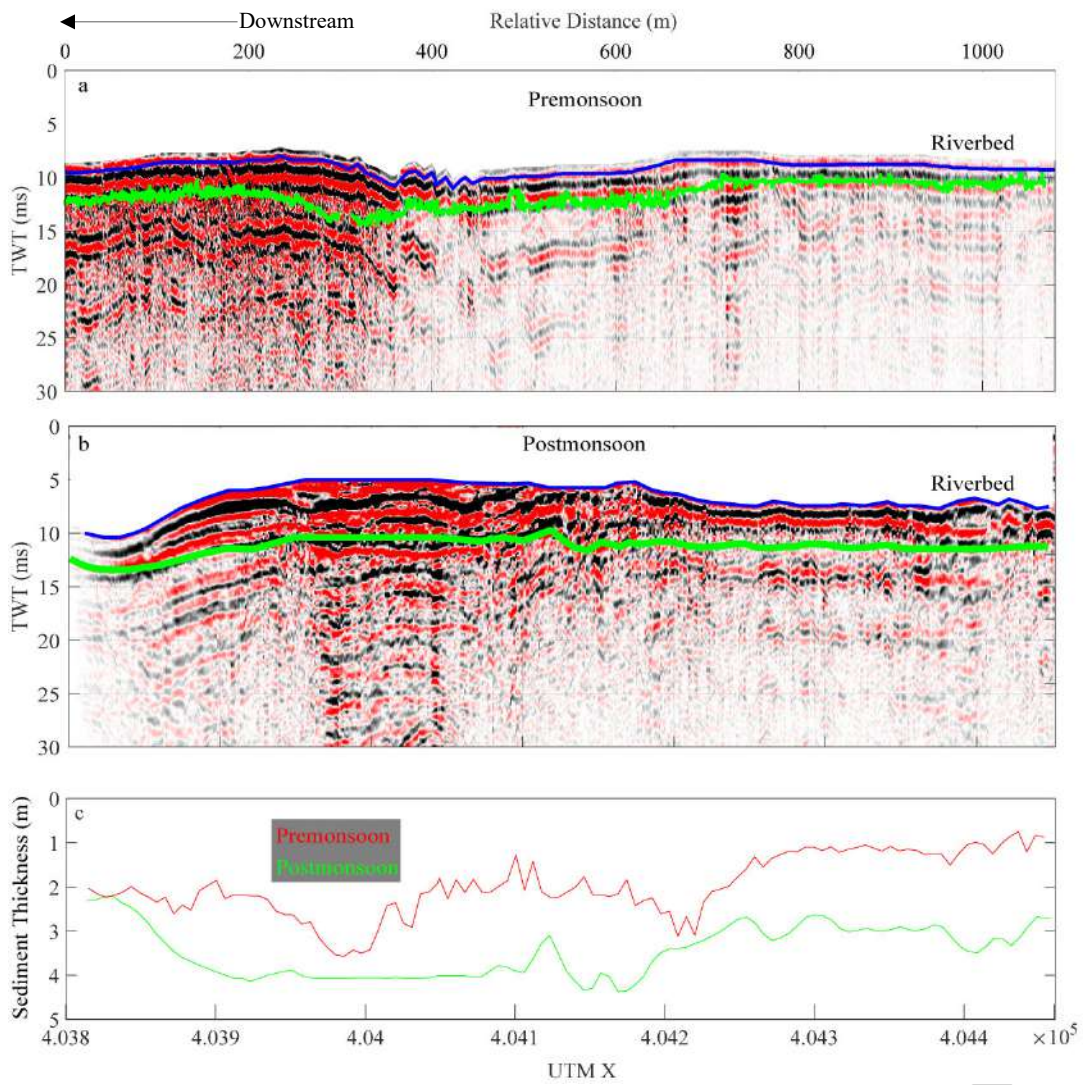


Figure 43. High-resolution seismic data: a) pre-monsoon seismic data, b) post-monsoon seismic data, c) sediment thickness variation between the survey period near the Sanvordem - Baag Shirfod region.

Chapter 7. Conclusions

Based on the side scan sonar imaging, single beam echosounder bathymetry and high resolution seismic (HRS), morphological features of riverbed have been interpreted across a stretch of 53 km of Zuari river. The side scan sonar image shows various geomorphological features like ripple marks (associated with sand), rock outcrops, riverbanks, erosion features, mud zones and shadow zones of the road and railway bridges across the Zuari river. Apart from this, active sand mining zones in different regions of Zuari river have also been identified. The single beam echo sounding data is used for estimating the depth of the riverbed and the high-resolution seismic data is utilized for estimating the sediment thickness.

The microscopic grain size analysis shows a decrease in grain size when moving from Sanvordem to the river mouth. The bulk sediment grain size in most of the samples is dominated by sand fraction. Most of the stations contain a considerable amount of iron oxide, quartz, phyllite, and fewer lithic fragments. Sorting of acquired sediment samples is consistent with respect to their location in the river. It varies from well sorted to poorly sorted having yellow to brownish colour. Poorly sorted sediment upstream Sanvordem reflects presence of local sediment sources through the channel course and well sorted sediment downstream Sanvordem reflects sediment travelled sufficiently long distance before they settle and absence of nearby sediment source in this zone suggesting there no significant river bank erosion in this zone.

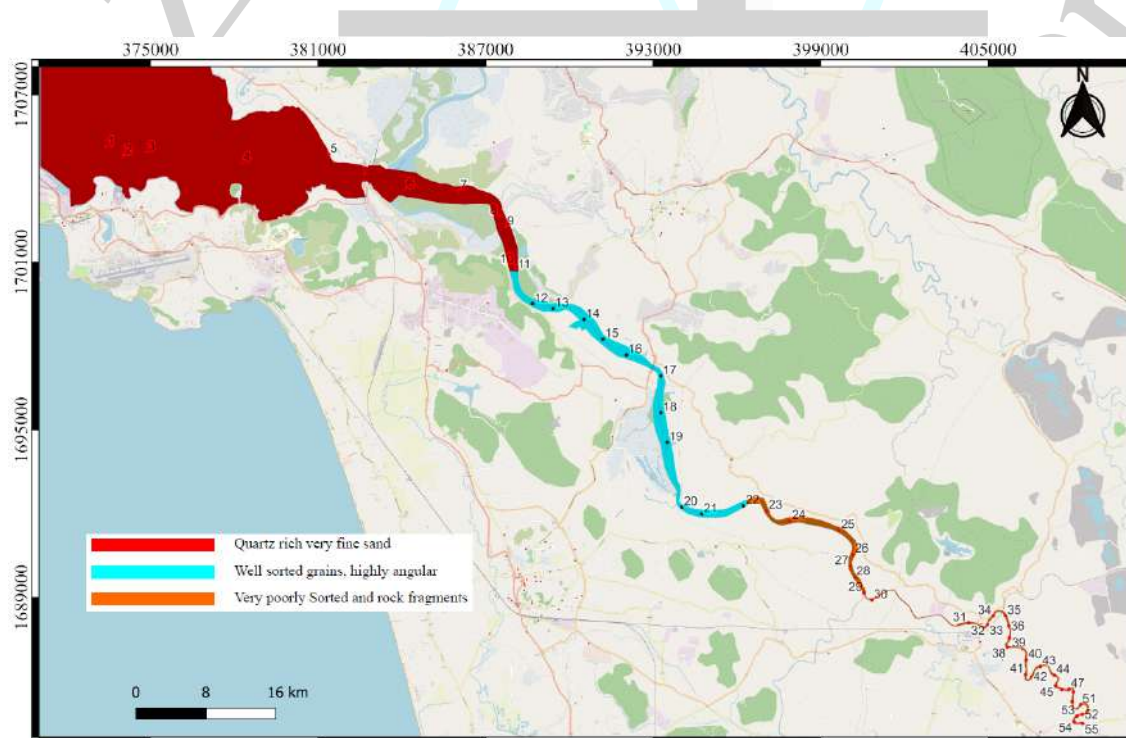


Figure 44. Sand sediment grain size distribution from upstream to river mouth

The comparative analysis of pre- & post-monsoon side scan sonar images revealed substantial geomorphological changes through the Zuari River course. Based on the observed geomorphological changes, the Zuari River can be classified into three different regions **1. Sangmeshwar temple to Sanvordem bridge**, thinning of sediment bar/lag and bedrock exposure are prevalent in this region indicating predominant erosion. Although, some locations show sediment deposition as well as local sediment redistribution. **2. Downstream Sanvordem to Borim bridge**, these changes indicate that the sediment eroded from the upstream Sanvordem bridge is deposited in the Sanvordem-Baag Xelvona region. And further downstream, the sediments transported from the Kushawati river and Guirdolim rivulet might have also contributed to the sediment supply to the region. **3. Downstream Borim bridge**, the region downstream of the Borim bridge shows minor changes in the riverbed morphology. A negligible amount of sediments reaches up to this extent of the river. The analysis of pre-and post-monsoon seismic data revealed significant to insignificant aggradation/degradation of the riverbed through the Zuari river. At a few locations in the upstream region, aggradation/degradation of the riverbed are significant, whereas it is largely insignificant in the downstream region. However, the integrated analysis of SSS and HRS data in respective regions revealed that irrespective of the magnitude, the identified deposition/erosion can only be categorized as local in nature and reflect the local adjustment of the river during the monsoon season.

Based on the EIA/EMP study by NIO in Zuari river, five feasible sand mining regions have been identified (Fig.45). These regions have been evaluated based on detail studies of impact on the environment and biodiversity.

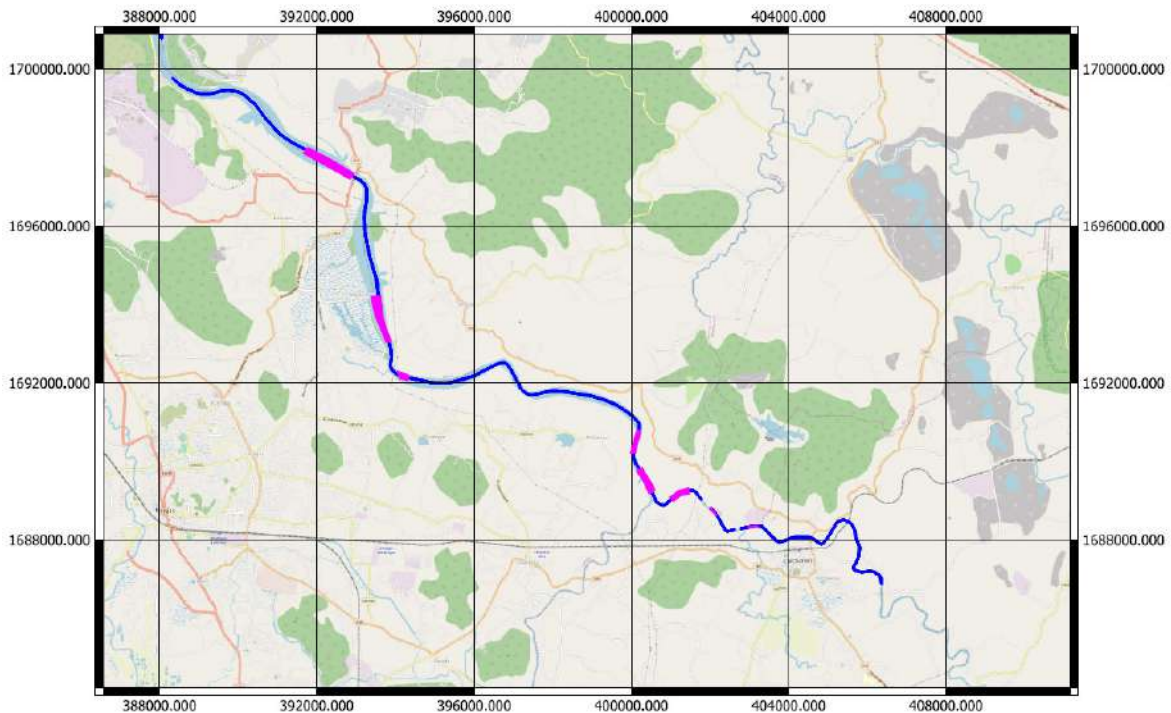


Figure 45. Possible Sand mining regions after considering EIA/EMP studies

Geo-Morphological studies for Zuari River - 2022

Availability of sand (volume and weight) for sustainable mining (3-meter mining) along with total sand deposits have also been provided in table 8. The total sand volume is estimated using the sediment thickness (data riverbed to bed rock thickness) derived from high resolution seismic and width of the sand distribution (based on the riverbed characteristics such as ripple marks etc.) was derived from side scan sonar image along the length of the river. considering the effective bulk density of the sediment 1.6 gm/cc, total weight of sediment (sand) available in the minable zones of Zuari river have also been estimated (Table 8). Later a constraint of 3 meter for mining have been applied to get volume and weight of the minable sand in the identified regions (Table 8).

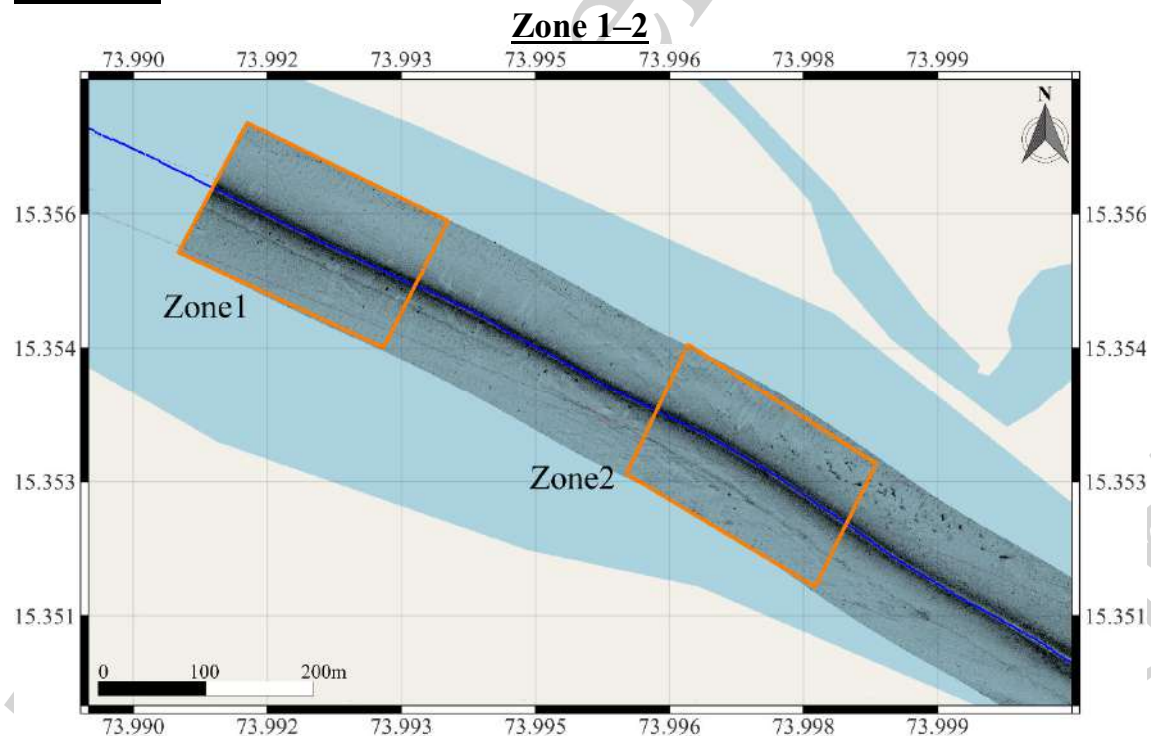
Table 8. Total Volume (Cubic m) and Weight (Ton) in selected regions and volume (cubic m) and weight (ton) within 3meter mining depth

S. No	Region	Length (m)	Volume (Cubic m)	Weight (Tons)	Volume (Cubic m) for 3m thickness	Weight (Tons) for 3m thickness
1	Borim Bridge	1600	2731608.20	4370573.12	411681.48	658690.37
2	Rachol- Shi-roda	2200	1923124.64	3076999.43	432219.00	691550.00
3	Chandor- Ponchwadi	2200	2506997.45	4011195.92	549391.63	879026.61
4	Bag-Xelvona	1800	1038169.0	1661070	287541.5	460066.4
5	Ponchwadi- Odar	1600	191191.0	305905.72	244861.0	391777.0
	Total =	9400	8391090.29	13425744.19	1925694.61	3081110.38

Annexure 1

Detail locations and estimates of prospective sand mining zones for Zuari River

Locations



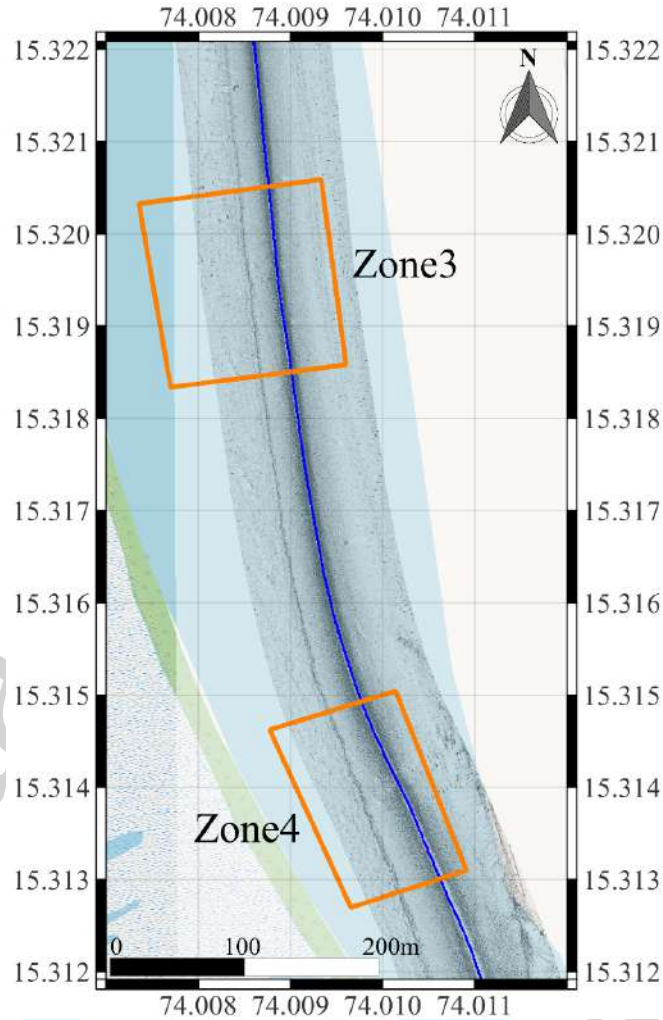
Zone-1 Block Coordinates

S. No.	Longitude	Latitude
1	73.994020	15.355421
2	73.993299	15.354006
3	73.991004	15.355068
4	73.991771	15.356515

Zone-2 Block Coordinates

S. No.	Longitude	Latitude
1	73.998813	15.352697
2	73.998127	15.351324
3	73.996018	15.352584
4	73.996706	15.354038

Zone 3 – 4

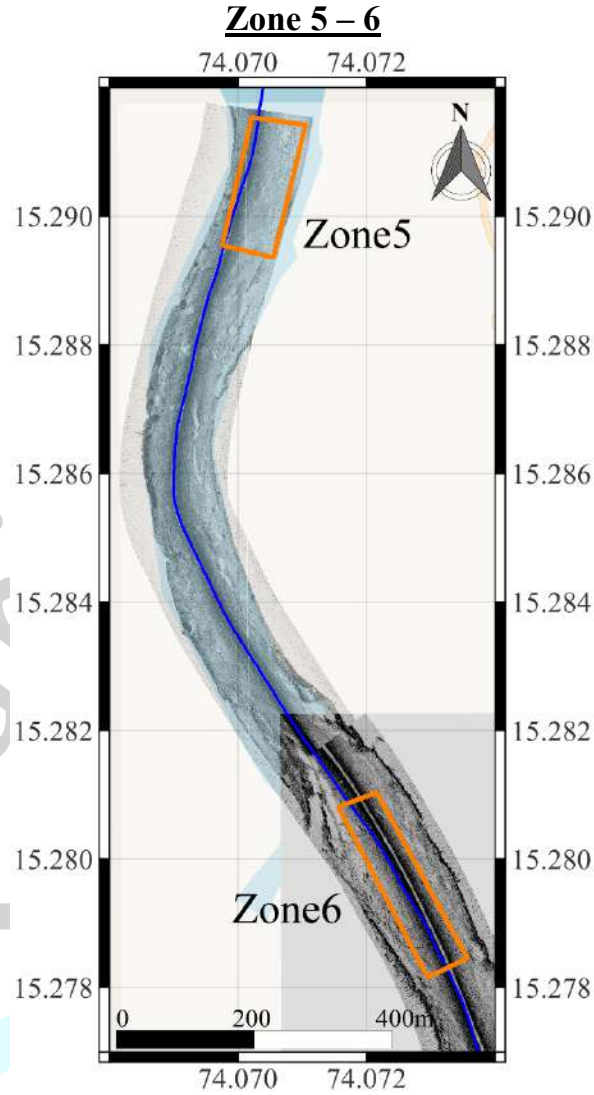


Zone – 3 Block Coordinates

S. No.	Longitude	Latitude
1	74.0096	15.31858
2	74.0077	15.31834
3	74.00736	15.32033
4	74.00933	15.32059

Zone – 4 Block Coordinates

S. No.	Longitude	Latitude
1	74.010907	15.313097
2	74.009654	15.312695
3	74.008775	15.314622
4	74.010140	15.315042

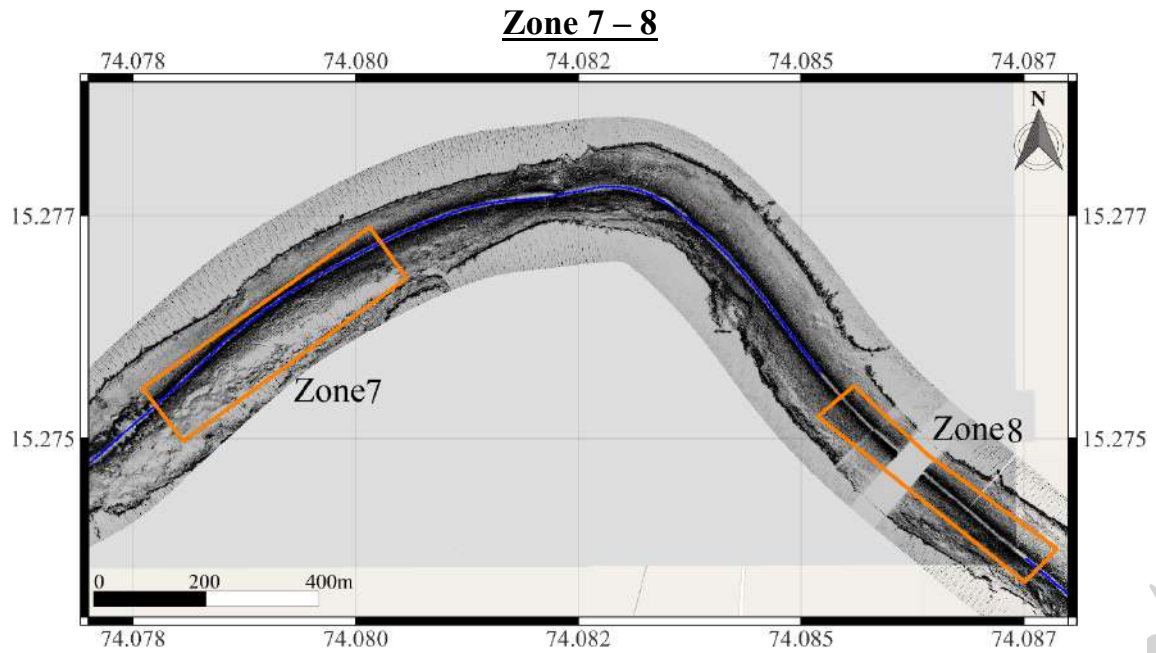


Zone – 5 Block Coordinates

S. No.	Longitude	Latitude
1	74.071049	15.291420
2	74.070787	15.290228
3	74.070105	15.290350
4	74.070381	15.291505

Zone – 6 Block Coordinates

S. No.	Longitude	Latitude
1	74.073567	15.278457
2	74.072950	15.278158
3	74.071557	15.280809
4	74.072155	15.281034



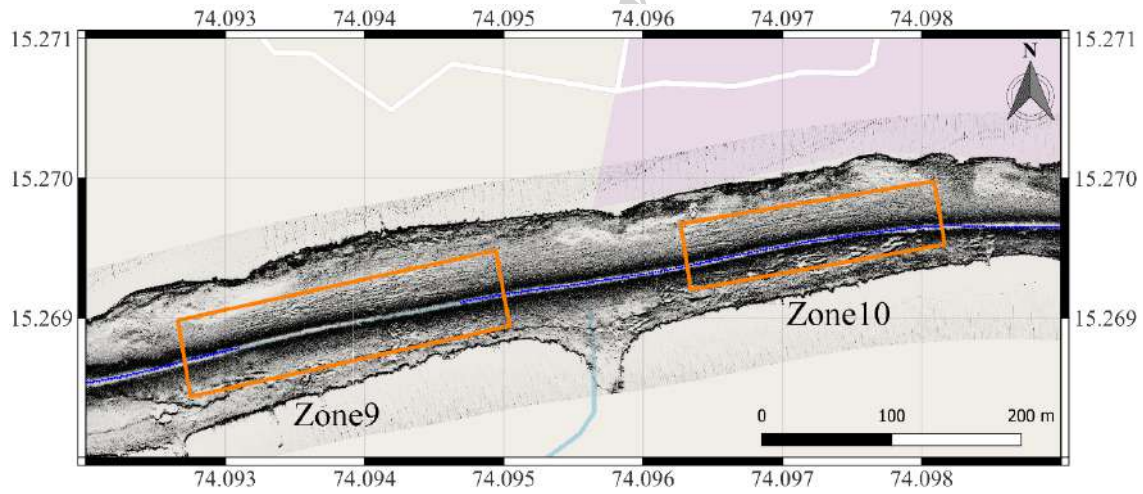
Zone – 7 Block Coordinates

S. No.	Longitude	Latitude
1	74.080569	15.276798
2	74.078068	15.274969
3	74.077605	15.275563
4	74.080158	15.277368

Zone – 8 Block Coordinates

S. No.	Longitude	Latitude
1	74.086426	15.274810
2	74.087870	15.273763
3	74.087510	15.273389
4	74.085189	15.275248
5	74.085591	15.275589

Zone 9 – 10



Zone – 9 Block Coordinates

S. No.	Longitude	Latitude
1	74.095041	15.268940
2	74.092750	15.268435
3	74.092661	15.268982
4	74.094942	15.269482

Zone – 10 Block Coordinates

S. No.	Longitude	Latitude
1	74.098164	15.269524
2	74.096341	15.269202
3	74.096270	15.269674
4	74.098089	15.269978

Estimates of available sand in the prospective Sand Mining Zones

S. No.	Zones	Area (ha)	Volume (Cubic m)	Weight (Tons)
1	Zone1	4.8	68,614	1,09,700
2	Zone2	4.5	68,360	1,02,240
3	Zone3	4.6	72,036	1,15,258
4	Zone4	3.4	43,221	69,154
5	Zone5	2.04	62,680	1,00,288
6	Zone6	2.32	82,408	1,31,853
7	Zone7	2.69	47,923	76,677
8	Zone8	1.66	28,753	46,006
9	Zone9	1.53	32,648	52,236
10	Zone10	1.02	27,206	43,530

